ASSESSMENT AND ENHANCEMENT OF THE TRANSIENT STABILITY OF DFIG BASED WIND FARM USING ANFIS

(A Case Study of ADAMA II Wind Farm)

A Thesis Submitted

In Partial Fulfillment of the Requirements

For the Degree of

Master of Science

In

Power System and Energy Engineering

By

TESFAYE BELAY

DEPARTMENT OF ELECTRICAL ENGINEERING

HAWASSA UNIVERSITY INSTITUTE OF TECHNOLOGY

HAWASSA (ETHIOPIA)

April, 2021

ASSESSMENT AND ENHANCEMENT OF THE TRANSIENT STABILITY OF DFIG BASED WIND FARM USING ANFIS

(A CASE STUDY OF ADAMA-II WIND FARM)

By

TESFAYE BELAY

A THESIS SUBMITTED TO THE SCHOOL OF ELECTRICAL AND COMPUTER ENGINEERING, INSTITUTTE OF TECHNOLOGY

SCHOOL OF GRADUATE STUDIES

HAWASSA UNIVERSITY

HAWASSA, ETHIOPIA

IN PARTIAL FULLFILLMENT OF THE REQUIREMENT FOR THE DEGREE

OF MASTER OF SCIENCE IN POWER SYSTEM AND ENERGY ENGINEERING

April, 2021

EXAMINER'S APPROVAL SHEET

We, the undersigned, members of the Board of examiners of the final open defense by **Tesfaye Belay Mengistu** have read and evaluated his/her thesis entitled "'**Assessment and enhancement of the transient stability of DFIG based wind farm using ANFIS**", and examined the candidate. This is, therefore, to certify that the thesis has been accepted in partial fulfillment of the requirements for the degree of **Masters of Science in Electrical and Computer Engineering.**

Advisors:

Dr. Baseem Khan (PHD)	----------	----------
Advisor	signature	date
Issaias Gedey (MSc)	----------	----------
Co-advisor	signature	date
Mr. Mesfin J	----------	----------
Name of the chairperson	signature	date
Dr. Muluneh Lemma	----------	----------
Name of external examiner	signature	date
Mr.Mulualem T.	----------	----------
Name of internal examiner I	signature	date
Mr. Mesfin J	----------	----------
Name of internal examiner II	signature	date
----------	----------	----------
SGS Approval	signature	date

Hawassa University, Hawassa, Ethiopia

April, 2021

ADVISOR'S APPROVAL SHEET

This is to certify that the thesis entitled "'**Assessment and enhancement of the transient stability of DFIG based wind farm using ANFIS**" submitted in partial fulfillment of the requirements for the degree of master's with specialization in **Power System and Energy Engineering**, the graduate program of the Department/School of Electrical and Computer Engineer, and has been carried out by **Tesfaye Belay Mengistu ID No- PGPOsyR/008/11**, under my/our supervision. Therefore, I/we recommend that the student has fulfilled the requirements and hence hereby can submit the thesis to the department.

Advisors:

Dr. Baseem Khan (PHD) ---------- ----------

Advisor signature date

Issaias Gedey (MSc) ---------- ----------

Co-advisor signature date

Hawassa University, Hawassa, Ethiopia

April, 2021

Declaration

I hereby declare that the thesis ‘’Assessment and enhancement of the transient stability of DFIG based wind farm using ANFIS (Case Study Adama II wind Farm)’’ is my unique work and has not been presented for a degree in any other university, and all source of materials used for this thesis has been duty acknowledged.

Name:-Tesfaye Belay

Signature: _____

This thesis has been submitted for examination with my support as a university advisor.

Advisor:

Dr. Baseem Khan (PHD)

Signature: _____

Co-Advisor

Issaias Gedey (MSc)

Signature: _____

HAWASSA, ETHIOPIA

April, 2021

Acknowledgments

Primarily, praise and thank God, the Almighty, for His showers of blessings throughout my effort to complete the thesis effectively. This thesis is finalized with a prayer of numerous and the love of my family and friends. However, few persons that I would like to particularly acknowledge and extend my heartfelt gratitude to have made the completion of this thesis possible. With the biggest contribution to this thesis, I would like to thank my advisor Dr.Baseem Khan (Ph.D.) had given me his full support in guiding me with inspiring suggestions and reassurance to go ahead in all the time of the thesis. I would also like to thank co-advisor Mr. Issaias.Gedey (MSc) for his kind support during this work. Also, I would like to extend my thanks to Mr. Mesfin Fanuel, ahead of the electrical and computer engineering Department, for providing us with the adequate infrastructure in carrying the work. I am also thankful to Mr. Issaias Gedey Coordinator, Power stream department, for the motivation and inspiration that triggered me for the thesis and to the Adama II wind farm staff, for providing me all the materials and required data for my thesis.

Next, I would like grateful thank to the School of Electrical and Computer Engineering staff, especially all Power Engineering staff for their positive attitude to do this thesis.

Last but not the least; I would like to thank my family for giving birth to me in the first place and supporting me spiritually throughout my life and all the persons who have supported me to finish the thesis work directly or indirectly.

Abstract

Wind power is the greatest existing and used form of renewable energy in the world. Mixing the different wind farms to the national grid introduces new challenges regarding power system stability, among power system stability concerns; transient stability is one that significantly affects the grid. The objective is to assess and enhance the transient stability of DFIG based on wind farms, to model PI control for speed and slip control generator, to improve transient stability using thyristor control series capacitor (TCSC), to conduct during pre-fault, during fault, and post fault conditions. The methods to gathering data are through review of different papers, by asking the site workers, preparing questions for the worker, and from nameplates of equipment. The result consists of four conditions, the first condition is pre-fault conditions, the systems have no disturbance, the second condition is during a fault condition, all systems are disturbed, the third condition is posted fault conditions in this systems have no disorder and the fourth is the improvement of the systems by using TCSC, TCSC is injecting reactive power to the fault area and remove the fault from the systems or back to normal operations. Generally, stability has contained three scenarios pre-fault, during the fault, and post-fault condition. In Matlab Simulink, the pre-fault and post-fault have no disturbance, but during fault conditions, the systems disturbed and the disturbed systems are solved by TCSC at the improved conditions of the systems.

Keywords: - ANFIS; DFIG; PI; TCSC; Wind turbine

Table of Content

List of Table

List of Figure

List of Abbreviation

AC	Alternating Current
ANFIS	Adaptive neuro fuzzy interference systems
ANN	Artificial neuro fuzzy interference Systems
CCA	Critical Clearing Angle
CCT	Critical Clearing Time
DC	Direct Current
DFIG	Double fed induction generator
DSTATCOM	Distribution STATCOM
ELD	Economic load dispatch
ESS	Energy storage Systems
FACTS	Flexible alternator current transmission systems
FLC	Fuzzy Logic Controllers
GSC	Gird side Converter
HAWT	Horizontal Axis Wind Turbine
IGBTs	Insulated Gate Bipolar Transistors
LVRT	Low Voltage Ride Though
MATLAB	Matrix Laboratory
PID	Proportional integral derivative
PMSG	Permanent magnet Synchronous Generator
PSCAD	Power System Computer Aided Design
PSO	Particles swarm Optimizations
RSC	Rotor side converter
SCADA	Supervisory Control and Data Acquisition
SSSC	Static Synchronous series compensations
STATCOM	Static synchronous compensator
SVC	Static Var compensator
TCSC	Thyristor controlled series capacitors
TRASI	Transient rotor angle stability index
TSAT	Transient security analysis tool

TSAI	Transient rotor angle stability index
TSI	Transient stability index
UPFC	Unified power flow control
UPQC	Unified power Quality controllers
VAWT	Vertical Axis Wind Turbine
VFC	Variable frequency control
VSC	Voltage source converter
WE	Wind energy
WECS	Wind energy conversion systems
WF	Wind Farm
WPP	Wind Power Plant
WT	Wind Turbine
WTG	Wind turbine generator

List of Symbol

C_1	Positive Sequence capacitor
C_0	Zero Sequence capacitor
X_m	Magnetizing reactance
V_b	Base voltage
L	length of transmission line
S	Apparent power
R_1	Positive Sequence resistance
R_0	Zero Sequence resistance
L_1	Positive Sequence inductor
L_0	Zero Sequence inductor
t_c	Time clearing fault
δ_c	Angle clearing fault
Q_m	Magnetizing reactive power
Q_r	Reactive power of rotor
Q_s	Reactive power of stator
V_r	Rotor voltage
V_s	Stator voltage
E	Energy
MVA	Mega volt amperes
MW	Mega Watt
P	Power
V	Wind speed
η	Efficiency

Chapter One

1. Introduction

1.1.Background

Electrical power is a widely used form of energy for our community such as for home, industry, government and non-government work area s and another service; energy source are categorized into two forms, a renewable and nonrenewable energy source. The renewable energy source is recycled form of energy such as hydropower, solar, wind and etc and non-renewable energy source is non-recycled energy form such as coal, petroleum, natural gas and etc in [1].

Ethiopia has used large hydropower plants when compared to the wind power plant. Adama II wind power plant is one of Ethiopian wind energy is used now which located about 7 km from Adama and 95 km from Addis Ababa, at elevations of 1741~2173 m. At the middle of the environmental position of the wind power plant is 39° 12' 10" E, 8° 34' 18" N. at the ground surface of the wind. It is a good site for wind power plants in [2]. The site is located near Great Rift Valley.

Ethiopia has been large wind power potential. According to data, the capability ranges from 2005MW -18645MW at a wind speed of 7.5~8.8m/s and more than 8.8m/s at 50m height of the tower. This shows that there is a good condition to construct a wide scale wind power plant. Technically, wind energy can be the second best important resource next to hydropower power generation in Ethiopia. As wind energy is renewable unpolluted energy with short assembly periods, it has the substantial advantage of rapid results. Thus, Ethiopia electric power cooperation (EEPCO) has scheduled to use wind power plants to respond to the lack of electric power in [3].

Wind energy is defined as the change of wind to produce electricity. A generator can translate mechanical power into electricity. There are two kinds of wind turbine arrangements used to convert wind power to electricity, that is horizontal axis wind turbines (HAWT) and Vertical axis wind turbine (VAWT). Wind turbine categorized into two depends on the speed that is variable speed and fixed speed wind turbine generators in [4]. The best common variable speed wind turbines are double fed induction generator wind turbine (DFIG WT) and permanent magnet synchronous generator wind turbine (PMSG WT). Double fed induction

generator (DFIG) is a generating principle widely used in a wind turbine for variable wind speed and it's based on the induction generator through a multiphase wound rotor and multiphase slip ring assembly with brushes for contact to the rotor winding. A Permanent magnet synchronous generator (PMSG) is a generator when the excitation field is provided through a Permanent magnet in place of a coil. The term synchronous mentions here the fact that the rotor and magnetic field rotate at the same speed. The influence of wind energy on the dynamic performance of power structures throughout different operation conditions with wide penetration on the grid will be studied. At last, the study of the impact of WE on power system transient stability has become a very significant matter. The variable frequency converter (VFC) protections of rotor side converter (RSC) and grid side converter (GSC) coupled by interconnected to Dc link capacitor. The VFC regulates the reactive and active power of the generator and accomplishing quick dynamic reply through short harmonic distortion and control only a very little fraction (25-30%) of the whole power in [4]. Wind power predicting is Unpredictability, intermittency, and non-displaced features of WPPs can cause a stability problem. A supplementary exact estimate model of wind farm not only accelerates the combination of wind power to the grid but also prepares the power systems works by delivering climate warnings, thus enhancing stability. Wind power predicting methods are categorized into three, Physical Approach, Statistical Approach, and Learning Approach. Learning Approach is the latest method of wind forecasting.

1.2.Power Systems

Power systems today more complex systems through hundreds of generation and load midpoints being connected via transmission lines. The power system can be characterized into four stages: i) generation, ii) transmission iii) distribution and iv) utilization (load). The basic arrangement of power systems is shown in the figure below. Power system contains renewable energy source and nonrenewable energy sources. The wind is one of the renewable energy sources.

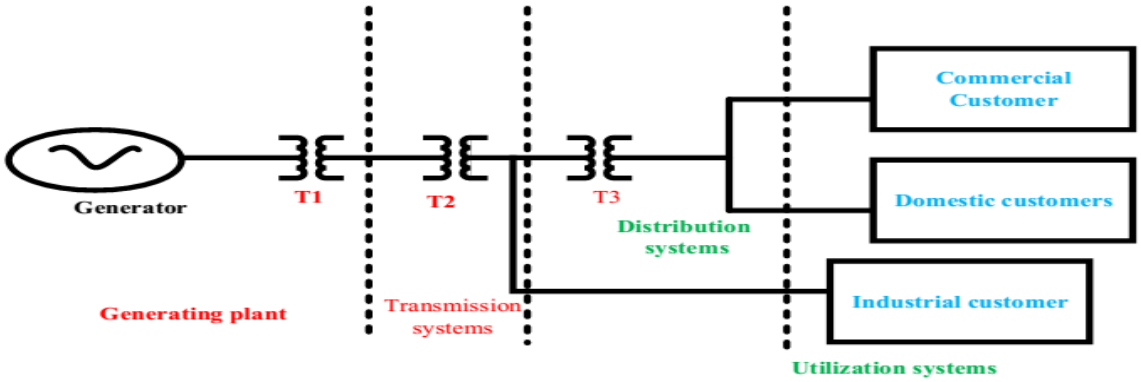

Figure 1-1 Structures of power systems

Power system is an extremely nonlinear scheme that works in a regularly varying environment; generator outputs, loads, topology, and key operating parameters variation continually.

1.3.Power System Stability

Power system stability is a capacity to back to usual or steady working situations later having been endangered to some form of disorder. Stability is directed at the planning level when new generating, and transmitting facilities are developed in [5]. Three kinds of stability are there:-

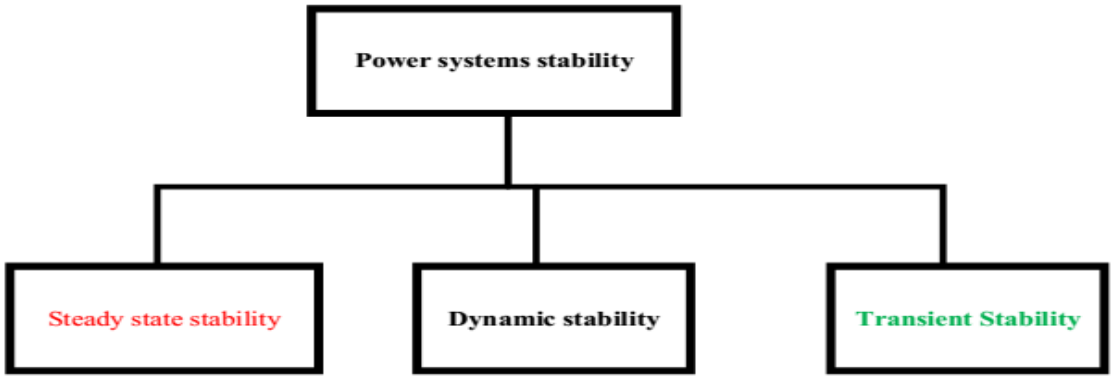

Figure 1-2 Power system stability

Steady state stability:-

Steady state stability is the ability of the power system to maintain its initial condition after small changes or to reach a condition very close to the original one when the fault is still present.

Dynamic stability:-

Dynamic stability is focus on the response to minor instabilities that happen on the system, generating alternations.

Transient stability

Transient stability is dealing with a capacity of a power system to keep constant when exposed to a huge or severe disorder such as loss of generator, loss of load, or a transmission line fault in [4].

1.4.Statement of the Problem

Double fed induction generator (DFIG) becomes one of the most popular generators in variable speed wind turbines. DFIG has advantages of low weight, high efficiency, and low cost. Therefore, one of the main problems is sensitivity to any grid faults. The DFIG is very sensitive to any grid disturbance due to grid fault. High current will pass through the stator and rotor winding, stability problem, and a very high DC voltage would be induced in the converter circuit. During grid disturbance, it's subjected to stability problems such as wind turbine generators outages, loss of rotor angle, and loss of loads, or transmission line fault. Thyristor control series capacitor (TCSC) is a flexible alternator current transmission systems (FACTS) device essential to inject the amount of reactive power based on fault power to the cluster to remove the faults. Adama II wind farm is utilized DFIG for power generation and has been used capacitor bank for their systems but even through the problems under fault condition will there.

1.5.Objective

1.5.1. General Objective

The main objective of this thesis is Assessment and enhancement of the transient stability of a double-fed induction generator based on a wind farms using ANFIS.

1.5.2. Specific Objectives

- To model controller speed of the rotor using a PI, in order to stabilize rotor speed and slip of the generator.
- To show input/output characteristics of systems using ANFIS.
- To improve the transient stability of the systems using TCSC device.
- To conduct systems during pre-fault, during fault, and post-fault conditions of the grid.

- To conduct faulty system with MATLAB/SIMULINK.

1.6.Scope of the thesis

Scope of thesis will be presented like the observed wind climate; the Wind Atlas and also the reposition of the wind turbine generators for better power output are the kind of results. The restriction of wind energy is that no electrical power generated when the wind speed low. The main scope of this thesis deals with the mathematical calculation of transmission line parameter, and Transient stability analysis, designing of PI controllers, and enhancement of the transient stability of DFIG grid connected control schemes. The analysis is done by taking the DFIG based wind energy of Adama II a case study to investigate the enhancement of the transient stability of DFIG and it will simulate by using MATLAB/SIMULINK software under various operating conditions.

1.7.Significance of the study

This work provides important insight into potential improvements to the studied wind farm and can be used as an input for other existing wind farms and for those which are under construction. It also helps to:

- ✓ Understand the operational challenges of a power system containing a large wind farm.
- ✓ Evaluate the possible solutions for improved performance of grid connected wind farms, and comply with grid connection requirements (grid codes).
- ✓ Investigate the applicability of FACTS devices in improving dynamic performance of wind farms.
- ✓ It is significantly the good performance of wind turbine Systems.

1.8. Motivation of this Thesis

The major issues during grid interconnection are severe loss of generator, loss of load and transmission line due to grid fault; high current will pass through rotor and stator winding, sudden wind gust, grid abnormality (voltage sags and voltage swell), frequency variations and also very high DC voltage would be induced current on converter circuit and the DFIG windings. Thyristor controlled series capacitor (TCSC) is a flexible AC transmission system that is essential to avoid the disconnection of the cluster from the grid during fault conditions and protect the other cluster from the dangerous effect of the

electric fault. The main motivation for choosing a TCSC is FACTS device in a wind farm is its ability to provide fast and inject reactive power support at PCC either by supporting or absorbing reactive power into the system. The proposed system is applied on the Adama II wind farm in Ethiopia as a case study.

1.9. Outline of this thesis

The thesis is classified into five chapters. Chapter one includes an introduction, background, power systems, and power systems stability, and problem statement, objective of the thesis, scope, significance, and motivation. In the second chapter, Literature reviews, the basic theory regarding the thesis. Chapter three covers methodology, Introduction to DFIG, discus different controllers, etc. Chapter four is the result and discussion. At the last, chapter five is conclusions, recommendations and future Work of a thesis.

Chapter Two

2. Literature Review

2.1.Introduction

The wind is one of the most widely used non-conventional sources of energy. The majority of wind farms use a variable speed wind turbine generator (WTGs) equipped with a double-fed induction generator due to their benefits over other WTGs and it investigates the effects of different faults on transient stability. The analysis is done on a 6-bus test system during transient fault and loss of excitation in the synchronous generator. The stator flux-oriented vector control method used for both stator and rotor side converter (RSC) is planned to mitigate the DFIG influence on the system's stability. The speed control is performed through a slower electromagnetic torque control in partial load conditions. The speed control is considered for reasonable pitch angle control and the fault simulation using the Neplan program, by considering different fault disturbance natures in [6].

Wind energy conversion system (WECS), the wind energy is converted into mechanical energy in a turbine by aerodynamic principle and again converted into electrical energy in the generator by the principle of electromagnetic induction. Based on the Betz limit, the wind turbine has no convert more than 59.3% of the kinetic energy of the wind into mechanical energy. Maximum power point tracker (MPPT) Controller is designed to use the minimum power extracted from the wind efficiently. The rotor speed is controlled according to the variation of wind speed by using Adaptive Neuro-Fuzzy Inference System (ANFIS) based MPPT. The doubly-Fed Induction Generator is the machine uses widely in Wind Energy Conversion Systems in [7].

The stability of the control grid is a critical precondition for safe and efficient power system service. A correspondingly aggregated double-fed induction generator (DFIG) powered through a gearbox analogy with an equally aggregated wind turbine (WT) regulates the operating output of the wind farm. A proportional–integral–derivative controller (PID) established damping controller, PID with Fuzzy Logic Controller (FLC), and an adaptive network-based fuzzy inference system (ANFIS) controller of the proposed STATCOM is intended to add enough damping properties to the controlling modes of the studied system during diverse working circumstances. The STATCOM is suggested and is attached to the

system's PCC to provide suitable reactive control. For the STATCOM, a PID damping controller was developed using a unified approach focused on modal regulator theory to delegate the studied Synchronous Generator (SG)'s mechanical mode and exciter mode in [8]. Double fed induction generator has a wound stator that consists of three copper windings through a 120° spatial offset in generators with two poles although those with four poles have six windings at 60° offsets. The stator is linked, either directly or through a transformer based on the level of voltage output in relation to the grid voltage. Accordingly, it presents a brief introduction of the DFIG on the wind energy conversion systems (WECS) cover its operation, construction, merits, demerits, modeling, control types, levels of faults, their proposed solutions, and finally simulation. The doubly-fed induction generator (DFIG) in a WECS is a well-recognized technology, has been used in wind power generation for some years, and having a great world market share due to its many advantages in [9].

Static Synchronous Compensator (STATCOM) is a flexible AC transmission systems (FACTS) device that has the ability to absorb or inject fastly the reactive power with power grid entirely through means of electronic processing of the voltage and current waveforms in a voltage source converter (VSC) and it provides an optimized STATCOM control for wind electric generators. The transient behavior of fixed-speed wind farms can be enhanced by inserting large amounts of reactive power during fault recovery. When integrated into the power system, large wind farms pose stability and control matters. Therefore, it will provide the use of a Static Synchronous Compensator (STATCOM) along through wind farms to stabilizing the grid voltage after grid-side instabilities such as a momentary trip of a wind turbine, three-phase short circuit, and fault sudden load changes, FACTS devices are power electronics-based reactive Compensators that are connected to a power system and are capable of enhancing the power system transient performance and the quality of supply in [10].

The increasing penetration of wind energy to the conventional power system due to the fast growth of energy demand has led to the concern to different wind turbine generator technologies. These papers emphasize improving the transient instability (TS) of a permanent magnet synchronous generator (PMSG) established on a power system during three-phase fault conditions using FACTS devices. In fault conditions, the frequency of the power system

reduces and eventually leads to speed differences among the grid and the interconnected wind generator. Under the revision of an international electrical and electronic engineering (IEEE-14) bus system using PSAT as a simulation tool, the integrated critical clearing time through a PMSG-based wind turbine is improved through three self-regulating FACTS devices such as UPFC, STATCOM, and TCSC. In each case, the CCT was stated and the improvement time was recognized in [11].

Doubly-Fed Induction Generator (DFIG) systems control and widely used in the wind turbine system because of their advantages over other types of generators, such as working at different speeds and not requiring continuous maintenance. The responses of different types of faults have been presented like; two lines to ground faults and three lines to ground faults at different working conditions. Faults are connected to three proposed controllers; the first controller is the Proportional-Integral (PI), the second controller is PI-controller established on Particle Swarm Optimization (PI-PSO) method and STATCOM. The location of (STATCOM) is improving the system stability leads to enhance all the elements of power equality of the grid for the both abnormal and normal condition in [12].

The Unified Power Quality Controller (UPQC) device is a combination of a series active filter and a shunt active filter and utilizes the UPQC to improve the low-voltage ride-through (LVRT) capability of the doubly fed induction generator (DFIG)-based wind energy conversion system (WECS) according to the grid connection requirement. The key purpose of a UPQC is to compensate for reactive power, voltage flicker, and harmonics. It has the ability to improving power quality at the point of installation on power distribution systems or industrial power systems. The unified power quality controller (UPQC) is applied to a wind energy conversion system employing a doubly fed induction generator to enhance the low voltage ride- through of the system during a three-phase ground fault in [13].

The scheme is a part of wind power in order to on-grid to the electrical power grid system. In this work, wind turbine driven is via DFIG which feeds ac power to the distribution network and has described the control scheme of doubly-fed induction generator (DFIG) wind energy conversion system using the ANFIS approach. The wind turbine driven through double fed induction generator is a part of a distributed generation that feeds AC power to the distribution network. In order to study the performance of the ANFIS controller, the different

abnormal conditions are examined even the worst case. The Simulation results indicate the good performance of the ANFIS control unit as stability of wind power system and enhancing power quality in [14].

FACTS devices are available that use power electronic components provide efficient solutions for improving power quality in Distribution network. The discussion is performance of three FACTS devices static synchronous series compensation (SSSC), distribution Static synchronous compensator (DSTATCOM), and Unified Power Quality Controller (UPQC) for mitigating voltage swells, sags, and harmonics injected into a DFIG based WECS. Integration of a wind farm with an electric grid is an issue that has gained attention due to poor power quality and unbalance power and frequency of the grid. Maintenance of power quality has become a significant factor in modern power systems in [15].

The fuzzy controllers are used for providing optimal proportional and integral gains under various operating conditions. The observation was the considerable improvement of the damping ratios of DFIG-based wind generation under all operating conditions especially, at medium wind speed and at weak grid strength. Fuzzy logic-based controllers for DFIG established wind turbine systems integrated into the infinite bus system have been recognized. Small signal analysis founded on system equations' linearization in the operating point's region has been used for the identification of low-frequency oscillations. The fuzzy logic controllers provide optimum proportional and integral gains under various operating conditions namely wind speed and grid strength in [16].

The study of the performance of Squirrel Cage Induction Generators (SCIG) wind farm, Double Feed Induction Generators (DFIG) wind farm, and a combined wind farm (CWF) during three-phase grid fault. Since the CWF is a combine of equal number of DFIGs and SCIGs, it incorporated the main advantages of both types of generators. Definitely, the SCIG has a little price, but its drawback lies in its negative impacts on system stability, especially when it operates without a shunt compensator. On the other hand, the DFIG, though more expensive, is better able to keep the stability of the system. The SCIG and DFIG wind farms are equipped with SSSC controllers to regulate the active and reactive line power flow. The outcomes of a comparative study of DFIG and SCIG wind farms with SSSC and integrated to wind farms without SSSC during a three-phase grid fault. In this case, the SCIG wind farm

suffers from a severe decrease in voltage at PCC subsequently with the fault occurrence until it reached zero before fault clearance and also, it can be observed that the CWF voltage at PCC during the fault period is greater than the voltage of DFIG wind farm without SSSC although the voltage of DFIG wind farm with SSSC is oscillated more in [17].

Table 2-1 Comparison of literature review

Author	Title	Methods	Advantages	Disadvantages
Akpeke, Muriithi and Mwaniki, et al., 2019 [11]	Contribution of FACTS Devices to the Transient stability improvement of a Power System integrated with a PMSG-based Wind Turbine	FACTS device like TCSC, UPFC, and STATCOM	Higher efficiency when compare to other wind turbine technologies	disconnecting wind farms from the grid at under fault conditions
Eskander et al., 2015[13]	Superiority of LVRT of Grid Connected Wind Energy Conversion System Using Unified Power Quality Controller	Using Unified Power Quality Controller	Reduce maintenance cost Fast recovery after fault.	High harmonic content. Increasing rotor speed.
Chowdhury et al., 2015 [20]	A review on transient stability of DFIG integrated power system	PI controller	Faster dynamic response with low harmonic distortion.	During fault DFIG disconnecting from the grid. Less efficiency.
Soued, Ramadan and Becherif, et al., 2019[6]	Effect of double-fed induction generator on transient stability analysis under different fault conditions	Crowbar	To protect DFIG-RSC from faults.	The total efficiency is low. There is no grid protection
Rashad, Kamel and Jurado, et al ., 2018 [17]	Stability improvement of power systems connected with developed wind farms using SSSC controller	SSSC	Low cost for SCIG. To control active and reactive power flow lines.	Negative impacts on power systems stability. less efficiency

Research Gap

Different researchers are proposed different methods used to improve power systems stability such as DVR, Crowbar protection, and FACTS devices and used different controllers but to keep the grid or wind farm cluster from the fault using FACTS devices better. The main problems of the papers in wind power plant has a problem when wind connected to the grid such as power quality problems like voltage sags, voltage swell, voltage dips, etc. power systems stability such as lack of wind speed makes generator outages due to generator outage loss of load occurs at the grid. The capacity of power generating is reduced so that to improve or enhance the systems using TCSC. Especially for transient stability improve TCSC is better performance to control when compared to other FACTS devices. In this thesis a case study of 153MW, Adama II wind farm is presented which consists of 102 DFIG based wind turbines each unit have 1.5 MW connected to the grid.

Chapter Three

3. Methodology and System Modeling

3.1.Introduction

The first step towards processing this thesis is started with reviewing the different papers, where all the theoretical information regarding the Assessment and enhancement of the transient stability of double fed induction generators regarded to wind farm using ANFIS are gathered and a comparison of previous similar research is studied. The work of different authors has been reviewed under literature review. Then the total task of data collection was accomplished through;

- ✓ From recorded datasheet and equipment-name plate
- ✓ By interviewing people working on the site and
- ✓ Through prepared questions

This work will discuss the assessment and improvement of the transient stability of DFIG based wind farms use ANFIS of Adama II wind farm to break associated through grid under three phase fault conditions. Previously wind turbine is disconnected during the fault conditions.

Enhancement Ways

Most researchers did on the improvement of low voltage ride-through capability of DFIG wind farm based on the wind turbine. The researcher did or problem identification is power quality problem like voltage swell, voltage sag, voltage dips wind turbine outages and frequency variations. That researcher was used a dynamic voltage regulator (DVR) and crowbar protection for improving low voltage ride through wind turbine and controller used PI, FLC, and ANN, but, the drawback of those devices were only used for single wind turbine and it is more prices in those researchers. When we come to my research the problem is regarding transient stability is concentrated to faults, large disturbances, generator outages, and loss of load at the grid. The problem is regarding generator outage, load decreases, or generally a fault at wind farm cluster. So that, in order to remove a fault from a wind farm cluster using FACTS is better when compared to another method to improve transient stability. There are different FACTS devices such as STATCOM, SSS, D-STATCOM, TCSC and etc. For transient stability improve TCSC is better performance when compared to other

FACTS devices. In this case, TCSC is connected to the grid in order to serve all clusters, when a fault occurs TCSC is injecting into every cluster faulted in order to remove the fault from the cluster. This means TCSC is connected on the point of common coupling or it is connected to the grid whatever the disturbance occurs for every wind turbine line by injecting reactive power to the line to improve the disturbance.

3.2.Double Fed Induction Generator Modeling

The overall arrangement of double-fed induction generators established WT has presented in the Figure 3 1. DFIG contains WT, gearbox, a wound rotor induction generator, back-to-back converter, and their controllers. The induction generator stator is directly linked to the grid; however, the rotor is fed through a back-to-back Voltage source converter. Crowbar is needed during grid faults to keep the RSC after overcurrent in the rotor circuit.

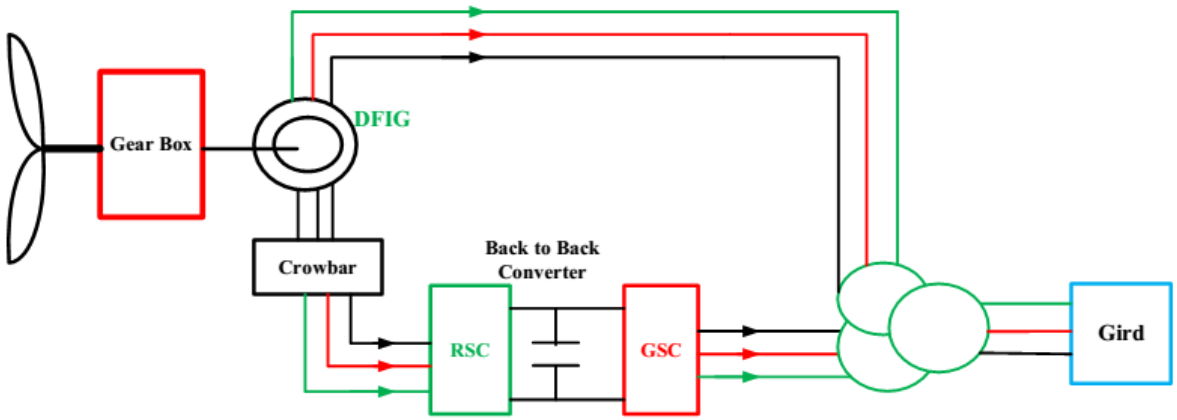

Figure 3-1 Modeling of DFIG with a crowbar [18]

DFIG shares common of the market related to other variable speed wind generators as shown in the figure below the stator is straight organized to the grid and the rotor and the rotor through a bidirectional converter. The vector control method is needed for decoupled functions of real and reactive power. RSC attracts the DFIG and GSC brings/absorbs the active power to/from the grid.

Reactive power drawn through DFIG is taken as:

$$Q_m = \frac{3V_s^2}{2X_m} \quad (3.1)$$

$$Q_s = Q_m + \frac{Q_r}{s} \quad (3.2)$$

Q_m Reactive power for magnetization of DFIG, V_s stator voltage, and Xm is a magnetizing reactance. Q_sAnd $Q_r$is a reactive power of the stator and rotor correspondingly. S is a slip of the generator in [18]. The unit working of the Power factor is essential below normal situations, Qs=0.

- ✓ The control of RSC accepts two mention signals; torque essential for removing maximum power and reactive power wanted for the unity power factor functions of DFIG
- ✓ The GSC control takes the set-points for DC link voltage and reactive power the DFIG can be linked to the low grid without dropping its stability.

3.3. Objective function

Improve DFIG in the grid-connected systems is mainly to minimize power losses, minimize price and maximize the stability and reliability of the systems.

3.3.1. Cost analysis of TCSC

Construction of new transmission lines is hard for environmental political causes. Hence, the power transmissions are motivated closer to their restrictions endangering the system security. The techniques needed for optimal placement and setting of FACTS device can be approximately categorized into two methods: [19]

i) Index-based methods: - the precedence list is made to decline solutions space created on feeling indexes with detail to each line and bus.

ii) Optimization-based methods: - needed either conventional or heuristic optimization approaches such as simulated support, Tabu search, or Particle swarm (PSO).

The range of cost of FACTS devices is obtainable in Siemens AG Database. A polynomial cost function of FACTS devices is resulting and used for FACTS allocation study as in. The investment costs of TCSC

$$C_{TCSC} = 0.0015S_{TCSC}^2 - 0.713S_{TCSC} + 153.7 \quad (3.3)$$

From the formula above we can calculate the cost of TCSC can be as follows and in the Simulink result from figure 4-49 reactive power produced by TCSC is 17MVar in the improvement conditions.

$$C_{TCSC} = 0.0015 \times (17 \times 10^3)^2 - 0.713 \times 17 \times 10^3 + 153.7 \frac{\$}{kVar} = 573.08 \frac{\$}{kVar}$$

The overall investment cost of TCSC if the wind turbine works for 12 hours.

$$\mathrm{IC_{TCSC}} = \left(\frac{\mathrm{C_{TCSC} * S_{TCSC} * 1000}}{\text{time of the year in hours}}\right) \$/\mathrm{Year} \quad (3.4)$$

If the wind turbine works for 16 hours in one day, in the years it works about 5840 hours. Then the overall investment cost of TCSC is calculated as:

$$\mathrm{IC_{TCSC}} = \left(\frac{573.08 * 17 * 1000}{5840}\right) \$/\mathrm{Year} = 1668.2 \frac{\$}{year}$$

Year of back payment $= \frac{1668.2 \frac{\$}{year}}{573.08 \frac{\$}{kVar}} = 2.91 year$

3.4.Modeling of Adama II Wind Farm

The power system modeling, Adama II wind farm, for transient stability analysis in Matlab Simulink has been certain as a case study. The installed capacity of the wind farm is 153MWand individual wind turbine generates 1.5 MW. It takes 102 turbines and clustered into eight clusters. Each individual wind turbine generator (WTG) is connected to a 690 V bus. The wind turbines are connected through 33kV underground cables and overhead transmission lines of different lengths and capacities conditional on the location of each unit and the distance to the 33 kV collector bus. The combination is developed than a WPP via 102 wind turbines into a single turbine model has been made and the model has been verified with transient stability analysis.

3.4.1. Site Description

Adama II wind farm is placed in the middle of Ethiopia as shown in the figure below, approximately 95km east of the capital city, Addis Ababa, and 7km North-West of Adama city at an elevation of 1741~2173m. According to the feasibility study, the central geographical position of the wind park is 39° 12' 10"E, 8° 34' 18" N, and the average wind speed in the area is 9–10m/s. The farm has been used a doubly-fed induction generator (DFIG) type.

Figure 3-2 Location of Adama II Wind Farm [Google earth]

3.4.2. Layout of Adama II Wind Farm

The Adama II wind farm has 102 turbines. Each turbine is attached to a unit transformer that steps up the generator voltage (690 V) into a medium voltage level of 33 kV and all are grouped into eight clusters (cluster A to cluster H). Except one of the clusters that have eleven turbines, while the remaining seven clusters have thirteen turbines each, grouped together and a 33 kV overhead line connects each cluster to the main substation. The high voltage terminal side is connected to the Koka substation with a single 230 kV overhead transmission line. The layout of the Adama II wind farm is shown in the figure below. Cluster is a group of wind turbine that is located at a site to generate electricity.

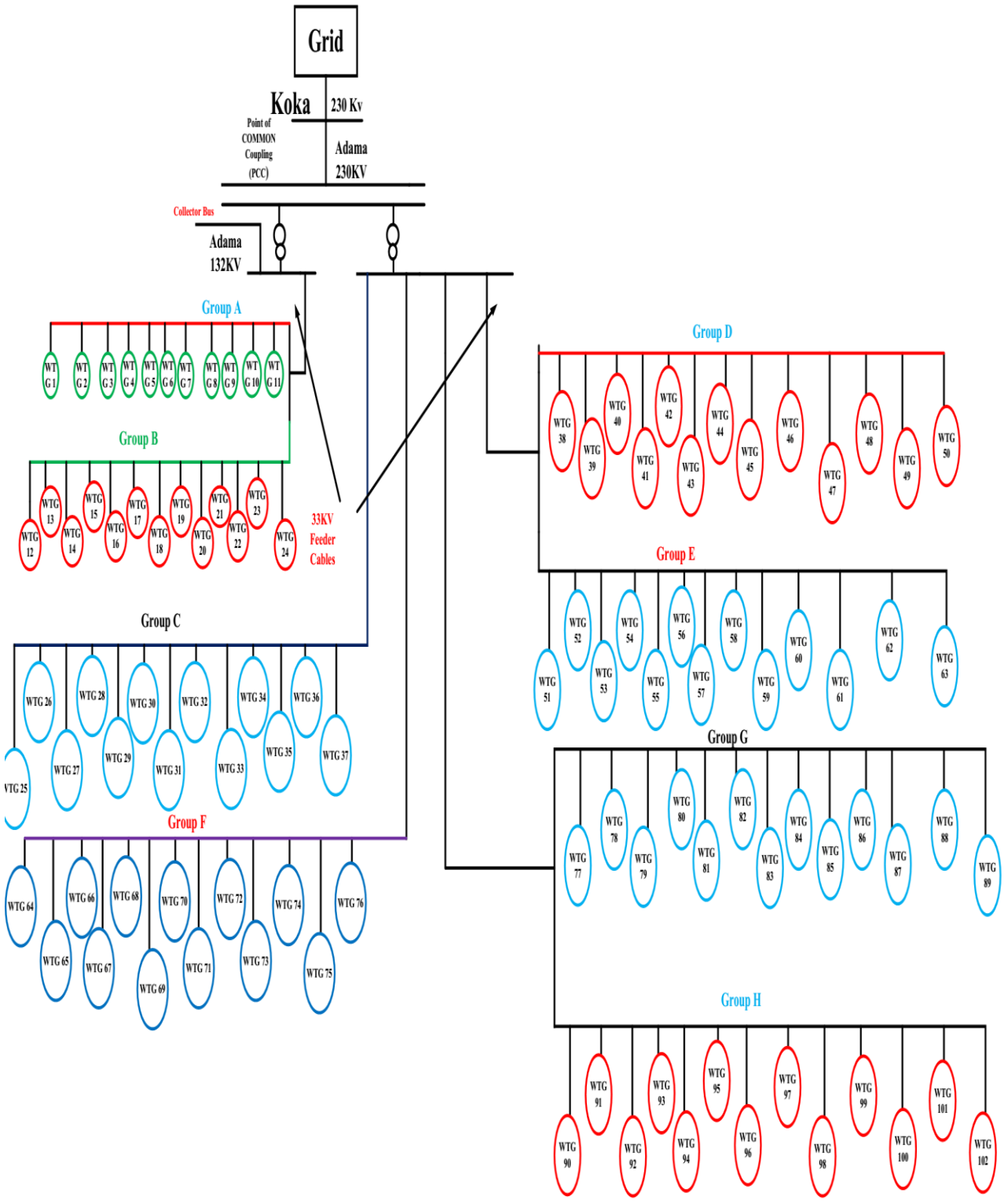

Figure 3-3 Layout of the Adama II wind farm

3.5.Transient stability assessment

Transient stability is the know-how of power systems to remains to a steady working principle later the happening of disorder variation topology. Transient stability assessments of power systems combine through DFIG are classifies into two ways one is the Qualitative assessment and the second Quantitative assessment in [20].

3.5.1. Qualitative assessment

Qualitative assessment is accepted available through seeing post fault formal of diverse double fed induction generator restriction. The constraints are listed below:

i. Rotor angle: once the rotor angle of the generator drops out of phase.

ii. Rotor speed/active power: While the rotor speed/ active power continuously increases without restrictions after the fault happens is called transient stability.

iii. Terminal voltage: Faster repair of generators terminal voltage after the fault takes good confidence on systems stability.

iv. Reactive power: when around a substantial reactive power request on the grid monitored by fault, the systems might smooth since transient stability.

3.5.2. Quantitative assessment

Quantitative assessment is accepted and obtainable by the succeeding transient formal quantity in units such as critical clearing time and critical clearing angles. The CCT is the greatest fault range for which the systems stay transient stable. The CCT is estimated considered from equal area criterion ideas in [20]. Transient rotor angle stability index (TRASI):

TRASI is the relative amount of rotor angle leaving ensuing transient fault is calculated as:

$$TRASI = \frac{360° - \delta_{max}^{Post}}{360° - \delta_{max}^{Pre}} \quad (3.5)$$

Where δ_{Max}^{Post} post max and δ_{Max}^{Pre} is the maximum post fault and per-fault rotor angle conversion in the network with cross ponding to the machine.

The harshness of a contingency and trajectory of the systems behind to disorder can be measured by calculating the transient stability index (TSI). The TSI is accomplished from the transient security assessments tool (TSAT) through investigating the index based on angle margin algorithm taken as:

$$TSI = \left(\frac{360° - \delta_{max}}{360° + \delta_{max}}\right) * 100 \qquad -100 < TSI < 100 \qquad (3.6)$$

Where δmax is the maximum angle existing from any two generators in the systems at the same time in the after fault reply. $TSI > 0$ and $TSI \leq 0$ relate to steady and unsteady situations correspondingly. The TRASI ranges from 0-1. The TSI (h) is calculated as:-

$$\eta = \left(\frac{360° - \delta_{max}}{360° + \delta_{max}}\right) * 100 \qquad (3.7)$$

Where δ_{max} is the maximum Angle

3.6.Comparisons of controllers

3.6.1. Artificial neural network

The artificial neural network (ANN) is a hugely similar arrangement that can study from the knowledge base. The accomplished by plotting a set of one or additional input set off one or more input to a model that can be with a new set of data. There are two types of neural networks, which are dynamic and static. The structure ANN contains three layers that are input layer, hidden layer, and output layer. The hidden layer is linked to the input and output layer through different sets of weights in [21].

Figure 3-4 Blocks of ANN

3.6.2. Fuzzy logic Controller

Fuzzy control is a control scheme constructed on a fuzzy logic calculated system that analog input numbers in relation to logic variables that select on the continuous number between 0-1 indifference to classic or digital logic, which function on discrete values of either 1 or 0. Fuzzy logic is frequently needed in machine controllers. The important making elements of an FLC are fuzzification units, fuzzy rationale thinking units, a study base, and de-fuzzification units in [22, 23].

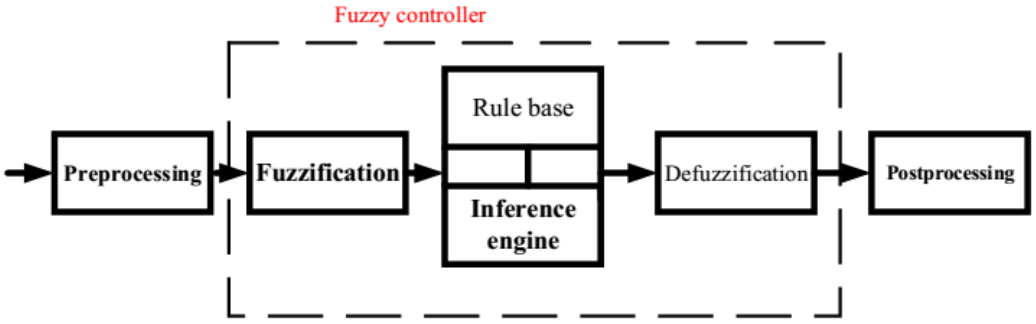

Figure 3-5 Block of FLC

3.6.3. Adaptive neuron fuzzy interference systems

ANFIS is an arrangement of an intelligent system that one of the greatest solutions in data modeling, where it's accomplished of reasoning and learning in an unclear and imprecise environment. It is an arrangement of two or more intelligent technology. This combination is done regularly to overcome single intelligent technologies. The fuzzy system cannot learn or familiarize itself with the new environment, while the ANN is ambiguous to the use. By combining these two methods, the ANN suits more transparent, and the fuzzy system receipts on the ability of learning. It depends on data that learn the rules and membership functions in [21].

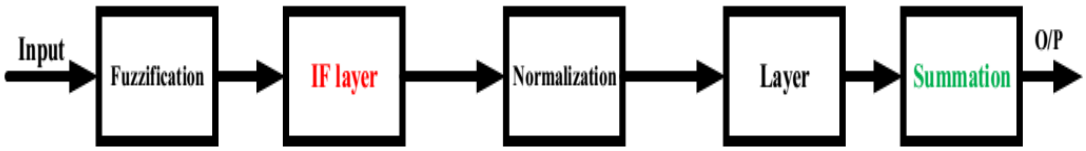

Figure 3-6 Layer of ANFIS

The input/output data stayed fed in the ANFIS models to remove the rule. The 'fuzzification' layer is usual and adjusts the constraints for the chosen membership. Both ANN and ANFIS model were advanced using Matlab.

The goal of an ANFIS is to mix the best features of fuzzy systems and ANNs. The benefits of an ANFIS related to a FIS are as follows:-

- An ANFIS can simulate and investigate the plotting relation between input and output data through a learning algorithm to optimize the parameters of a given FIS.
- A FIS is fully helpless on its membership functions. An ANFIS comprises networks that associate nodes and directional links, and some learning rules are related through these networks.
- The networks learn associations between inputs and outputs. An ANFIS can be skilled without any essential for the adept knowledge frequently essential for the standard fuzzy logic strategy.

Why ANFIS is select

- ❖ The ANFIS combines of the both artificial neural networks and fuzzy inference systems.
- ❖ The ANFIS has the ability to capture the nonlinear structure of a process, adaptation capability, and rapid learning capacity

3.6.3.1.Design of ANFIS based Controller

ANFIS is mixes of the best constructions of FLC and ANN, and it has the possibility to capture the incomes of both in a single framework. ANFIS is a type of ANN that is created on the Takagi-Sugeno fuzzy inference system, which is having one input as done output. By using an assumed data set, the toolbox function of ANFIS constructs a FIS. In order to have an idea of improved ANFIS design for future control, initial data is generated from the typical *PI* regulator and the data is kept in the workspace of MATLAB in [24]. Then the data before saved in the workspace is overloaded in the ANFIS command window to make an enhanced ANFIS architecture as shown in the figure below.

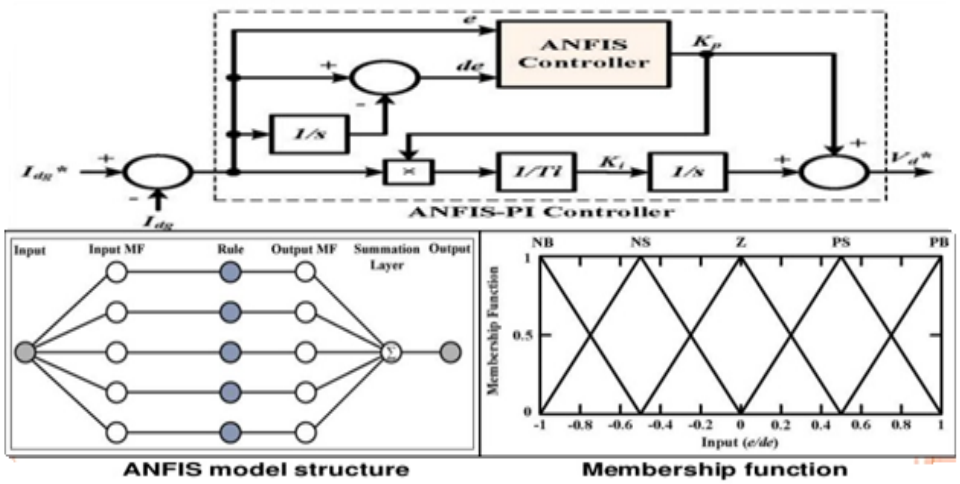

Figure 3-7 Structure of adaptive-neuro fuzzy interference systems

3.7.FACTS Device

The flexible ac transmission system is known as the FACTS device, became in the modern ways of a well-known word for advanced control in power systems through means of power electronic devices. In greatest of the tenders and the controllers are used to escape cost severe or landscape needful delays of power systems, for example like upgrades or additions of substations and power lines. The basic applications of FACTS-devices are: [25]

- Power flow control,
- Growth of transmission ability,
- Voltage control
- Reactive power compensation,
- Stability enhancement,
- Power quality improvement,

FACTS-devices consist of additional radical technology of voltage source converter (VSC) centered on the furthermost of VSC established on the furthermost on Insulated Gate Bipolar Transistors (IGBT) or Insulated Gate Commutated Thyristors (IGCT). FACTS devices are regularly observed as new technology, but hundreds of connections worldwide, particularly of SVC since early the 1970s with a total connected power of 90000 MVar, show the getting of these types of technology.

Table 3-1 Estimated number of installed FACTS devices and total installed power [25]

Type	Total installed power in MVA	Number
SVC	90000	600
STATCOM	3000	20
Series Compensation	350000	700
TCSC	2000	10
HVDC B2B	18000	45
HVDC VSC B2B	2250	1+(12with cable)
UPFC	250	2-3

3.7.1. Comparison of Various FACTS Devices

The TCSC used to control transient stability of systems and UPFC used to control for load flow and voltage control however STATCOM is used for voltage regulator in the small distribution system and the UPFC shows good outcomes of power system stability enlargement related to the other FACTS devices such TCSC, SSSC, and SVC.[26]

Table 3-2 Compare of different FACTS devices

No	FACTS Device	Transient Stability	Dynamic Stability	Load flow	Voltage Control
1	SVC	Low	Medium	Low	High
2	STATCOM	Medium	Medium	Low	High
3	UPFC	Medium	Medium	High	High
4	TCSC	High	Medium	Medium	Low
5	SSSC	Medium	Medium	Low	High

FACTS devices at a suitable place, wherever the reactive power upkeep is wanted the most, are an effective way to raise the voltage stability margin, and a comparison of Facts in terms of Cost can be as follows in [27].

Table 3-3 Comparison cost of capacitors and FACTS device

No	FACTS Controllers	Cost(USD)
1	Shunt capacitor	8/kVar
2	Series capacitor	20/kVar
3	SVC	40/kVar controlled rations

4	TCSC	40/ kVar controlled rations
5	STATCOM	50/kVar
6	UPFC series portions	50/kVar through the power
7	UPFC shunt portions	50/kVar control

3.8.Thyristor controlled series Capacitors

Thyristor-controlled series capacitors (TCSC) delivers powerful rates of monitoring and growing power transfer level of a system by the adjustable apparent impedance of a specific transmission line. Through the use of TCSC, the system will function stably at power levels well beyond those for which the system was formerly made without dropping the stability. TCSC is a parallel LC circuit, containing secure capacitive impedance$X_L(\alpha)$ that is in [23, 28]

$$X_{TCSC} = \frac{X_C X_L(\alpha)}{X_C(\alpha) - X_L} \quad (3.8)$$

Where $X_L = \omega L$ and α is the delay angle measure from the peak of the capacitor voltage.

Thus, TCSC works on the principle of controlling the transmission line impedance by changing its individual reactance X_{TCSC}.

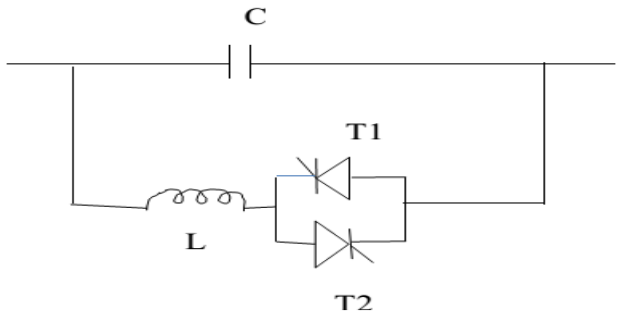

Figure 3-8 Thyristor -controlled series capacitor basic models [28]

The significant benefits of TCSC are listed below:-

i. Growths of dynamic stability of power transmission systems

ii. Improves stability

iii. Rejection of line overloads and decreases of loop flows

iv. Enhancement voltage control and reactive power balance

v. Elimination of sub-synchronous resonance risks (SSR)

vi. Damping of active power fluctuations and dynamic power flow regulator

vii. Minimizing system losses and optimizing load involvement between similar circuits/lines

3.8.1. Operation and control of TCSC

TCSC is a series controller capacitive reactance that can deliver a continuous regulator of power on the ac line terminated a wide range. The thyristor-controlled series capacitors operations are classified into three based on firing angles that is thyristor blocked mode, thyristor bypassed mode, and Veriner or partially conducting modes.

3.8.2. TCSC Model

A TCSC includes continuous time dynamics, rating voltage and current in the capacitors and reactor, and nonlinear, discrete switching behaviors of Thyristors. There are two models of thyristor control series capacitors.

1. Variable reactance model
2. Firing angle model

Some Assumption of models:

i. The transmission system works in a sinusoidal steady-state, with the only dynamics related to generators and PSS.

ii. The variables reactance TCSC model accepts the availability of continuous reactances range and is therefore suitable for multi-module TCSC arrangements.

TCSC has two models; from two models variable reactance model is better for Transient stability studies when associated with the firing angle model. The model of variable reactance is as follows:-

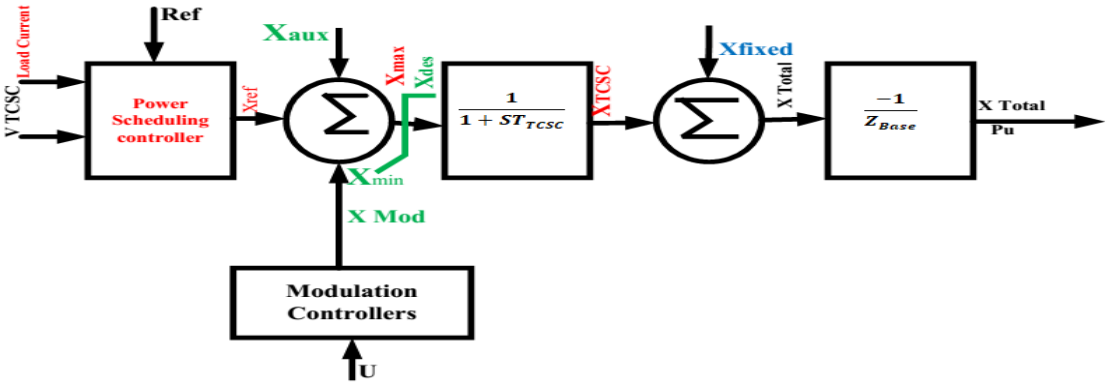

Figure 3-9Block diagram of the variable-reactance model of the TCSC

Where

X_{ref}:- Power scheduling controller based on power flow specification

X_{mod}: - Modulation controller for damping enhancement

X_{aux}: - External power flow controller

X_{des}: -The desired magnitude of TCSC

T_{TCSC}: - Time constant

X_{fixed} : - Reactance of TCSC installation's FC component

X_{ref}: - is generated from a power arrangement controller based on the power-flow requirement in the transmission line. The reference X_{ref}value may also be set directly by manual control in response to an order from an energy-control center, and it essentially represents the initial operating point of the TCSC; it doesn't include the reactance of fixed capacitors (if any). The reference value is modified by an extra input, X_{mod} from a modulation controller for such purposes as damping enhancement. X_{aux}, is can be obtained from an external power-flow controllers. A desired magnitude of TCSC reactance, X_{des} is obtained that is implemented after a finite delay caused by the firing controls and the natural response of the TCSC. This delay is demonstrated by a lag circuit taking a time constant, T_{TCSC} of typically 15–20 ms. The resulting X_{TCSC} is additional to the X_{fixed} , which is the reactance of the TCSC installation's fixed capacitor component

$$Z_{base} = \frac{(kV_{TCSC})^2}{MVA_{sys}} \quad (3.9)$$

Where

kV_{TCSC}: - The rms line to line voltage of TCSC in kilovolts (kV)

MVA_{sys}: - The 3-phase MVA base of the powers system

3.9. Design of Proportional-Integral Controller

The old-style proportional-integral (PI) controller is usually adopted with either stator voltage orientation (SVO) or stator flux orientation. In this PI controller, perfect regulation is only achievable for the DC components, the steady state mistake is zero and a lot of derivatives can be obtained at high frequency terms. There are typically two control plans for the variable-speed wind turbine. Pitch angle regulation is required in situations above the esteemed wind speed when the rotational speed is kept continuous. Based on the general description, the PI controller is adopted in the rotor circuit of DFIG.

The importance of the control can be summarized in three goals:

1. Enhancing the power output while a wind speed is less than rated wind speed

2. Keeping the rotor power at design restrictions while a wind speed is exceeding rated wind speed

3. Reduce the weakness loads of the turbine mechanical components.

In active Proportion-Integral-Derivative (PID) pitch controller, the sensitivity of aerodynamic power to the rotor combined blade pitch angle is negative. With positive control gains, the derivative term will increase the effective inertia of the drive-train. Because of the above reasons I recommend using a proportion integral (PI) controller.

Theoretical technique to compute PI-controller Gain

Change in the pitch angle is:

$$\dot{\beta} = \frac{\beta_d - \beta}{\tau\beta} \tag{3.10}$$

$$\frac{\beta}{\beta_d} = \frac{1}{\tau\beta + 1} \tag{3.11}$$

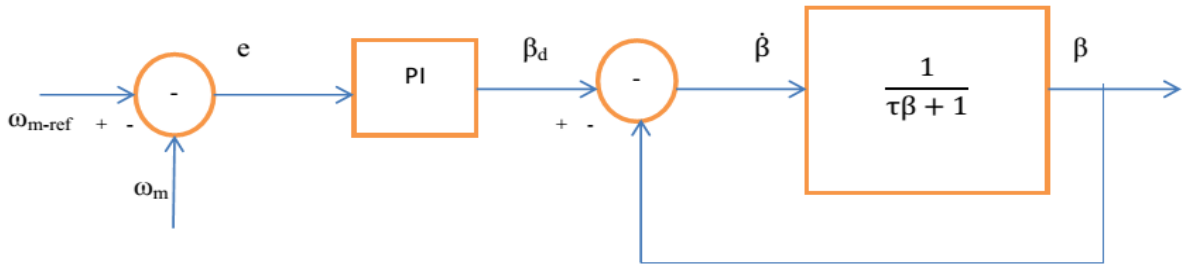

Figure 3-10 PI controller system

The output signal from PI-controller is βd as showing in the figure above, which also contains the actuator‘s transfer function that got from the above equation. The PI-controller and wanted pitch angle can be expressed as follows:

$$\beta_d = K_P e + K_i \int e dt \tag{3.12}$$

Where, $e = \omega_{m-ref} - \omega_m$, ω_{m-ref} is a rated rotor speed (reference generator speed).

To find the solution, let be x

$$x = K_i \int e d_t \; or \; \frac{d_x}{d_t} = K_i e \tag{3.13}$$

$\beta_d = K_{pe} + K_i \int e dt$ And $x = K_i \int e dt$ from this equation, the partial derivatives of βd with respect to e, is expressed as follows

$$\frac{d\beta_d}{de} = \frac{d(K_p e + K_i \int e dt)}{de} \tag{3.14}$$

$$\frac{d\beta_d}{de} = K_p + \frac{dx}{dt} \rightarrow K_p + \frac{K_i e}{de/dt} \quad (3.15)$$

For an adjustable slip asynchronous generator, the variation range of e is very small. Moreover, Kp is far greater than K_i. Equation (above) can be simplified as follows:

$$K_p = \frac{d\beta_d}{de} \rightarrow d\beta_d = \beta_d(\beta_{d0} - \text{initial value}) \quad (3.16)$$

To find the direct relation between β and βd we reduce inner closed loop for the actuator in above Figure above, to the forward path and assuming τβ =1 sec. then we obtain the transfer function:

For fault condition the equations become:

$\frac{\beta}{\beta d} = \frac{1}{\tau_\beta + 1} = \frac{1}{s+2}$ $in\ transient\ state, let\ s = t,\ \frac{\beta}{\beta d} = \frac{1}{s+2} = \frac{1}{t+2} \rightarrow \beta d = (t+1)\beta,$ then $K_p\ and\ K_i$ is as follows

$$K_p = \frac{(t+2)\beta}{\omega_{m,ref} - \omega m} \quad (3.17)$$

$$K_i = \frac{1}{\omega_{m,ref} - \omega m} * \left(\frac{(t+2)\beta}{\omega_{m,ref} - \omega m} - K_p\right) * \frac{\partial \Delta\omega}{\delta t} \quad (3.18)$$

3.10. Load Model

Load refers to a group of devices that consumes energy from the supply lines. The design and operations of the power system are critically influenced by the nature of the load. The following three ways of load model are used in power systems.

I. Constant current model

The constant current model in this model voltage is assumed to vary and the current drawn by the load is constant. So that:-

$$I_1 = I_2 \quad (3.19)$$

For two power systems the constant current mode has two real power means P_1 and P_2 and two reactive power means Q_1 and Q_2can be as follows:

For real power systems:

$$P_1 = V_1 I_1 \cos\varphi_1 \quad (3.20)$$

$$P_2 = V_2 I_2 \cos\varphi_2 \quad (3.21)$$

From equation 3.20 and 3.21 when solve for $I_1\ and\ I_2$ respectively and apply equation 3.19 we get:

$$I_1 = I_2 = \frac{P_1}{V_1 \cos\varphi_1} = \frac{P_2}{V_2 \cos\varphi_2} \quad (3.22)$$

Assumes if $\cos\varphi_1$is equal to $\cos\varphi_2$ is unity the power is:-

$$P_2 = \frac{V_2}{V_1} P_1 \quad (3.23)$$

For reactive power constant current model

$$Q_1 = V_1 I_1 \sin\varphi_1 \quad (3.24)$$

$$Q_2 = V_2 I_2 \sin\varphi_2 \quad (3.25)$$

From equation 3.24 and 3.25 when solve for $I_1\ and\ I_2$ respectively and apply equation 3.19 we get:

$$I_1 = I_2 = \frac{Q_1}{V_1 \sin\varphi_1} = \frac{Q_2}{V_2 \sin\varphi_2} \quad (3.26)$$

Assumes if $\sin\varphi_1$is equal to $\sin\varphi_2$ is unity the power is

$$Q_2 = \frac{V_2}{V_1} Q_1 \quad (3.27)$$

For constant current model power directly proportional to voltage.

II. Constant impedance model

The constant impedance model is the model in which the impedance of the load remains constants.

$Z = \frac{V}{I}$ Is constant (3.28)

III. Constant power model

The constant power model is the model when the power is constant (demand) regardless of voltage. Adama wind farm has eight loads from load A-H. For Power invariance, we have eight loads. We have considered two power invariances$P_1\ and\ P_2$. We divided eight loads into two power systems.

For real Power model

$$P_1 = P_A + P_B + P_C + P_D \quad (3.29)$$

$$P_2 = P_E + P_F + P_G + P_H \quad (3.30)$$

$$P_1 = P_2 \quad (3.31)$$

When apply equation (3.31) for all clusters we get:

$$P_A + P_B + P_C + P_D = P_E + P_F + P_G + P_H \quad (3.32)$$

Where $P_A, P_B, P_C, P_D,\ P_E,\ P_F, P_G\ and\ P_H$ are real powers of the wind farm from cluster A up to cluster H.

The real power one and two is:-

$$P_1 = V_1 I_1 \cos\varphi_1 \quad (3.33)$$

$$P_2 = V_2 I_2 \cos\varphi_2 \quad (3.34)$$

When apply equation (3.31) for all clusters we get:

$$V_1 I_1 \cos\varphi_1 = V_2 I_2 \cos\varphi_2 \quad (3.35)$$

For reactive Power model

$$Q_1 = Q_A + Q_B + Q_C + Q_D \quad (3.36)$$

$$Q_2 = Q_E + Q_F + Q_G + Q_H \quad (3.37)$$

$$Q_1 = Q_2 \quad (3.38)$$

When apply equation (3.38) for all clusters we get:

$$Q_A + Q_B + Q_C + Q_D = Q_E + Q_F + Q_G + Q_H \quad (3.39)$$

Where $Q_A, Q_B, Q_C, Q_D, Q_E, Q_F, Q_G and\ Q_H$ are real powers of the wind farm from cluster A up to cluster H.

The reactive power one and two is:-

$$Q_1 = V_1 I_1 \sin\varphi_1 \quad (3.40)$$

$$Q_2 = V_2 I_2 \sin\varphi_2 \quad (3.41)$$

When apply equation (3.38) for all clusters we get:

$$V_1 I_1 \sin\varphi_1 = V_2 I_2 \sin\varphi_2 \quad (3.42)$$

3.10.1. Load Flow Analysis

Load flow analysis is the most frequently performed systems study by electric utilities. There are three classifications of buses:-

I. Slack (swing) bus: - is used as a reference bus in order to meet the power balance conditions. Known quantities $|V|\ \delta$ and unknowns quantities P and Q

II. Generator (PV) bus: - is voltage control bus. The base is connected to the generator unit in which output power generated by this bus can be controlled by adjusting the prime mover and voltage can be controlled by adjusting excitations of the generator. Known quantities $|V|\ and$ P and unknowns quantities δ and Q

III. Load (PQ) bus: - this non-generator bus that can be obtained from historical data, records, measurement and forecast. Known quantities P and Q and unknowns quantities$|V|, and\ \delta$.

There three methods used for load flow analysis used :-

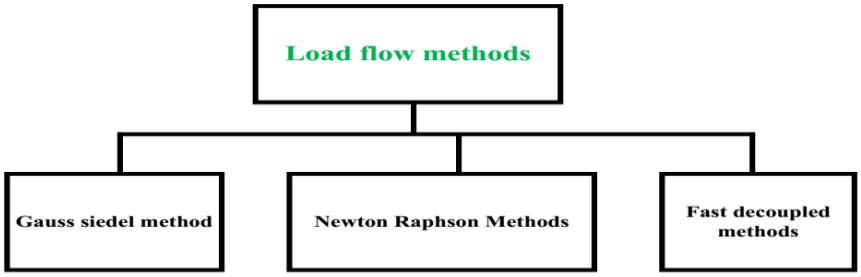

Figure 3-11Load flow analysis methods

Gauss seidel Methods is one the simplest iterate method, which used for solving linear equations and solving a set of non-linear load flow equations in power flow analysis.

Newton Raphson methods are an iterative technique for solving a set of various nonlinear equations with an equal number of unknowns.

Fast Decoupled method is a program that employing sparse matrix techniques needs less computer storage and running time.

So that Adama wind farm has eight loads and one grid. So we have eight load and one grid, from eight load one load is generate power 16.5 MW other seven load is 19.5MW each and one grid comes from koka power generation is 230Kv connected to the grid. The consideration is two loads and one slack bus as follows:-

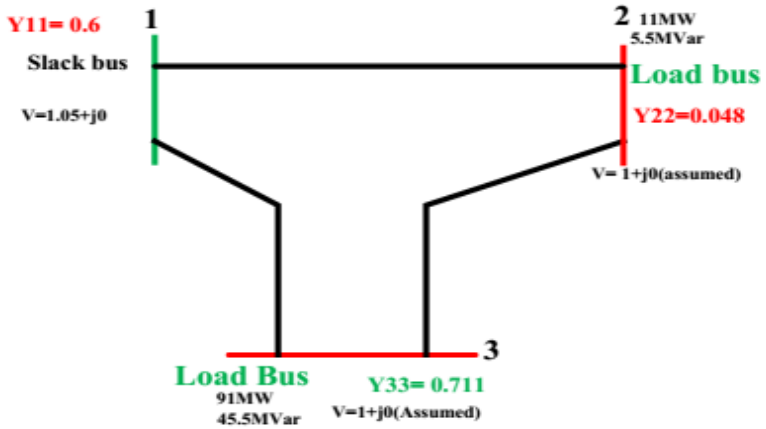

Figure 3-12 load flow bus

For a grid connected systems Adama wind farm have eight loads from that one cluster A have load is produced 16.5MW as load bus one and the left seven load (Load B-H) has load generate bus second and The reference or slack bus 230Kv which comes from Koka power stations. According to IEEE three bus systems the figure shown above.

Formulation of Ybus Matrix

We have three bus systems; accordingly to arrangement of wind turbines or the amount of power generated by systems classifies into two load buses and one slack bus.

$$Y_{bus} = \begin{bmatrix} Y_{11} & Y_{12} & Y_{13} \\ Y_{21} & Y_{22} & Y_{23} \\ Y_{31} & Y_{32} & Y_{33} \end{bmatrix} \quad (3.43)$$

From appendix A we have reactance at each load. Load bus one have reactance 0.048, load bus two has load from B-H and have reactance 0.711 and slack bus reactance is 0.6 s per unit value for each reactance.

$$Y_{11} = 0.6 \quad (3.44)$$

$$Y_{22} = 0.048 \quad (3.45)$$

$$Y_{33} = 0.711 \quad (3.46)$$

Those above one is the self-reactance for each buses and the required value isY_{12}, $Y_{23,}$$and$ Y_{13}

$$Y_{12} = -Y_{21} \quad (3.47)$$

$$Y_{23} = -Y_{32} \quad (3.48)$$

$$Y_{13} = -Y_{31} \quad (3.49)$$

The formula is there how to calculate $Y_{11,}$ $Y_{22}$$and$ Y_{33} based on this we find the above required.

$$Y_{12} + Y_{13} = 0.6 \quad (3.50)$$

$$Y_{12} + Y_{23} = 0.048 \quad (3.51)$$

$$Y_{13} + Y_{23} = 0.711 \quad (3.52)$$

We have three equations solve by simultaneous equations and combine equation 3.51 into 3.50.

$$Y_{13} = 0.552 + Y_{23} \quad (3.53)$$

Combine equation 3.53 into 3.52 we get:

$$0.711 = 0.552 + Y_{23} + Y_{23} \quad (3.54)$$

Then apply equation 3.47 up to 3.49 is as follows:

$$Y_{23} = 0.08$$

$$Y_{13} = 0.631$$

$$Y_{12} = -0.031$$

So that the Ybus matrix from equation 3.43 can be shown below:

$$Y_{bus} = \begin{bmatrix} 0.6 & 0.031 & -0.631 \\ 0.031 & 0.048 & -0.08 \\ -0.631 & -0.08 & 0.711 \end{bmatrix}$$

To calculate the voltage and phase angle at bus two and three by using gauss siedel method can be as follows

The general formula for voltage magnitude and phase angel at each bus can be as follows:-

$$V_P^{(K+1)} = \frac{1}{Y_{PP}}\left[\left(\frac{P_P - jQ_P}{V_P^K}\right) - \sum_{q=1}^{P} Y_{pq} V_q^{(K+1)} - \sum_{q=P+1}^{n} V_q^K\right] \quad (3.55)$$

Where q ≠p

From the figure of load flow bus we have Ybus matrix, then calculate magnitude of voltage and phase angle based on the above formula and base power is 100MVA.

Real and reactive power at each can be as follows

$P_2 = 0 - 0.11 = -0.11$Pu

$Q_2 = 0 - 0.055 = -j0.055$Pu

$P_3 = 0 - 0.91 = -0.91$Pu

$Q_3 = 0 - 0.455 = -j0.455$Pu

At bus two (load bus one)

$$V_2^1 = \frac{1}{Y_{22}}\left[\frac{P_2 - jQ_2}{V_2} - Y_{21}V_1 - Y_{23}V_3\right] \quad (3.56)$$

$V_2^1 = \frac{1}{j0.048}\left[\frac{-0.11+j0.055}{1-j0} - j0.031(1.05 + j0) - (-j0.631)1 + j0\right]$=0.918+j0.115Pu

At bus three (load bus two)

$$V_3^1 = \frac{1}{Y_{33}}\left[\frac{P_3 - jQ_3}{V_3} - Y_{31}V_1 - Y_{32}V_2\right] \quad (3.57)$$

$V_3^1 = \frac{1}{j0.711}\left[\frac{-0.91+j0.455}{1-j0} + j0.631(1.05 + j0) + j0.08(1 + j0)\right]$=0.9476+j0.284Pu

3.11. Design of Transmission line parameter

Synchronous generator performs very complicatedly, so, attaining a thorough model is really impossible for such generators; however, representing of the synchronous generator is

important for the investigation of the power system stability [29-30]. This particular model consists of 102 two-winding transformers, 102 lines, and 8 loads.

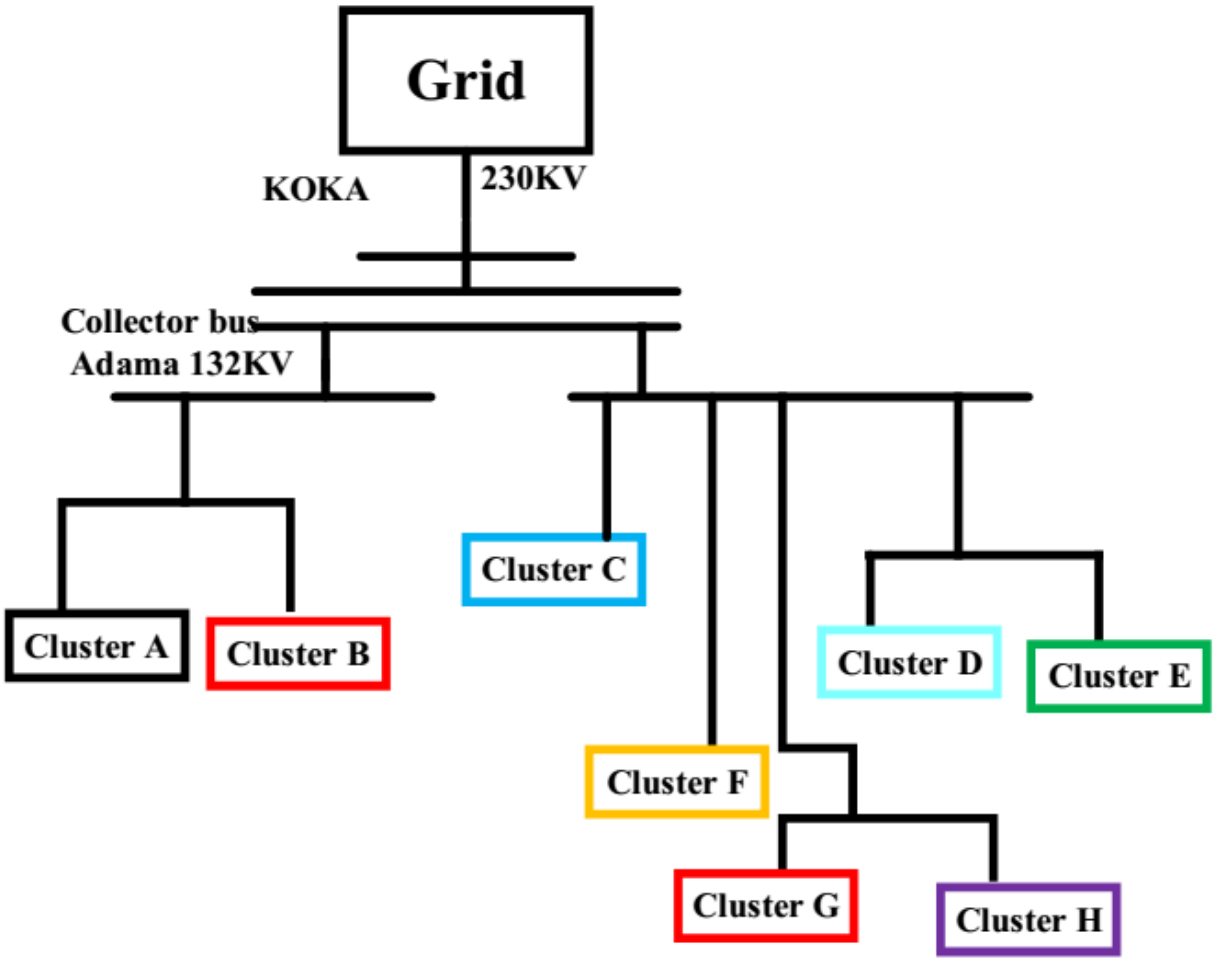

Figure 3-13 Adama wind farm clusters

Adama II wind turbine Consider the following data:-

$$V_b = 230KV$$

$$S_b = 100MVA$$

Where V_b and S_b are base voltage and base power respectively

The formula which is used for length of transmission can be as follows [23-24]:-

$$L = \frac{\sqrt{XB}}{2\pi f} * V \qquad (3.57)$$

Where L is length of transmission line in kilometer, X is reactance per unit, B is susceptibility per unit, f is systems frequency, and V is speed of light in kilometer per second, but speed of light in meter per second is$3 \times 10^8 m/s$ when change to km/s it become is$3 \times 10^5 m/s$.

Transmission line parameter calculation is as follows:-

Transmission line parameter is consists of resistance, capacitance and inductance, and some formula can be used for calculation is:-

$$\mathrm{R_{actual}} = \mathrm{R_{Base}} * \mathrm{R_{Pu}} \quad (3.58)$$

$$\mathrm{X_{actual}} = \mathrm{X_{Base}} * \mathrm{X_{Pu}} \quad (3.60)$$

$$\mathrm{B_{actual}} = \mathrm{B_{Base}} * \mathrm{B_{Pu}} \quad (3.61)$$

$$\mathrm{R_{Base}} = \mathrm{X_{Base}} = \frac{\mathrm{V_b}^2}{\mathrm{S_b}} \quad (3.62)$$

$$\mathrm{B_{Base}} = \frac{\mathrm{S_b}}{\mathrm{V_b}^2} \quad (3.63)$$

Transmission line parameter, sequence of transmission line parameter can be as follows:-

Positive and zero sequence Resistance can be:-

$$R_1(\frac{\Omega}{Km}) = \frac{R_{actual}}{line\ length} \quad (3.64)$$

$$R_0(\frac{\Omega}{Km}) = 3 * R_1(\frac{\Omega}{Km}) \quad (3.65)$$

Positive and zero sequence capacitance can be:-

$$C_{actual} = \frac{B_{actual}}{2\pi f} \quad (3.66)$$

$$C_1(\frac{\mathrm{F}}{Km}) = \frac{C_{actual}}{line\ length} \quad (3.67)$$

$$C_0(\frac{\mathrm{F}}{Km}) = 3 * C_1(\frac{\Omega}{Km} \quad (3.68)$$

Positive and zero sequence inductance can be:-

$$L_{actual} = \frac{X_{actual}}{2\pi f} \quad (3.69)$$

$$L_1(\frac{\mathrm{H}}{Km}) = \frac{L_{actual}}{line\ length} \quad (3.70)$$

$$L_0(\frac{\mathrm{F}}{Km}) = 3 * L_1(\frac{\mathrm{H}}{Km}) \quad (3.71)$$

For cluster A

The formula which is used for length of transmission can be as follows:-

$$\mathrm{L} = \frac{\sqrt{XB}}{2\pi f} * V$$

For this formula we calculate Susceptibility (B) is equal to

$$B = \frac{(l2\pi f)^2}{xV^2} = \frac{(4.86 \times 2 \times \pi \times 50)^2}{0.048(3 \times 10^5)^2} = 5.39621 \times 10^{-4}$$

Base resistance is calculate as

$$R_{Base} = X_{Base} = \frac{{V_b}^2}{S_b} = \frac{(230 \times 10^3)^2}{100 \times 10^6} = 529\Omega$$

$$R_{actual} = R_{Base} * R_{Pu} = 529 \times 0.122 = 64.538$$

Base susceptibility is calculate as

$$B_{Base} = \frac{S_b}{{V_b}^2} = \frac{100000000}{(230 \times 10^3)^2} = 1.89 \times 10^{-3}$$

$$\mathrm{B_{actual}} = \mathrm{B_{Base}} * \mathrm{B_{Pu}} = 1.89 \times 10^{-3} \times 5.39621 \times 10^{-4} = 1.02 \times 10^{-6}$$

Positive and zero sequence resistance calculate as:-

$$\mathrm{R_1}(\frac{\Omega}{\mathrm{Km}}) = \frac{\mathrm{R_{actual}}}{\text{line length}} = \frac{64.538}{4.86} = 13.28\ \Omega/\mathrm{Km}$$

$$R_0(\frac{\Omega}{Km}) = 3 * R_1(\frac{\Omega}{Km}) = 3 \times 13.28 = 39.84\Omega/\mathrm{Km}$$

Positive and zero sequence capacitance calculate as:-

$$\mathrm{C_{actual}} = \frac{\mathrm{B_{actual}}}{2\pi \mathrm{f}} = \frac{1.02 \times 10^{-6}}{2\pi \times 50} = 3.25 \times 10^{-9}$$

$$\mathrm{C_1}(\frac{\mathrm{F}}{\mathrm{Km}}) = \frac{\mathrm{C_{actual}}}{\text{line length}} = \frac{3.25 \times 10^{-9}}{4.86} = 6.69 \times 10^{-10} F/Km$$

$$\mathrm{C_0}(\frac{\mathrm{F}}{\mathrm{Km}}) = 3 * \mathrm{C_1}(\frac{\mathrm{F}}{\mathrm{Km}}) = 3 \times 6 \times 10^{-10} F/Km = 2.006 \times 10^{-9} F/Km$$

Positive and zero sequence inductance can be:-

$$\mathrm{X_{actual}} = \mathrm{X_{Base}} * \mathrm{X_{Pu}} = 529\Omega \times 0.048 = 25.392$$

$$\mathrm{L_{actual}} = \frac{\mathrm{X_{actual}}}{2\pi \mathrm{f}} = \frac{25.392}{2\pi \times 50} = 0.0809\mathrm{H/Km}$$

$$\mathrm{L_1}(\frac{\mathrm{H}}{\mathrm{Km}}) = \frac{\mathrm{L_{actual}}}{\text{line length}} = \frac{0.0809}{4{,}86} = 0.01664\mathrm{mH/Km}$$

$$\mathrm{L_0}(\frac{\mathrm{F}}{\mathrm{Km}}) = 3 * \mathrm{L_1}(\frac{\mathrm{H}}{\mathrm{Km}}) = 3 \times 0.01664\mathrm{mH/Km} = 0.0499\mathrm{mH/Km}$$

For cluster B

The formula which is used for length of transmission can be as follows:-

$$\mathrm{L} = \frac{\sqrt{XB}}{2\pi f} * V$$

For this formula we calculate Susceptibility (B) is equal to

$$\mathrm{B} = \frac{(\mathrm{l2\pi f})^2}{\mathrm{xV^2}} = \frac{(6.18 \times 2 \times \pi \times 50)^2}{0.048(3 \times 10^5)^2} = 8.717 \times 10^{-4}$$

Base resistance is calculate as

$$R_{Base} = X_{Base} = \frac{V_b{}^2}{S_b} = \frac{(230 \times 10^3)^2}{100 \times 10^6} = 529\Omega$$

$$R_{actual} = R_{Base} * R_{Pu} = 529 \times 0.126 = 66.65$$

Base susceptibility is calculate as

$$B_{Base} = \frac{S_b}{V_b{}^2} = \frac{100000000}{(230 \times 10^3)^2} = 1.89 \times 10^{-3}$$

$$B_{actual} = B_{Base} * B_{Pu} = 1.89 \times 10^{-3} \times 8.717 \times 10^{-4} = 1.648 \times 10^{-6}$$

Positive and zero sequence resistance calculate as:-

$$R_1(\frac{\Omega}{Km}) = \frac{R_{actual}}{\text{line length}} = \frac{66.65}{6.18} = 10.785\ \Omega/\text{Km}$$

$$R_0(\frac{\Omega}{Km}) = 3 * R_1(\frac{\Omega}{Km}) = 3 \times 10.785 = 32.35\Omega/\text{Km}$$

Positive and zero sequence capacitance calculate as :-

$$C_{actual} = \frac{B_{actual}}{2\pi f} = \frac{1.648 \times 10^{-6}}{2\pi \times 50} = 5.248 \times 10^{-9}$$

$$C_1(\frac{F}{Km}) = \frac{C_{actual}}{\text{line length}} = \frac{5.248 \times 10^{-9}}{6.18} = 8.492 \times 10^{-10} F/Km$$

$$C_0(\frac{F}{Km}) = 3 * C_1(\frac{F}{Km}) = 3 \times 8.492 \times 10^{-10} F/Km = 2.55 \times 10^{-9} F/Km$$

Positive and zero sequence inductance can be:-

$$X_{actual} = X_{Base} * X_{Pu} = 529\Omega \times 0.068 = 35.97$$

$$L_{actual} = \frac{X_{actual}}{2\pi f} = \frac{35.97}{2\pi \times 50} = 0.1146 H/Km$$

$$L_1(\frac{H}{Km}) = \frac{L_{actual}}{line\ length} = \frac{0.1146}{6.18} = 0.0185 H/Km$$

$$L_0(\frac{F}{Km}) = 3 * L_1(\frac{H}{Km}) = 3 \times 0.0185 H/Km = 0.0556 H/Km$$

For cluster C

The formula which is used for length of transmission can be as follows:-

$$L = \frac{\sqrt{XB}}{2\pi f} * V$$

For this formula we calculate Susceptibility (B) is equal to

$$B = \frac{(l2\pi f)^2}{xV^2} = \frac{(9.27 \times 2 \times \pi \times 50)^2}{0.093(3 \times 10^5)^2} = 1.0122 \times 10^{-3}$$

Base resistance is calculate as

$$R_{Base} = X_{Base} = \frac{V_b{}^2}{S_b} = \frac{(230 \times 10^3)^2}{100 \times 10^6} = 529\Omega$$

$$R_{actual} = R_{Base} * R_{Pu} = 529 \times 0.231 = 122.2$$

Base susceptibility is calculate as

$$B_{Base} = \frac{S_b}{{V_b}^2} = \frac{100000000}{(230 \times 10^3)^2} = 1.89 \times 10^{-3}$$

$$\mathrm{B_{actual}} = \mathrm{B_{Base}} * \mathrm{B_{Pu}} = 1.89 \times 10^{-3} \times 1.0122 \times 10^{-3} = 1.9 \times 10^{-6}$$

Positive and zero sequence resistance calculate as:-

$$\mathrm{R_1}(\frac{\Omega}{\mathrm{Km}}) = \frac{\mathrm{R_{actual}}}{\text{line length}} = \frac{122.2}{\mathbf{9.27}} = 13.18\ \Omega/\mathrm{Km}$$

$$R_0(\frac{\Omega}{Km}) = 3 * R_1(\frac{\Omega}{Km}) = 3 \times 13.18 = 39.55\Omega/\mathrm{Km}$$

Positive and zero sequence capacitance calculate as:-

$$\mathrm{C_{actual}} = \frac{\mathrm{B_{actual}}}{2\pi \mathrm{f}} = \frac{1.9 \times 10^{-6}}{2\pi \times 50} = 6.051 \times 10^{-9}$$

$$\mathrm{C_1}(\frac{\mathrm{F}}{\mathrm{Km}}) = \frac{\mathrm{C_{actual}}}{\text{line length}} = \frac{6.051 \times 10^{-9}}{9.27} = 0.653 \times 10^{-10} F/Km$$

$$\mathrm{C_0}(\frac{\mathrm{F}}{\mathrm{Km}}) = 3 * \mathrm{C_1}(\frac{\mathrm{F}}{\mathrm{Km}}) = 3 \times 0.653 \times 10^{-10} F/Km = 1.96 \times 10^{-9} F/Km$$

Positive and zero sequence inductance can be:-

$$\mathrm{X_{actual}} = \mathrm{X_{Base}} * \mathrm{X_{Pu}} = 529\Omega \times 0.093 = 49.197$$

$$\mathrm{L_{actual}} = \frac{\mathrm{X_{actual}}}{2\pi \mathrm{f}} = \frac{49.197}{2\pi \times 50} = 0.1567\mathrm{H/Km}$$

$$\mathrm{L_1}(\frac{\mathrm{H}}{\mathrm{Km}}) = \frac{\mathrm{L_{actual}}}{\text{line length}} = \frac{0.1567}{\mathbf{9.27}} = 0.0169\mathrm{H/Km}$$

$$\mathrm{L_0}(\frac{\mathrm{F}}{\mathrm{Km}}) = 3 * \mathrm{L_1}(\frac{\mathrm{H}}{\mathrm{Km}}) = 3 \times 0.0169\mathrm{H/Km} = 0.0507\mathrm{H/Km}$$

For cluster D

The formula which is used for length of transmission can be as follows:-

$$\mathrm{L} = \frac{\sqrt{XB}}{2\pi f} * V$$

For this formula we calculate Susceptibility (B) is equal to

$$\mathrm{B} = \frac{(\mathrm{l}2\pi \mathrm{f})^2}{\mathrm{xV}^2} = \frac{(4.86 \times 2 \times \pi \times 50)^2}{0.048(3 \times 10^5)^2} = 5.39621 \times 10^{-4}$$

Base resistance is calculate as

$$R_{Base} = X_{Base} = \frac{{V_b}^2}{S_b} = \frac{(230 \times 10^3)^2}{90 \times 10^6} = 587.78\Omega$$

$$R_{actual} = R_{Base} * R_{Pu} = 587.78 \times 0.192 = 112.85$$

Base susceptibility is calculate as

$$B_{Base} = \frac{S_b}{{V_b}^2} = \frac{90000000}{(230 \times 10^3)^2} = 1.701 \times 10^{-3}$$

$$\mathrm{B_{actual}} = \mathrm{B_{Base}} * \mathrm{B_{Pu}} = 1.701 \times 10^{-3} \times 5.39621 \times 10^{-4} = 9.179 \times 10^{-7}$$

Positive and zero sequence resistance calculate as:-

$$\mathrm{R}_1(\frac{\Omega}{\mathrm{Km}}) = \frac{\mathrm{R}_{\mathrm{actual}}}{\text{line length}} = \frac{112.85}{\mathbf{10.21}} = 11.0533\ \Omega/\mathrm{Km}$$

$$R_0(\frac{\Omega}{Km}) = 3 * R_1(\frac{\Omega}{Km}) = 3 \times 11.0533 = 33.16\Omega/\mathrm{Km}$$

Positive and zero sequence capacitance calculate:-

$$\mathrm{C}_{\mathrm{actual}} = \frac{\mathrm{B}_{\mathrm{actual}}}{2\pi \mathrm{f}} = \frac{9.179 \times 10^{-7}}{2\pi \times 50} = 2.92 \times 10^{-9}$$

$$\mathrm{C}_1(\frac{\mathrm{F}}{\mathrm{Km}}) = \frac{\mathrm{C}_{\mathrm{actual}}}{\text{line length}} = \frac{2.92 \times 10^{-9}}{4.86} = 6 \times 10^{-10} F/Km$$

$$\mathrm{C}_0(\frac{\mathrm{F}}{\mathrm{Km}}) = 3 * \mathrm{C}_1(\frac{\mathrm{F}}{\mathrm{Km}}) = 3 \times 6 \times 10^{-10} F/Km = 1.8 \times 10^{-9} F/Km$$

Positive and zero sequence inductance can be:-

$$X_{actual} = X_{Base} * X_{Pu} = 587.78\Omega \times \mathbf{0.106} = 62.31$$

$$L_{actual} = \frac{X_{actual}}{2\pi f} = \frac{62.31}{2\pi \times 50} = 0.19832 H/Km$$

$$L_1(\frac{\mathrm{H}}{Km}) = \frac{L_{actual}}{line\ length} = \frac{0.19832}{\mathbf{10.21}} = 0.0194 H/Km$$

$$L_0(\frac{\mathrm{F}}{Km}) = 3 * L_1(\frac{\mathrm{H}}{Km}) = 3 \times 0.0194 H/Km = 0.0583 H/Km$$

For cluster E

The formula which is used for length of transmission can be as follows:-

$$\mathrm{L} = \frac{\sqrt{XB}}{2\pi f} * V$$

For this formula we calculate Susceptibility (B) is equal to

$$\mathrm{B} = \frac{(\mathrm{l}2\pi \mathrm{f})^2}{\mathrm{xV}^2} = \frac{(4.86 \times 2 \times \pi \times 50)^2}{0.048(3 \times 10^5)^2} = 5.39621 \times 10^{-4}$$

Base resistance is calculate as

$$R_{Base} = X_{Base} = \frac{{V_b}^2}{S_b} = \frac{(230 \times 10^3)^2}{90 \times 10^6} = 587.78\Omega$$

$$R_{actual} = R_{Base} * R_{Pu} = 587.78 \times \mathbf{0.228} = 134.01$$

Base susceptibility is calculate as

$$B_{Base} = \frac{S_b}{{V_b}^2} = \frac{90000000}{(230 \times 10^3)^2} = 1.701 \times 10^{-3}$$

$$\mathrm{B}_{\mathrm{actual}} = \mathrm{B}_{\mathrm{Base}} * \mathrm{B}_{\mathrm{Pu}} = 1.701 \times 10^{-3} \times 5.39621 \times 10^{-4} = 9.179 \times 10^{-7}$$

Positive and zero sequence resistance can be:-

$$\mathrm{R}_1(\frac{\Omega}{\mathrm{Km}}) = \frac{\mathrm{R}_{\mathrm{actual}}}{\text{line length}} = \frac{134.01}{\mathbf{10.61}} = 12.63\ \Omega/\mathrm{Km}$$

$$R_0(\frac{\Omega}{Km}) = 3 * R_1(\frac{\Omega}{Km}) = 3 \times 12.63 = 37.89\Omega/\mathrm{Km}$$

Positive and zero sequence capacitance calculate as:-

$$\mathrm{C_{actual}} = \frac{\mathrm{B_{actual}}}{2\pi \mathrm{f}} = \frac{9.179 \times 10^{-7}}{2\pi \times 50} = 2.92 \times 10^{-9}$$

$$\mathrm{C_1}(\frac{\mathrm{F}}{\mathrm{Km}}) = \frac{\mathrm{C_{actual}}}{\text{line length}} = \frac{2.92 \times 10^{-9}}{4.86} = 6 \times 10^{-10} F/Km$$

$$\mathrm{C_0}(\frac{\mathrm{F}}{\mathrm{Km}}) = 3 * \mathrm{C_1}(\frac{\mathrm{F}}{\mathrm{Km}}) = 3 \times 6 \times 10^{-10} F/Km = 1.8 \times 10^{-9} F/Km$$

Positive and zero sequence inductance can be:-

$$X_{actual} = X_{Base} * X_{Pu} = 587.78\Omega \times \mathbf{0.11} = 64.66$$

$$L_{actual} = \frac{X_{actual}}{2\pi f} = \frac{64.66}{2\pi \times 50} = 0.206 H/Km$$

$$L_1(\frac{\mathrm{H}}{Km}) = \frac{L_{actual}}{line\ length} = \frac{0.206}{\mathbf{10.61}} = 0.0194 H/Km$$

$$L_0(\frac{\mathrm{F}}{Km}) = 3 * L_1(\frac{\mathrm{H}}{Km}) = 3 \times 0.0194 H/Km = 0.0582 H/Km$$

For cluster F

The formula which is used for length of transmission can be as follows:-

$$\mathrm{L} = \frac{\sqrt{XB}}{2\pi f} * V$$

For this formula we calculate Susceptibility (B) is equal to

$$B = \frac{(\mathrm{l}2\pi \mathrm{f})^2}{\mathrm{xV}^2} = \frac{(4.86 \times 2 \times \pi \times 50)^2}{0.048(3 \times 10^5)^2} = 5.39621 \times 10^{-4}$$

Base resistance is calculate as

$$R_{Base} = X_{Base} = \frac{{V_b}^2}{S_b} = \frac{(230 \times 10^3)^2}{90 \times 10^6} = 587.78\Omega$$

$$R_{actual} = R_{Base} * R_{Pu} = 587.78 \times 0.213 = 125.2$$

Base susceptibility is calculate as

$$B_{Base} = \frac{S_b}{{V_b}^2} = \frac{90000000}{(230 \times 10^3)^2} = 1.701 \times 10^{-3}$$

$$\mathrm{B_{actual}} = \mathrm{B_{Base}} * \mathrm{B_{Pu}} = 1.701 \times 10^{-3} \times 5.39621 \times 10^{-4} = 9.179 \times 10^{-7}$$

Positive and zero sequence resistance calculate:-

$$\mathrm{R_1}(\frac{\Omega}{\mathrm{Km}}) = \frac{\mathrm{R_{actual}}}{\text{line length}} = \frac{125.2}{\mathbf{10.95}} = 11.43\ \Omega/\mathrm{Km}$$

$$R_0(\frac{\Omega}{Km}) = 3 * R_1(\frac{\Omega}{Km}) = 3 \times 11.43 = 34.3\Omega/\mathrm{Km}$$

Positive and zero sequence capacitance calculate as:-

$$\mathrm{C_{actual}} = \frac{\mathrm{B_{actual}}}{2\pi \mathrm{f}} = \frac{9.179 \times 10^{-7}}{2\pi \times 50} = 2.92 \times 10^{-9}$$

$$\mathrm{C_1}(\frac{\mathrm{F}}{\mathrm{Km}}) = \frac{\mathrm{C_{actual}}}{\text{line length}} = \frac{2.92 \times 10^{-9}}{4.86} = 6 \times 10^{-10} F/Km$$

$$C_0(\frac{F}{Km}) = 3 * C_1(\frac{F}{Km}) = 3 \times 6 \times 10^{-10} F/Km = 1.8 \times 10^{-9} F/Km$$

Positive and zero sequence inductance can be:-

$$X_{actual} = X_{Base} * X_{Pu} = 587.78\Omega \times 0.113 = 66.42$$

$$L_{actual} = \frac{X_{actual}}{2\pi f} = \frac{66.42}{2\pi \times 50} = 0.211 H/Km$$

$$L_1(\frac{H}{Km}) = \frac{L_{actual}}{line\ length} = \frac{0.211}{\mathbf{10.95}} = 0.0193 H/Km$$

$$L_0(\frac{F}{Km}) = 3 * L_1(\frac{H}{Km}) = 3 \times 0.0193 H/Km = 0.0579 H/Km$$

For cluster G

The formula which is used for length of transmission can be as follows:-

$$L = \frac{\sqrt{XB}}{2\pi f} * V$$

For this formula we calculate Susceptibility (B) is equal to

$$B = \frac{(l 2\pi f)^2}{xV^2} = \frac{(4.86 \times 2 \times \pi \times 50)^2}{0.048(3 \times 10^5)^2} = 5.39621 \times 10^{-4}$$

Base resistance is calculate as

$$R_{Base} = X_{Base} = \frac{{V_b}^2}{S_b} = \frac{(230 \times 10^3)^2}{90 \times 10^6} = 587.78\Omega$$

$$R_{actual} = R_{Base} * R_{Pu} = 587.78 \times 0.268 = 157.53$$

Base susceptibility is calculate as

$$B_{Base} = \frac{S_b}{{V_b}^2} = \frac{90000000}{(230 \times 10^3)^2} = 1.701 \times 10^{-3}$$

$$B_{actual} = B_{Base} * B_{Pu} = 1.701 \times 10^{-3} \times 5.39621 \times 10^{-4} = 9.179 \times 10^{-7}$$

Positive and zero sequence resistance calculate as:-

$$R_1(\frac{\Omega}{Km}) = \frac{R_{actual}}{\text{line length}} = \frac{157.53}{\mathbf{10.72}} = 14.7\ \Omega/Km$$

$$R_0(\frac{\Omega}{Km}) = 3 * R_1(\frac{\Omega}{Km}) = 3 \times 11.43\ = 44.08\Omega/Km$$

Positive and zero sequence capacitance calculate:-

$$C_{actual} = \frac{B_{actual}}{2\pi f} = \frac{9.179 \times 10^{-7}}{2\pi \times 50} = 2.92 \times 10^{-9}$$

$$C_1(\frac{F}{Km}) = \frac{C_{actual}}{\text{line length}} = \frac{2.92 \times 10^{-9}}{4.86} = 6 \times 10^{-10} F/Km$$

$$C_0(\frac{F}{Km}) = 3 * C_1(\frac{F}{Km}) = 3 \times 6 \times 10^{-10} F/Km = 1.8 \times 10^{-9} F/Km$$

Positive and zero sequence inductance can be:-

$$X_{actual} = X_{Base} * X_{Pu} = 587.78\Omega \times 0.113 = 66.42$$

$$L_{actual} = \frac{X_{actual}}{2\pi f} = \frac{66.42}{2\pi \times 50} = 0.211 H/Km$$

$$L_1(\frac{\mathrm{H}}{Km}) = \frac{L_{actual}}{line\ length} = \frac{0.211}{\mathbf{10.72}} = 0.0197 H/Km$$

$$L_0(\frac{\mathrm{F}}{Km}) = 3 * L_1(\frac{\mathrm{H}}{Km}) = 3 \times 0.0197 H/Km = 0.0591 H/Km$$

For cluster H

The formula which is used for length of transmission can be as follows:-

$$\mathrm{L} = \frac{\sqrt{XB}}{2\pi f} * V$$

For this formula we calculate Susceptibility (B) is equal to

$$B = \frac{(l2\pi f)^2}{xV^2} = \frac{(4.86 \times 2 \times \pi \times 50)^2}{0.048(3 \times 10^5)^2} = 5.39621 \times 10^{-4}$$

Base resistance is calculate as

$$R_{Base} = X_{Base} = \frac{{V_b}^2}{S_b} = \frac{(230 \times 10^3)^2}{90 \times 10^6} = 587.78\Omega$$

$$R_{actual} = R_{Base} * R_{Pu} = 587.78 \times 0.204 = 119.91$$

Base susceptibility is calculate as

$$B_{Base} = \frac{S_b}{{V_b}^2} = \frac{90000000}{(230 \times 10^3)^2} = 1.701 \times 10^{-3}$$

$$\mathrm{B_{actual}} = \mathrm{B_{Base}} * \mathrm{B_{Pu}} = 1.701 \times 10^{-3} \times 5.39621 \times 10^{-4} = 9.179 \times 10^{-7}$$

Positive and zero sequence resistance can be:-

$$\mathrm{R_1}(\frac{\Omega}{\mathrm{Km}}) = \frac{\mathrm{R_{actual}}}{\text{line length}} = \frac{119.91}{\mathbf{10.56}} = 11.36\ \Omega/\mathrm{Km}$$

$$R_0(\frac{\Omega}{Km}) = 3 * R_1(\frac{\Omega}{Km}) = 3 \times 11.36\ = 34.07\Omega/\mathrm{Km}$$

Positive and zero sequence capacitance calculated as:-

$$\mathrm{C_{actual}} = \frac{\mathrm{B_{actual}}}{2\pi \mathrm{f}} = \frac{9.179 \times 10^{-7}}{2\pi \times 50} = 2.92 \times 10^{-9}$$

$$\mathrm{C_1}(\frac{\mathrm{F}}{\mathrm{Km}}) = \frac{\mathrm{C_{actual}}}{\text{line length}} = \frac{2.92 \times 10^{-9}}{4.86} = 6 \times 10^{-10} F/Km$$

$$\mathrm{C_0}(\frac{\mathrm{F}}{\mathrm{Km}}) = 3 * \mathrm{C_1}(\frac{\mathrm{F}}{\mathrm{Km}}) = 3 \times 6 \times 10^{-10} F/Km = 1.8 \times 10^{-9} F/Km$$

Positive and zero sequence inductance can be:-

$$X_{actual} = X_{Base} * X_{Pu} = 587.78\Omega \times 0.108 = 63.48$$

$$L_{actual} = \frac{X_{actual}}{2\pi f} = \frac{63.48}{2\pi \times 50} = 0.202 H/Km$$

$$L_1(\frac{\mathrm{H}}{Km}) = \frac{L_{actual}}{line\ length} = \frac{0.202}{\mathbf{10.56}} = 0.01914 H/Km$$

$$L_0(\frac{\mathrm{F}}{Km}) = 3 * L_1(\frac{\mathrm{H}}{Km}) = 3 \times 0.01914 H/Km = 0.0574 H/Km$$

Table 3-4 Transmission line parameter of Adama wind farm

Cluster	Length(Km)	R1($\frac{\Omega}{Km}$)	Ro($\frac{\Omega}{Km}$)	C1($\frac{F}{Km}$)	Co($\frac{F}{Km}$)	L1($\frac{H}{Km}$)	Lo($\frac{H}{Km}$)
A	4.86	13.28	39.84	6.69×10^{-10}	2×10^{-9}	0.01664	0.0499
B	6.18	10.785	32.35	$8.5 * 10^{-10}$	$2.6 * 10^{-9}$	0.0185	0.0556
C	9.27	13.18	39.55	0.653×10^{-10}	1.96×10^{-9}	0.0169	0.0507
D	10.21	11.0533	33.16	6.03×10^{-10}	1.809×10^{-9}	0.0194	0.0583
E	10.61	12.63	37.89	6.012×10^{-10}	1.804×10^{-9}	0.0194	0.0582
F	10.95	11.43	34.3	6.01×10^{-10}	1.803×10^{-9}	0.0193	0.0579
G	10.72	14.7	44.08	6.02×10^{-10}	1.806×10^{-9}	0.0197	0.0591
H	10.56	11.36	34.07	6.05×10^{-10}	1.81×10^{-9}	0.01914	0.0574

3.12. Equal- Area Criterion

The transient stability investigates include the purpose of whether stable or not are preserved subsequently the machine has been risked to simple disorders. This might be a rapid use of load, loss of load, loss of generation, and transmission line faults. This technique is established on the graphical analysis of the energy deposited in the revolving mass as an aid to conclude if the machine upholds its stability after interference in [32].

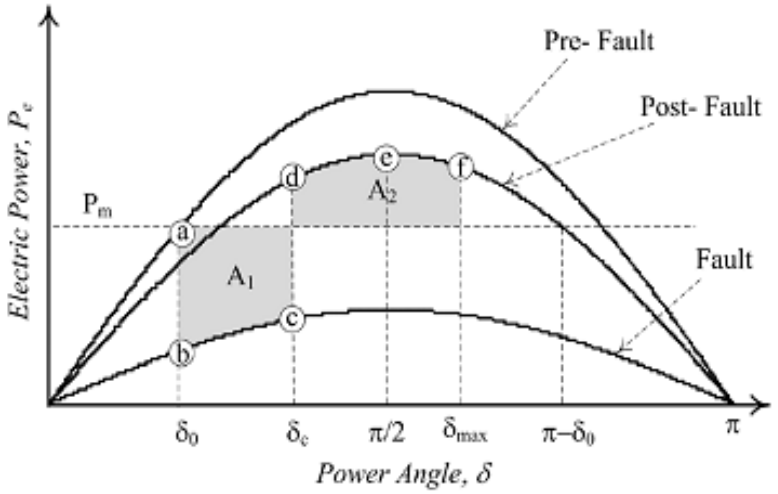

Figure 3-14Equal-area criterions [32]

The consequence is that the rotor swings to point ‘’d’’ and the angle δmax, at which point

Area A1 = Area A2=d

3.13. Designs for Transient Stability Analysis

3.13.1. Power Angle Curve

The DFIG is associated to infinite bus as shown in the figure below through a losses line, according to power system stability analysis stability cause by current smooth in the transmission line in [31-33].

Transmission line data for Adama II wind farm can be as follows:-

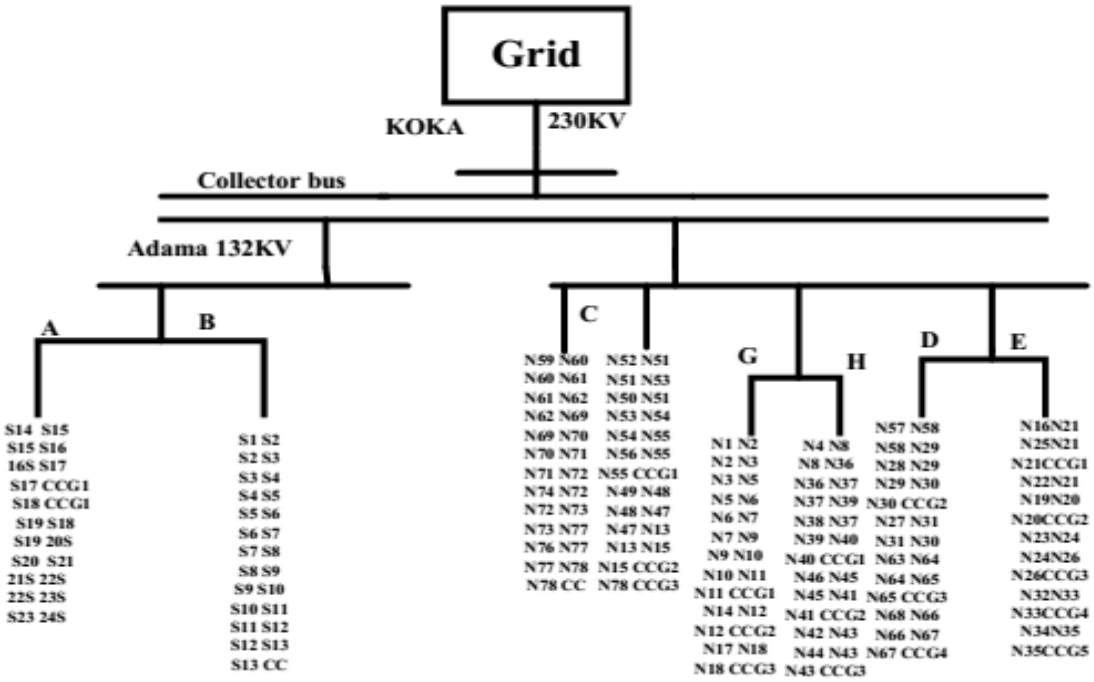

Figure 3-15Transmission line data of Adama II wind turbine

There are three condition of transient stability:-

1. Pre-fault conditions
2. During fault conditions
3. Post fault conditions

Pre fault electrical power is calculated as:-

$$P_{eI} = \frac{E*V}{X_I} \sin \delta \tag{3.72}$$

During fault condition electrical power is calculate as:-

$$P_{eII} = \frac{E*V}{X_{II}} \sin \delta \tag{3.73}$$

Post fault electrical power is calculate as:-

$$P_{eIII} = \frac{E*V}{X_{III}} \sin\delta \tag{3.74}$$

Clearing angle formula is as follows:-

$$\cos\delta_c = \frac{\left[P_i(\delta_{max}-\delta_0)*\frac{\pi}{180^\circ}-P_{eII}\cos\delta_0+P_{eIII}\cos\delta_{max}\right]}{P^{III}{}_{max}-P^{II}{}_{max}} \tag{3.75}$$

Time clearing fault is calculate as

$$t_c = \sqrt{\frac{2H(\delta_c-\delta_0)}{\pi f P_i}} \tag{3.76}$$

considering only cluster A for single representation of Adama wind farm have eight clusters from Cluster A-H, When a three phase fault is applies on one end of the line. This means when fault happen (applies) on cluster A. The Double fed induction generator is delivering 1.0 p.u.

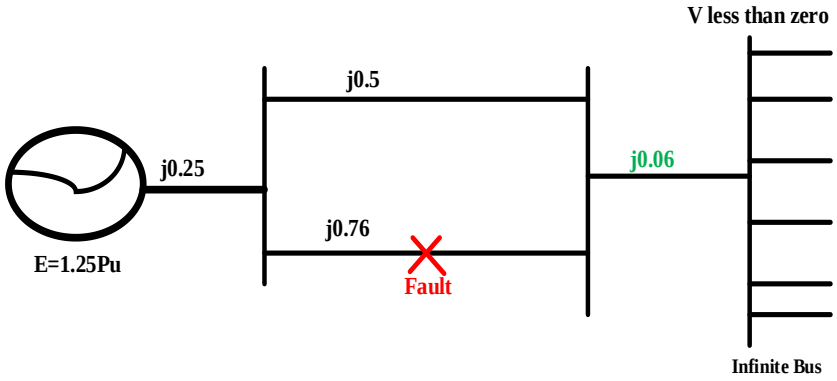

Solution:

Pre-fault condition

$$X^I = 0.25 + ((0.5x\ 0.76)/\ (0.5 + 0.76)) + 0.06 = 0.612$$

$$P_e{}^I = [|E||V|/X^I]\ \sin\delta = (1.25\ x\ 1.0\ /0.612)\ \sin\delta = 2.044\ \sin\delta$$

During fault

$$P_e{}^{II} = 0$$

Post fault condition

$$X^{III} = 0.25 + 0.63 + 0.06 = 0.94$$

$$Pe^{III} = [|E||V|/X^{III}]\ \sin\delta = (1.25\ X\ 1/0.94)\ \sin\delta = 1.3298\ \sin\delta$$

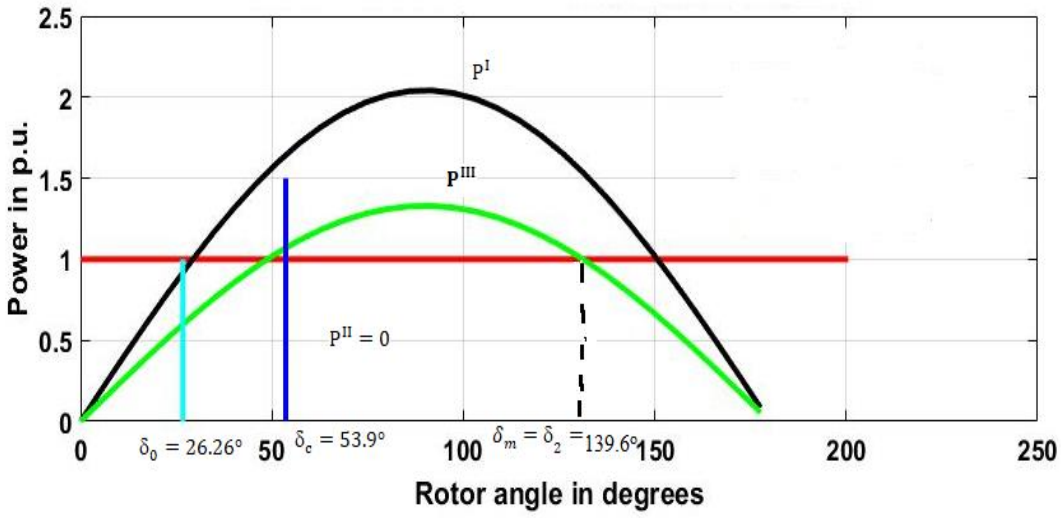

$$P_e^0 = P^I_{max} \sin\delta_0 = P_i;\ 2.044 \times \sin\delta_0 = 1.0$$

Therefore $\delta_0 = 26.62^o$

$$\delta_m = 180^o - \sin^{-1}\{P_i^0/P^{III}_{max}\}$$

$$= 180^o - \sin^{-1}\{1/1.543\} = 139.6^o$$

$$\cos\delta_c = [P_i(\delta_m - \delta_0) - P^{II}_{max}\cos\delta^0 + P^{III}_{max}\cos\delta_m]/[P^{III}_{max} - P^{II}_{max}] = [\,1(139.6^o - 26.62^o)(\pi/180) - 0 + 1.33\cos 139.6^o)]/[1.543 - 0]$$

$$= 1.4775$$

$$\delta_c = \cos^{-1}(1.4775) = 0.9419 \times 180/\pi = 53.9^o$$

$$\delta_c = 53.9^o$$

Assume if Inertia constant is equal to 6MJ/MVA and Time clearing fault is calculate as

$$t_c = \sqrt{\frac{2H(\delta_c - \delta_0)}{\pi f P_i}} = \sqrt{\frac{2 * 6(53.9° - 26.72°)}{180° * 50 * 1}} = 0.1463\ s$$

Chapter Four

4. Results and Discussion

4.1.Introduction

Power systems stability consists of three conditions or scenarios are there that is steady state stability, dynamic stability, and transient stability. Transient stability consists there conditions are there like pre-fault, during a fault and post fault. The simulation result contains four conditions are one at pre-fault conditions, the second is during faults, the third is post fault conditions, and the last one is the enhancement of the systems using or installing TCSC between grid and wind turbine or DFIG cluster. In this Simulation results, I classify systems at the wind turbine side, substation side, and grid sides. On each Matlab Simulink scenario I considered real and reactive power, pitch and speed of induction generators, current and voltage at a wind turbine, substation, and grid sides.

4.2.Modeling of DFIG in Matlab Simulink

The wind turbine and generators constitute the physical subsystems that are being simulated and the associated control blocks which are governing their behavior. The physical generator is simulated and then the measurable outputs are fed to the machine estimator, which computes the values of other variables which are not measurable but are necessary for the control. It is significant to keep this distinction between the physical systems and virtual control clear. This is because every signal in the models treated as the same and looks the same whether it is a real power or reactive power signal or an estimated value that would only exist in a microcontroller in the real world. The inverter dynamics are not considered in this work, so they appear in the model as simply a gain of one. Therefore this model must be taken for what it is: an ideal functional description of a DFIG wind turbine connected to a grid that treats each component in the most simple and fundamental way possible.

4.2.1. Thyristor -Controlled Series Capacitor

The thyristor-controlled series capacitor is a series-connected FACTS controller. TCSC delivers respected means of monitoring and aggregate power transfer level of a system by the variable apparent impedance of an exact transmission line. The thyristor-controlled series capacitor in mat lab Simulink is a combination of voltage sources converter as see in the figure below.

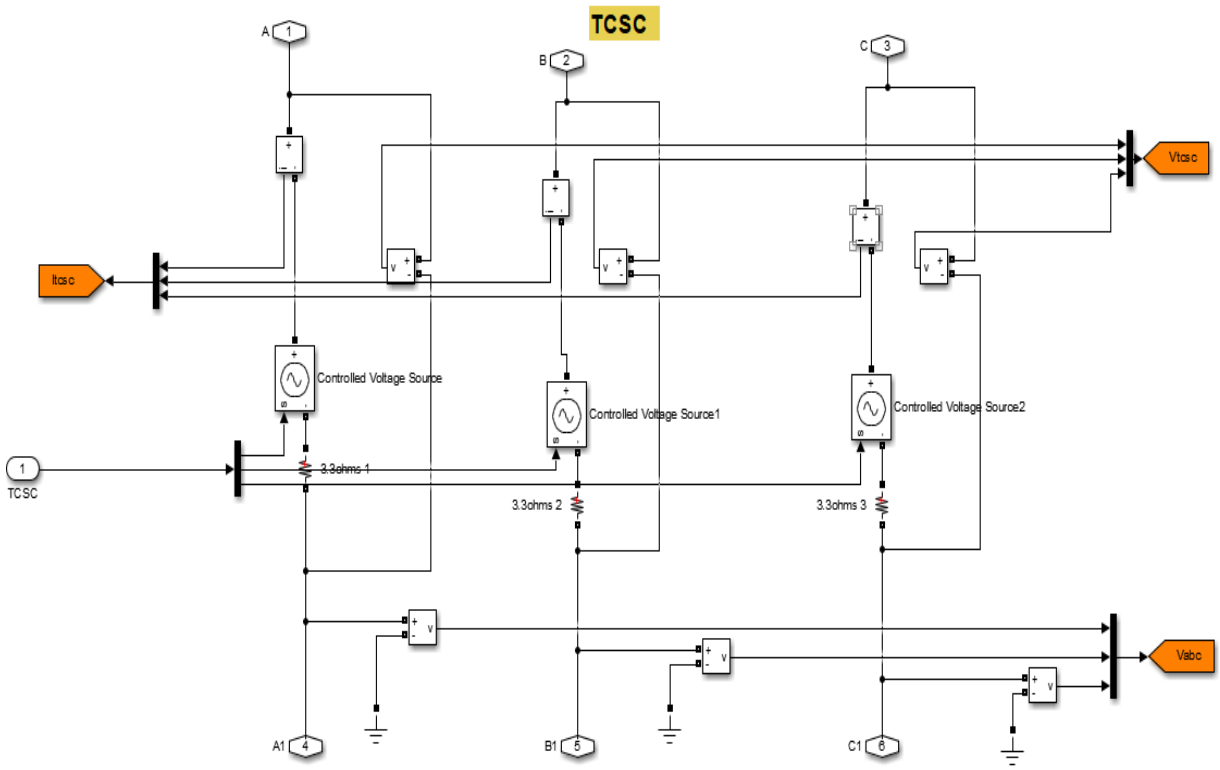

Figure 4-1 Structure of TCSC in Matlab Simulink

4.2.2. Adaptive neuro-fuzzy interference systems

The design of adaptive neuro-fuzzy interference systems in the mat lab coding by using input/output characteristics of Adama II wind farm. This means just wind speed is input for a wind turbine of DFIG. Coding is shown on appendixes of C and the input/output can be characteristics can be as follows:-

ANFIS information:

Number of nodes: 24

Number of linear parameters: 10

Number of nonlinear parameters: 15

Total number of parameters: 25

Number of trainings data pairs: 101

Number of checking data pairs: 0

Number of fuzzy rules: 5

Start training ANFIS...

1 0.0694086

2 0.0680259

3 0.066663

4 0.0653198

5 0.0639961

Step size rises to 0.011000 after epoch 5.

6 0.0626917

7 0.0612787

8 0.0598881

9 0.0585193

Step size rises to 0.012100 after epoch 9.

10 0.0571712

11 0.0557113

12 0.0542741

13 0.052858

Step size rises to 0.013310 after epoch 13.

14 0.0514612

15 0.0499449

16 0.0484475

17 0.0469667

Step size rises to 0.014641 after epoch 17.

18 0.0455003

19 0.0439022

20 0.0423184

Designated epoch numbers reached ANFIS training completed at epoch 20 and the ANFIS output and training data can be shown in the graph.

As seen from the figure below there is training data and ANFIS outputs, training data is the disturbance of input/output characteristics, this means the input is not reached synchronous speed or not nearly to synchronous speed of wind turbines, in this case, the out power got

from DFIG is low but ANFIS controllers use to enhance the input/output characteristics reach to synchronous and near to synchronous speed in order to produce power by DFIGs.

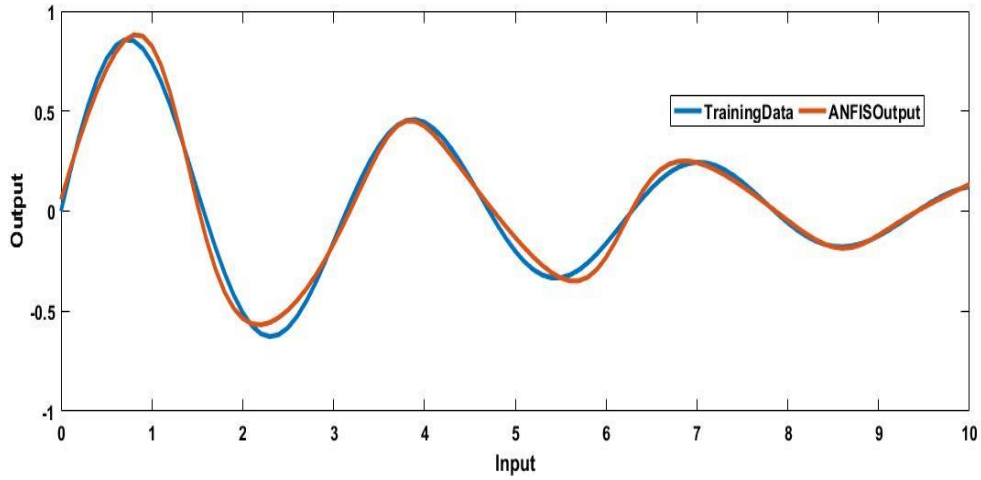

Figure 4-2 Input/output characteristics using ANFIS

Sample model ANFIS in Matlab Simulink

The matlab Simulink of an ANFIS has consists of step use as generator in a wind turbine, scope use for display the outputs and by using sample transfer function for Adama wind farms. The transfer function is consists three numbers one, two and three, the step is act as input of transfer function. This means just wind speed is input for wind turbine of DFIG. The Simulink is consists of Step, transfer function model, scope and fuzzy logic controllers and the model can be as follows.

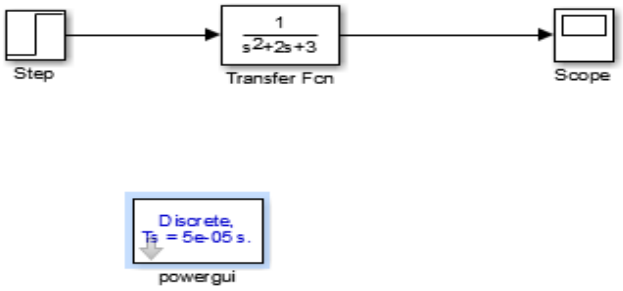

Figure 4-3Matlab Simulink model without ANFIS

The out of this model is disturbed as shown in figure below.

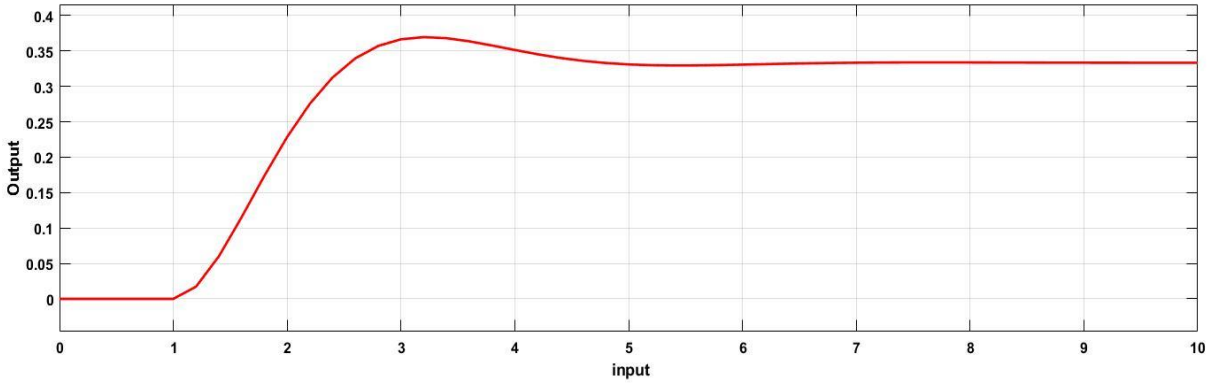

Figure 4-4the disturbed input/output of the systems

The out of this model is disturbed but by using ANFIS we can enhance the systems by adding fuzzy logic controllers as shown in figure.

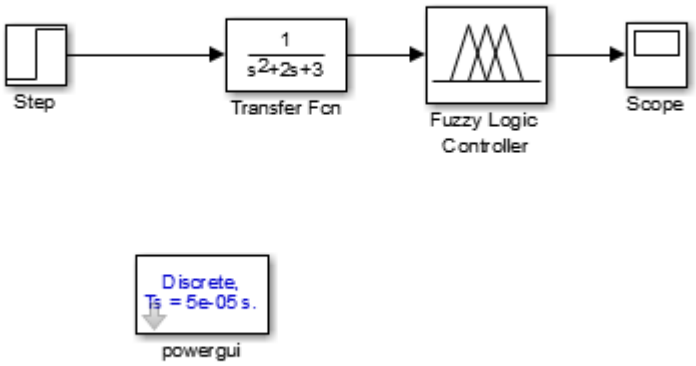

Figure 4-5Matlab Simulink model within ANFIS

Depend on the graph of above we have one input and one put for ANFIS. The input data of the above graph is:-

Table 4-1data of the step from transfer functions

No	Input	output
1	0.02	0.10
2	0.04	0.15
3	0.06	0.2
4	0.08	0.25
5	0.10	0.3
6	0.12	0.3
7	0.14	0.3
8	0.16	0.3
9	0.18	0.3
10	0.2	0.3
11	0.22	0.3

Then go to command writes ANFIS edit, and then the training data can be as follows:

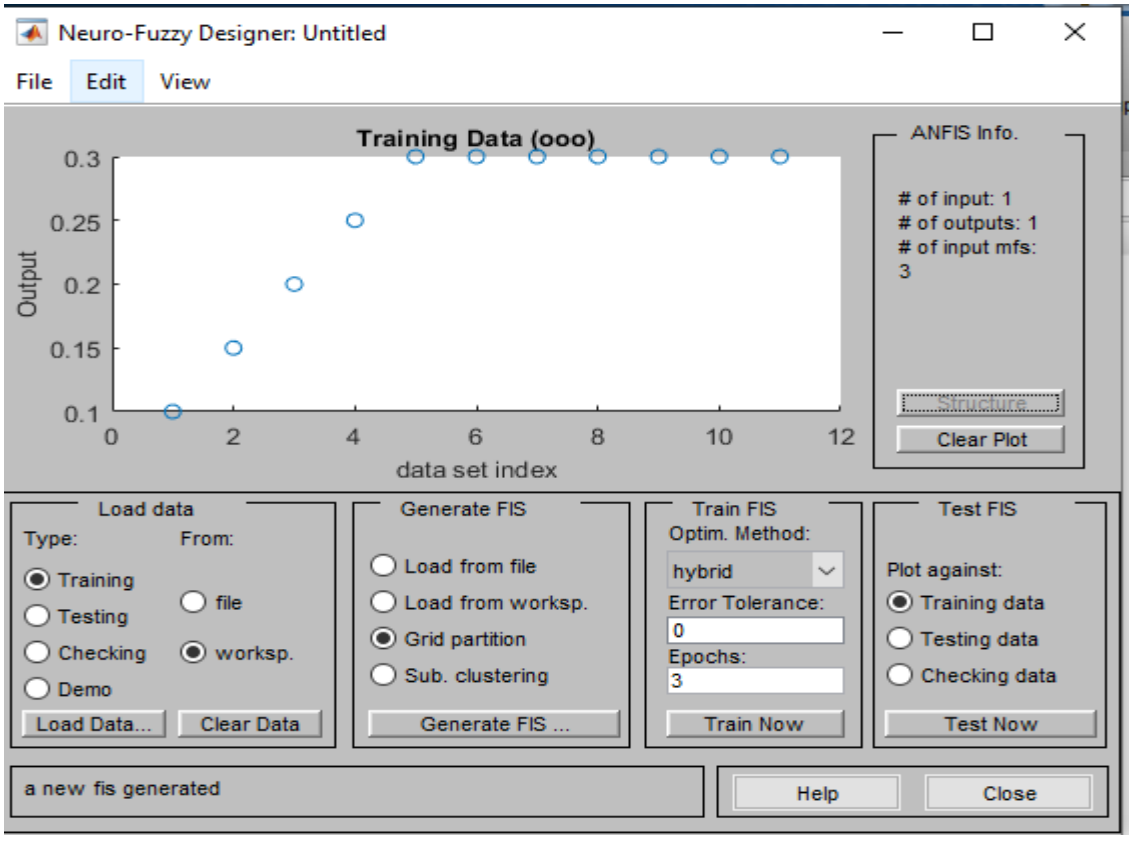

The ANFIS structure is as follows contain one input and one output

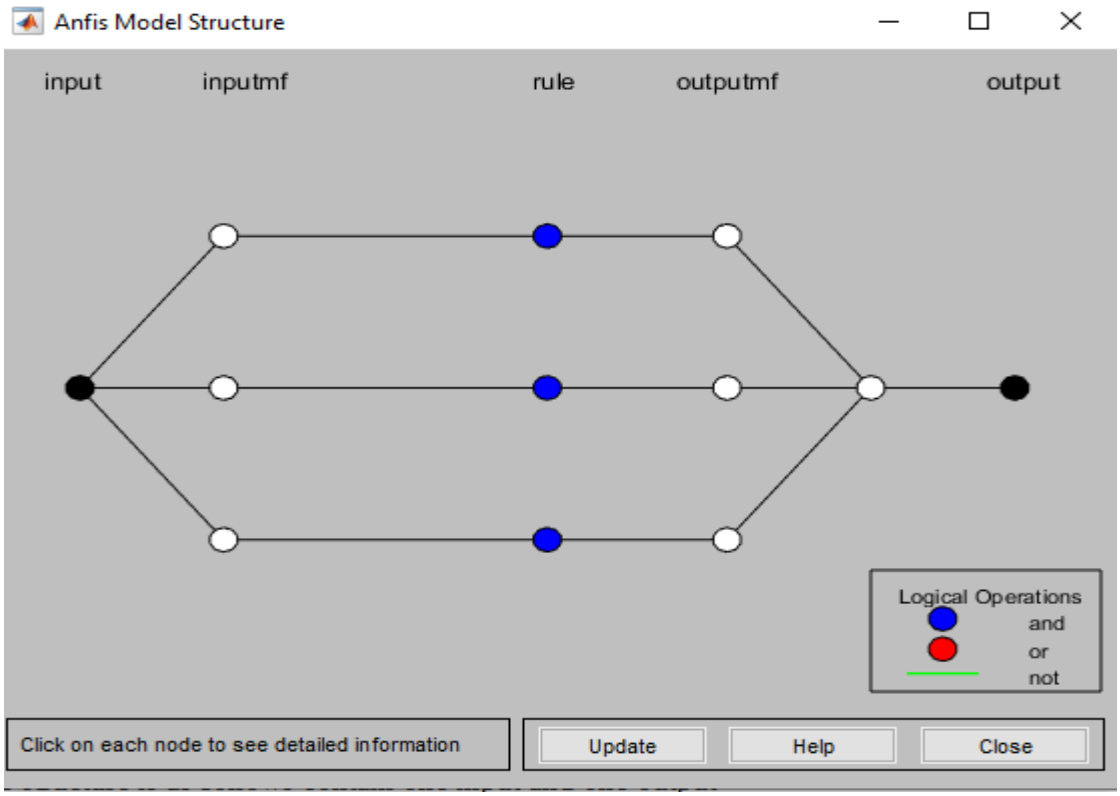

Make we train the input data until the error is goes to zero.

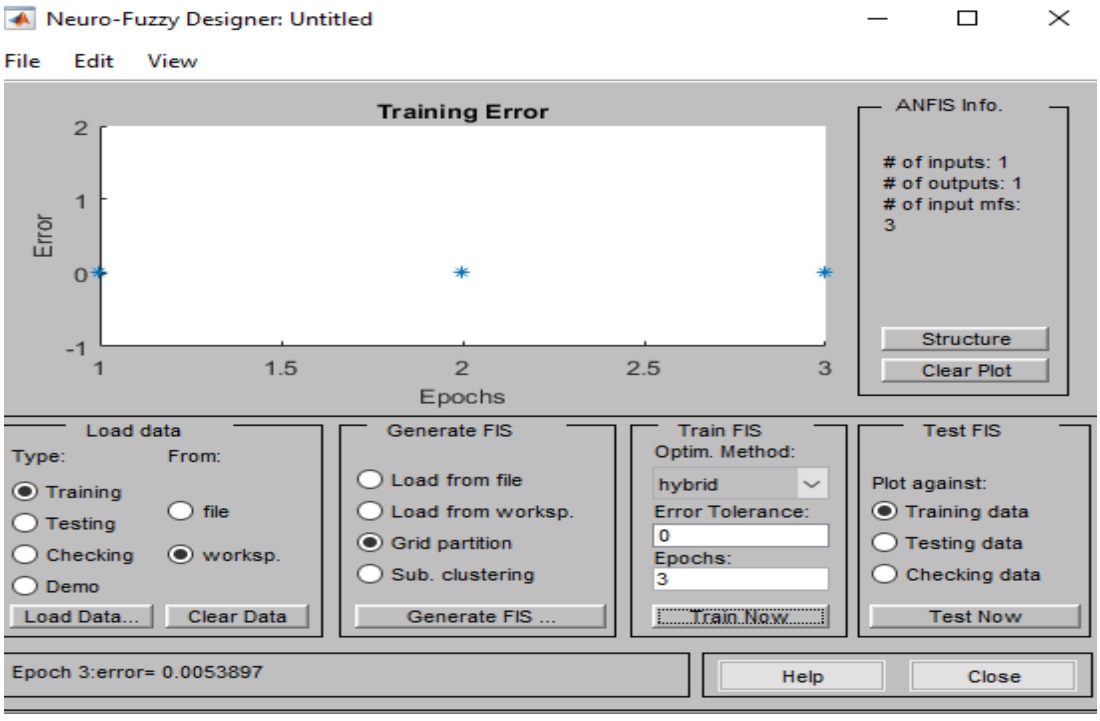

The check or test the error the systems or simple compare before and after systems enhanced.

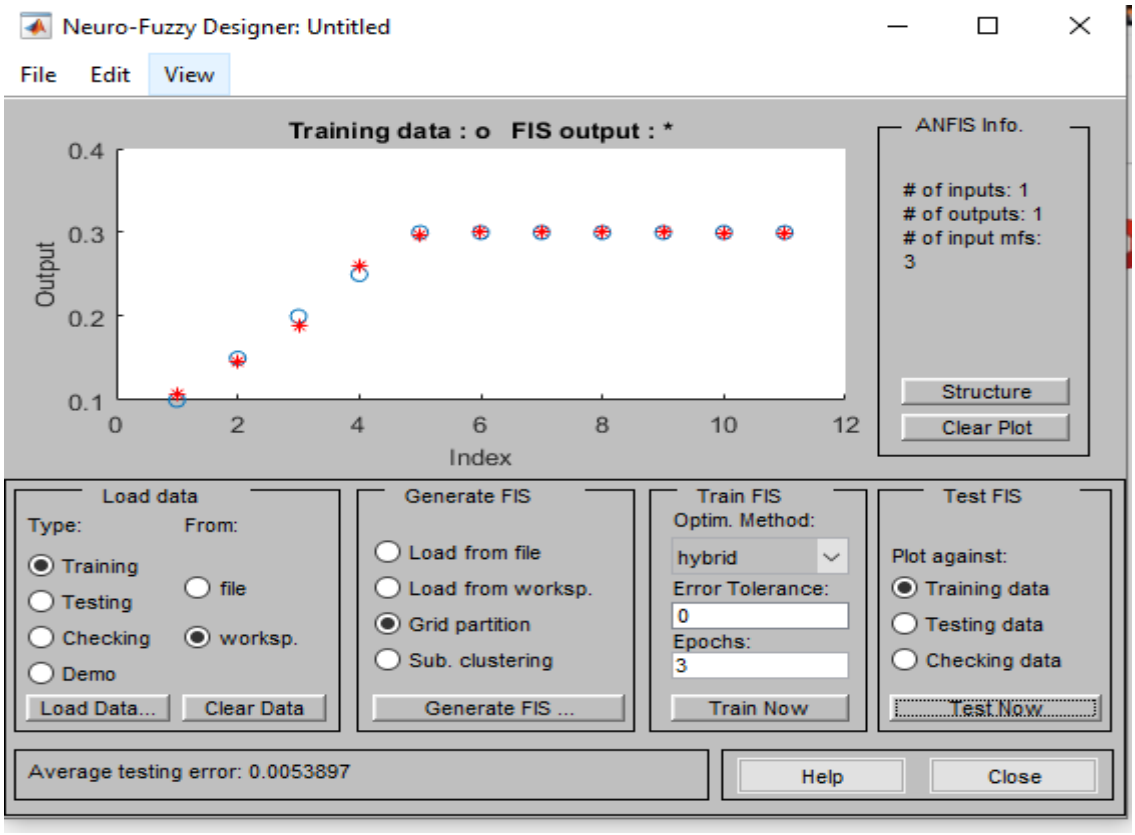

Then save the file to workspace and add to the fuzzy logic tools means shown in Figure 4-6, the enhancement systems can be show as the graph as follows.

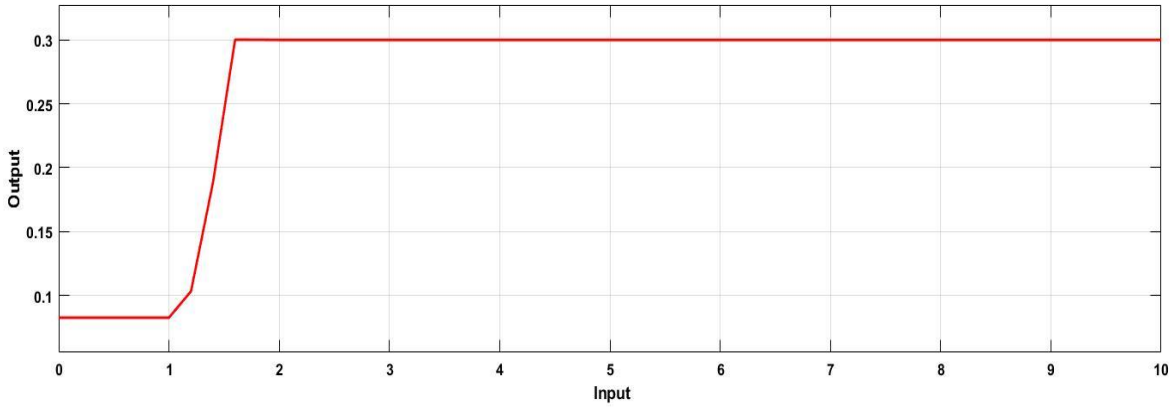

Figure 4-6 the enhancement of input/output of the systems

4.2.3. Proportional-Integral Controller

The main aim of the PI controller is to keep constant speed of the rotor at load during any unwanted disturbances occurs in the system and to stabilize rotor speed and slip of the generator. The PI controllers model in the Mat Lab/Simulink software in the system as shown in figure below:

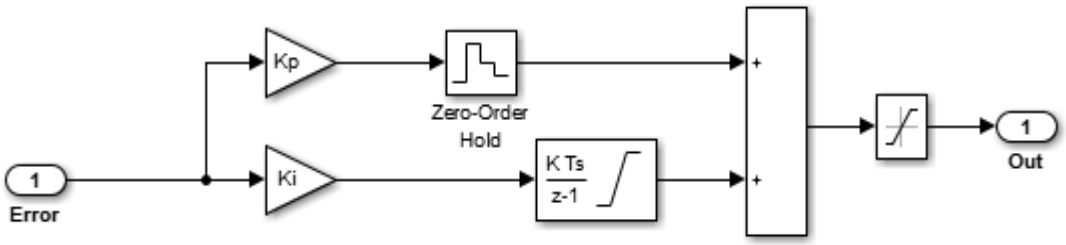

Figure 4-7Proportional integral controllers

4.2.4. Rotor side converter Control System

The rotor-side converter is used to regulator the wind turbine output and the voltage restrained at the grid terminal. The terminal voltage regulator is considered to control the terminal voltage to maintain a constant value such that the terminal of this wind turbine DFIG system can be shown as a variable wind speed. Rotor side converter consist four main model one is electromagnetic model, second is Voltage regulator, third one is Current regulator and the fourth one is index and phase of RSC. The structure can be as follows

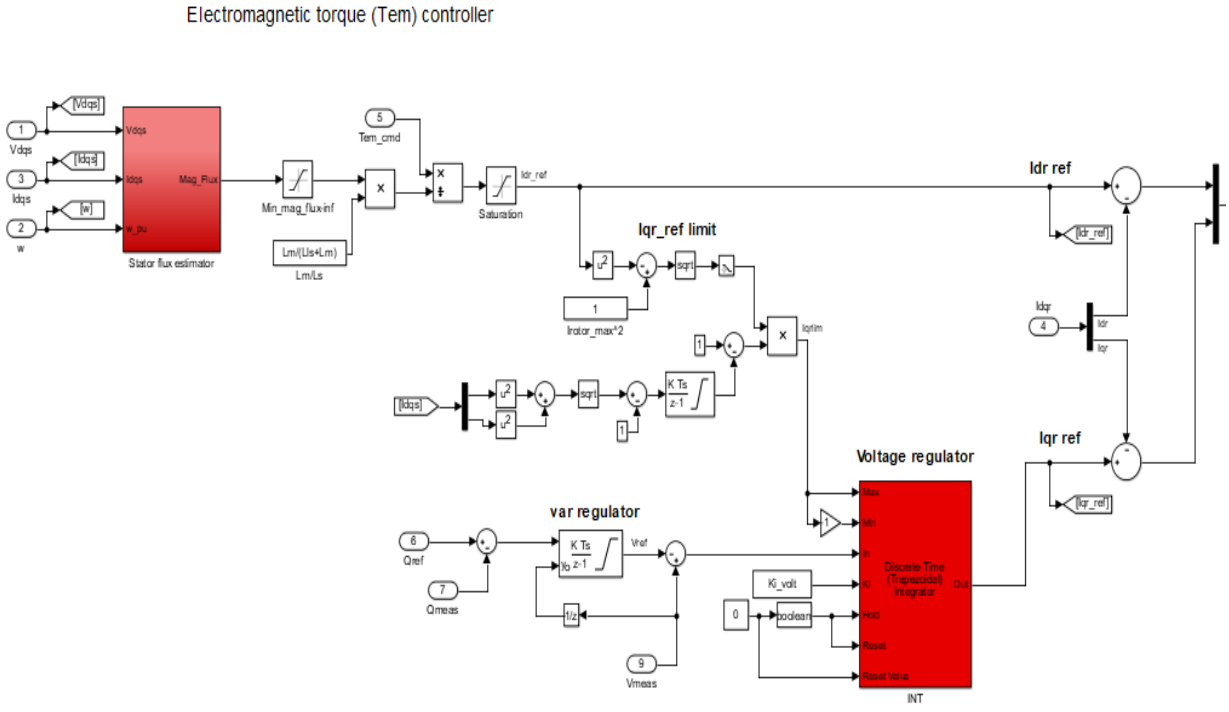

Figure 4-8 Electromagnetic torque controller and voltage regulator systems of RSC

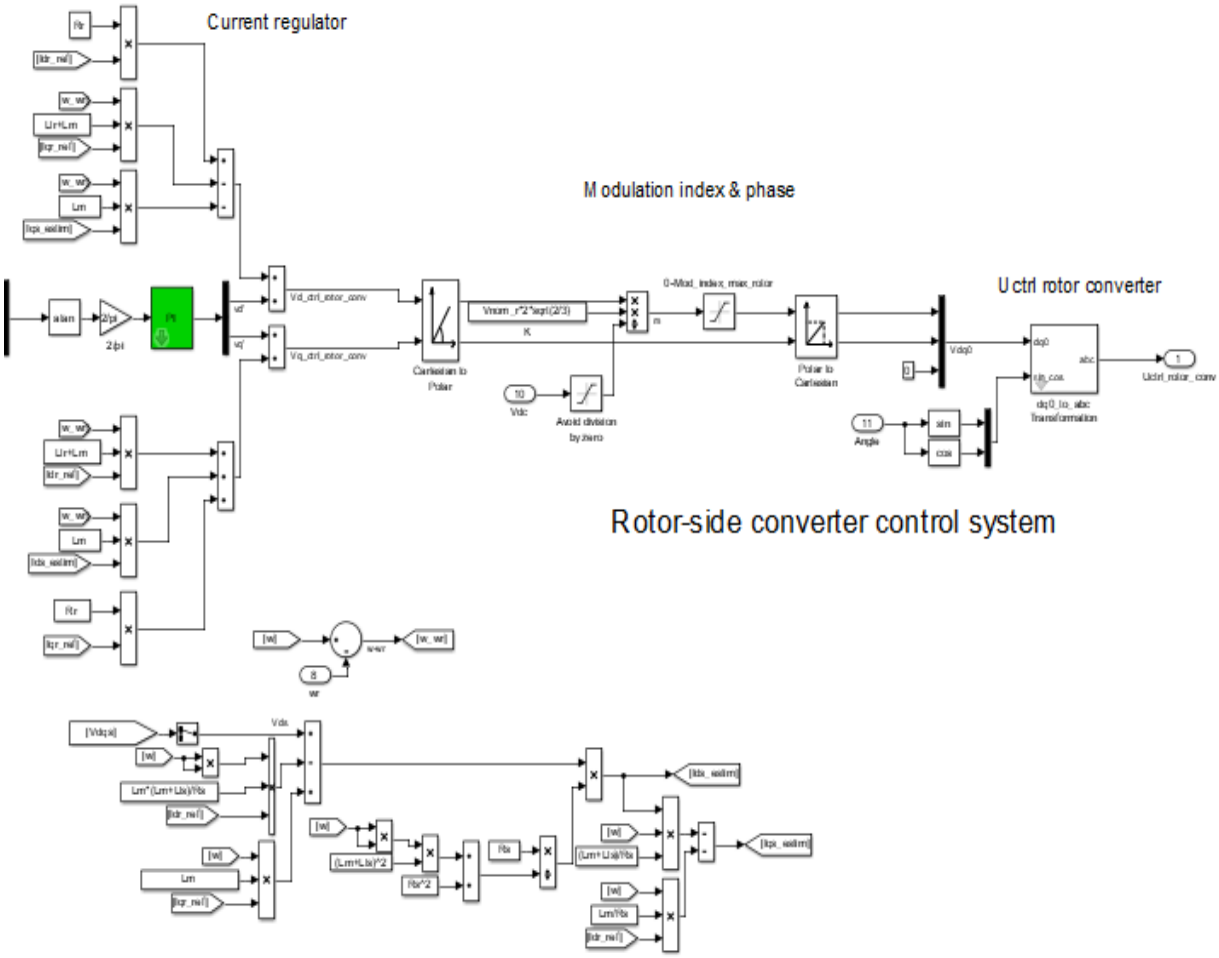

Figure 4-9 Current regulator and phase control systems of RSC

4.2.5. Grid Side Converter Control System

The Grid side converter is wanted to control the voltage of the DC-bus capacitor. For the grid-side controller the d-axis of the rotary reference frame used for d-q transformation is related with the order of grid voltage. The current controlling controls the magnitude and phase of the voltage produced by converter grid side converter (Vgc) from the Idgc_ref formed by the DC voltage regulator and specified Iq_ref reference. The current regulator is assisted by feed forward terms which estimate the grid side converter output voltage. The grid side converter can be as follows:-

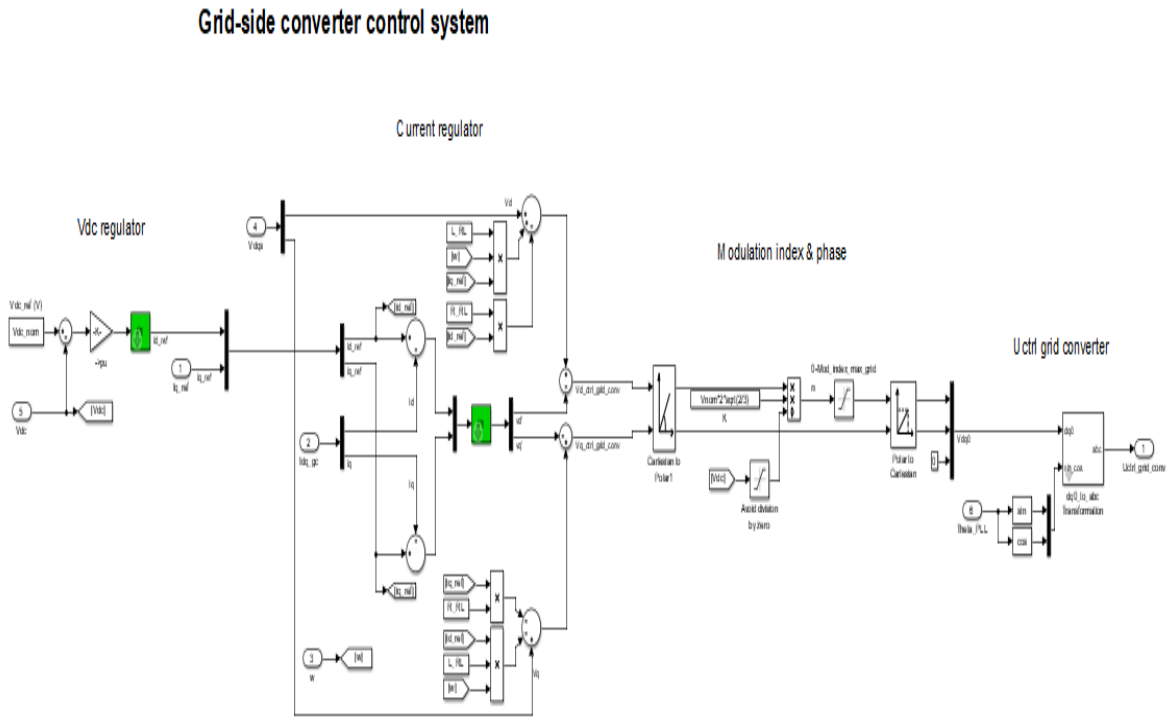

Figure 4-10 Structure of GSC control systems

4.3.Simulation Diagram of DFIG

This is the Simulink diagram for a doubly fed induction generator connected to grid side with wind turbine protection arrangements involved for security from three-phase faults. The system is connected to a 230kV, three phase source which is connected to a 16.5MW wind farm (11 of 1.5 MW each) via. Step down transformers, fault protection and pi- transmission line of 4,56km cover by wind farm of cluster A connected to 230kV koka generation, its far 10 km form Adama substation. The pitch angle is controlled in order to limit the generator output power at its minimal value for winds beyond the nominal speed (9.5m/s). In order to generate power the DSCIG speed essential be slightly above the synchronous speed. Speed varies approximately between 1p.u.After the active power extended its rated value the pitch angle controller try to increase the blade angle in order to protect the wind turbine from any

external damage. ANFIS- controller controls the speed of the rotor in order to get the maximum power from the wind and the result can be as follows:-

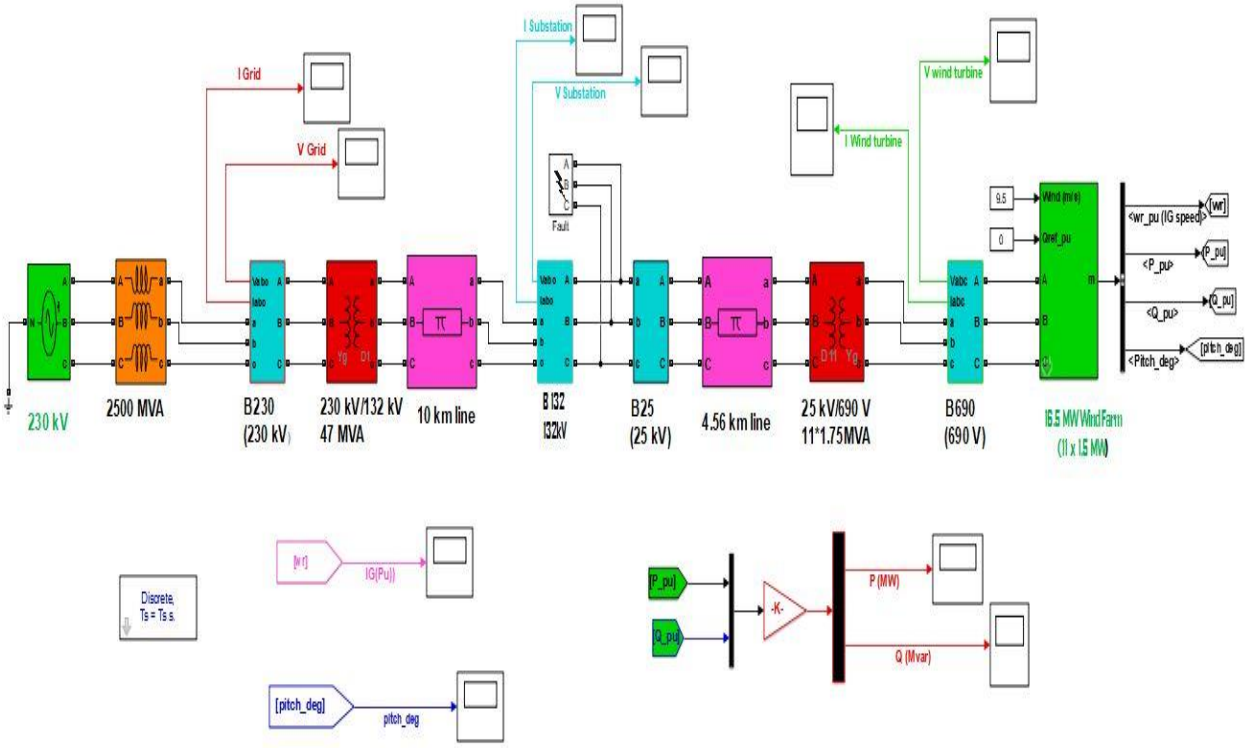

Figure 4-11 Simulink model of single cluster of Adama II wind farm

Transient stability analysis can be consists of three conditions are there:-

1. Pre-fault condition
2. During fault condition
3. Post-fault condition

4.3.1. Simulation result of DFIG Pre-fault condition

During pre-fault conditions the systems is stable means there is some disturbance at start point of the systems for a few mill second, after that systems is back to normal operation, and the simulation model can be as follows:-

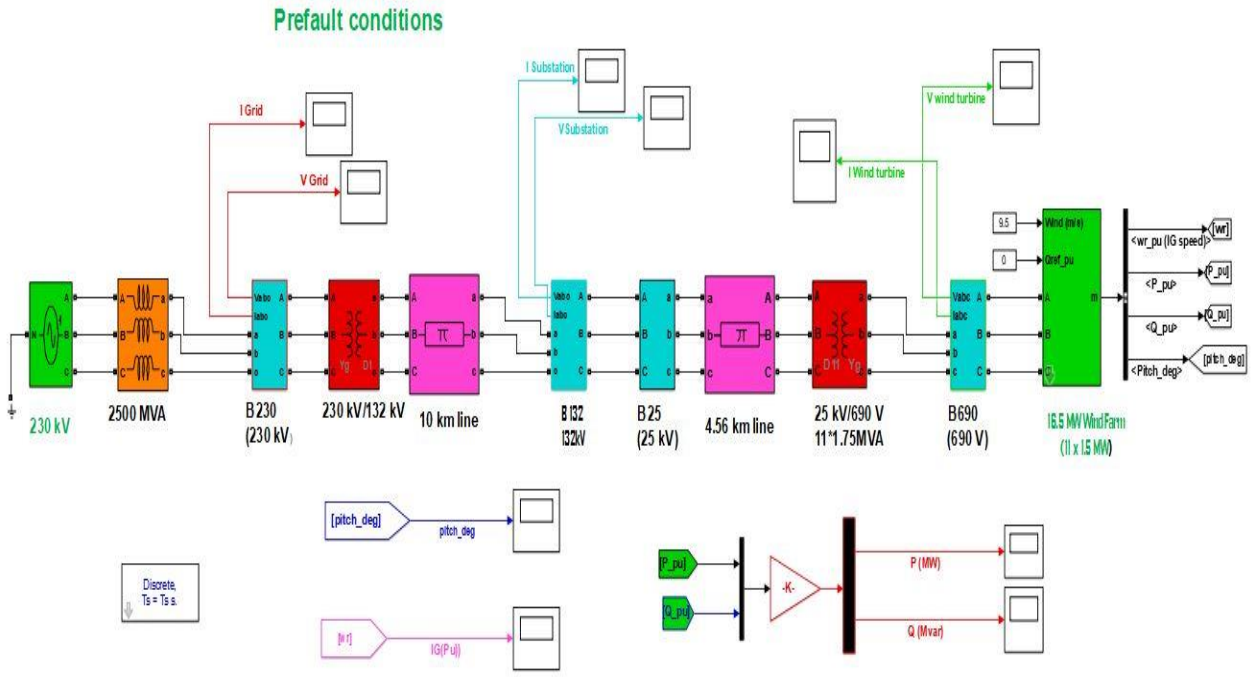

Figure 4-12 Simulation result of DFIG Pre-fault conditions

During pre-fault conditions the voltage is decreased at steady state or starting point of the systems at the ranges of time between 0to0.0125s. After the time of 0.0125s the level is increased to 6.75×10^{3}V during pre-fault condition.

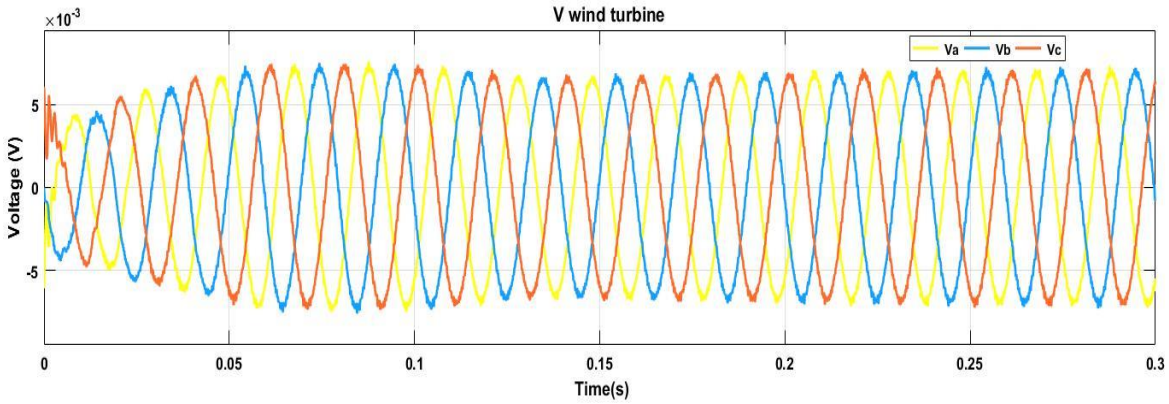

Figure 4-13 Voltage at Wind turbine side

During pre-fault conditions the current at wind turbine side is decreased during steady state or starting point of the systems at the ranges of time between 0to0.0125. This means the current is 2.25×10^{4}A during pre-fault condition.

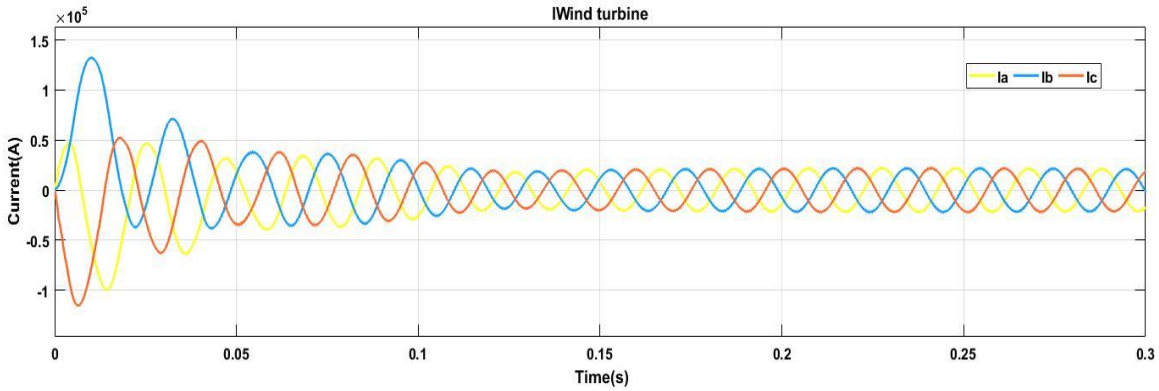

Figure 4-14 current at Wind turbine side

During pre-fault time there is no more loss of power is due load variation at starting point of the systems occurs in real power. In this case during pre-fault time ranges (0-0.015s) real power is around 0MW and after time ranges of start point or steady state real is back to normal condition around 14.89MW.

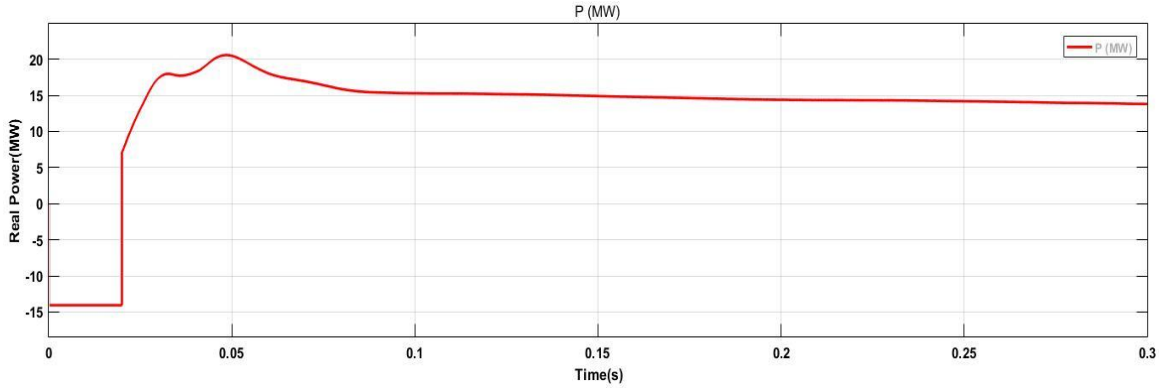

Figure 4-15 Real powers at Wind turbine side

During pre-fault time ranges the reactive power generated is not more as during fault conditions we see from the figure below. During pre-fault time ranges reactive power generated by DFIG is zero MVAr.

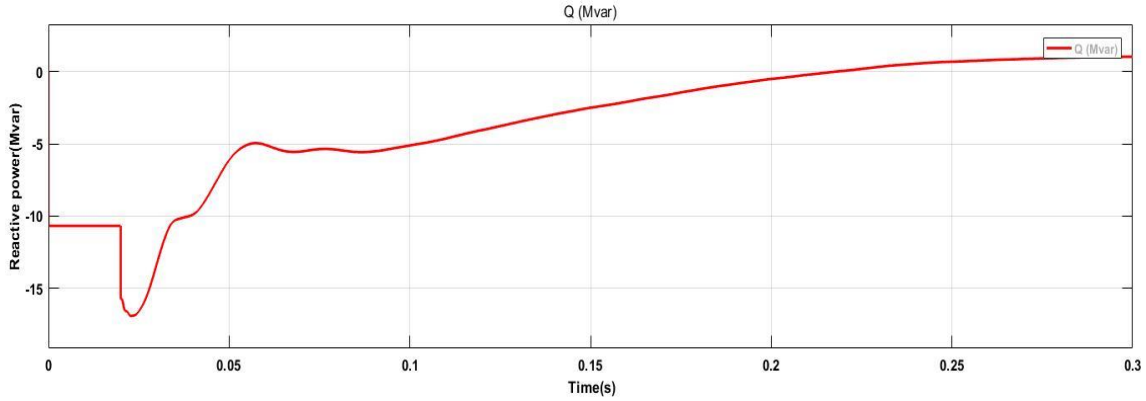

Figure 4-16 Reactive powers at Wind turbine side

The input angle or Pitch angle is increase until the steady state or starting point disturbance time range from 0s-0.06s, the DFIG angle start from 0 degrees to 0.489 degrees after the time ranges pitch angles goes to zero.

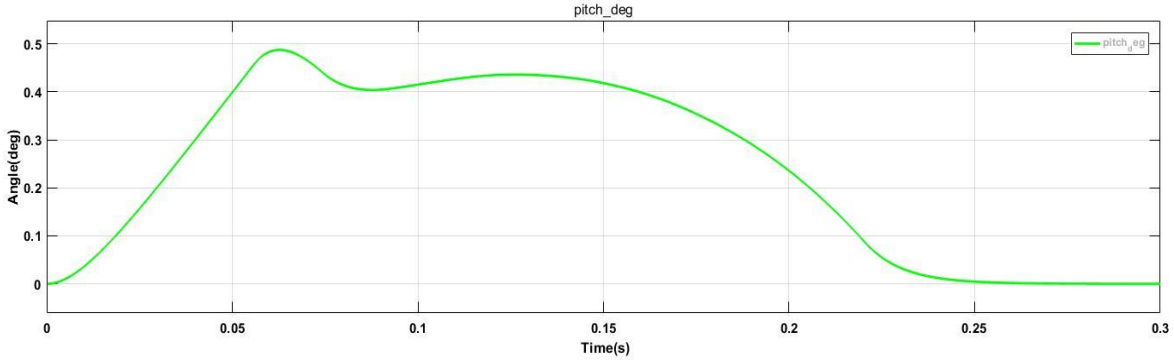

Figure 4-17 Pitch angle at Wind turbine side

The input speed of induction generator is around 9.5m/s. during pre-fault time ranges the speed of induction generator is grownup from 1.2pu to1.203pu at time ranges from 0to 0.0125s and after starting time means after 0.0125s is decline to near to 1.192pu.

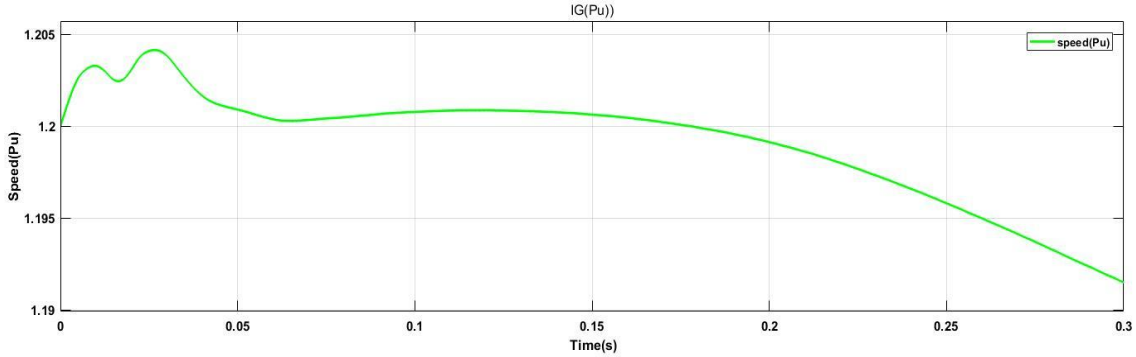

Figure 4-18 Induction generator speed at Wind turbine side

The voltage level at Adama substation during pre-fault conditions time ranges from0to 0.03s, the voltage is reduced 1.15Pu and after starting point of time ranges voltage level is back increase to normal operation which is 1.32Pu.

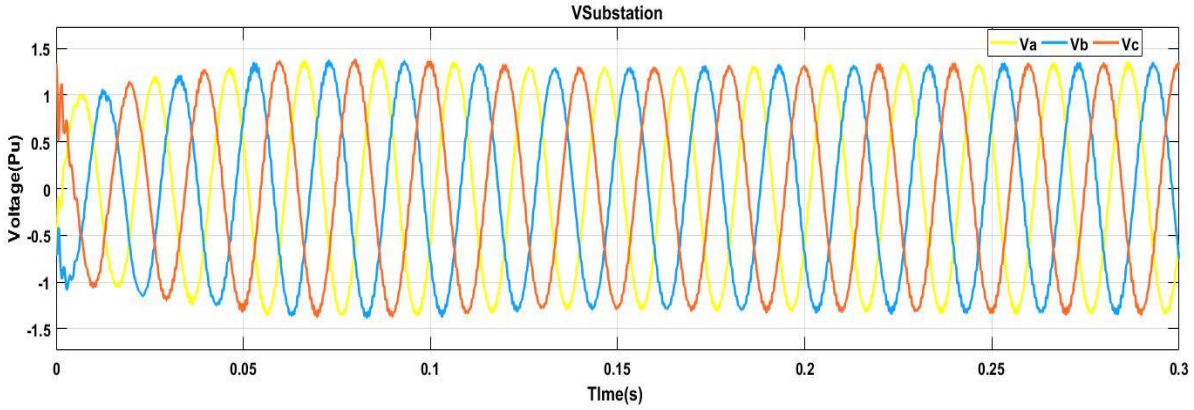

Figure 4-19 Voltage at Adama substations side

In pre fault conditions the current level at Adama substation is distributed at starting point high current fluctions and after starting point of the systems back to normal operations.

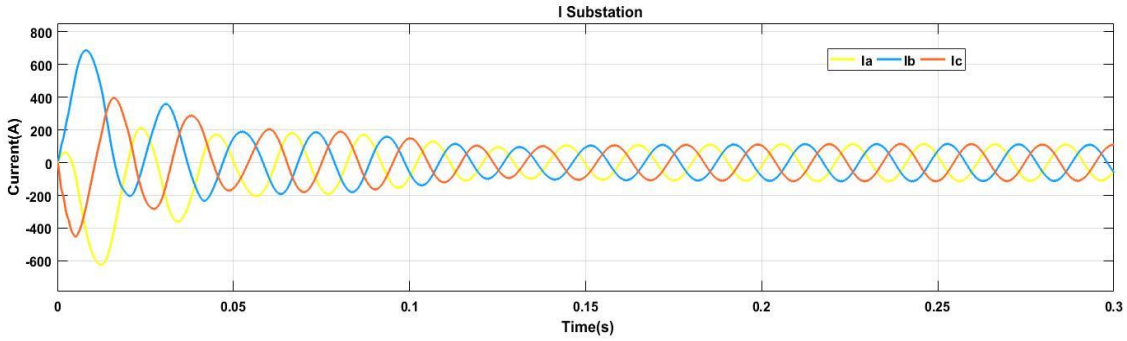

Figure 4-20 Current at Adama substations side

Voltage Level is normal at starting point and the normal operation of voltage is around 1Pu at all-time ranges. The voltage level at grid side is constants for all time variations, shown in Figure4-21.

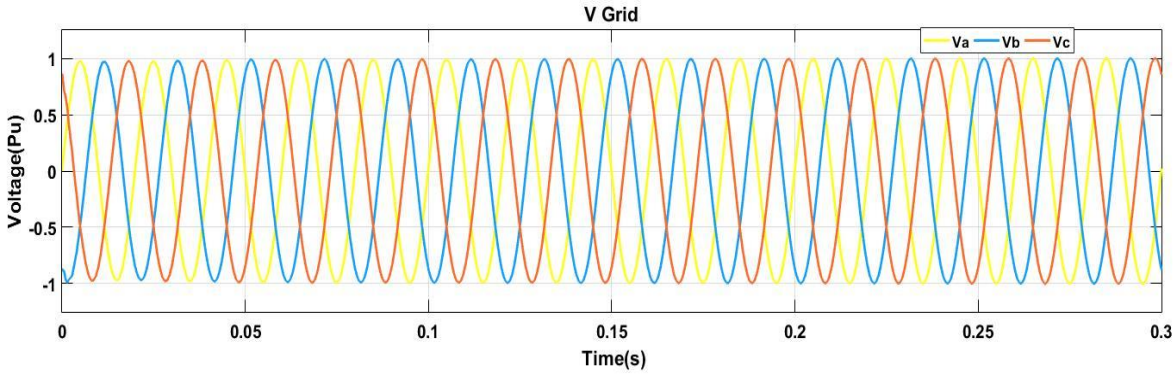

Figure 4-21Voltages at grid side

Current level is grow during starting point time ranges is high current ranges and after starting point of time seconds the current level is decreased as we see from figure below.

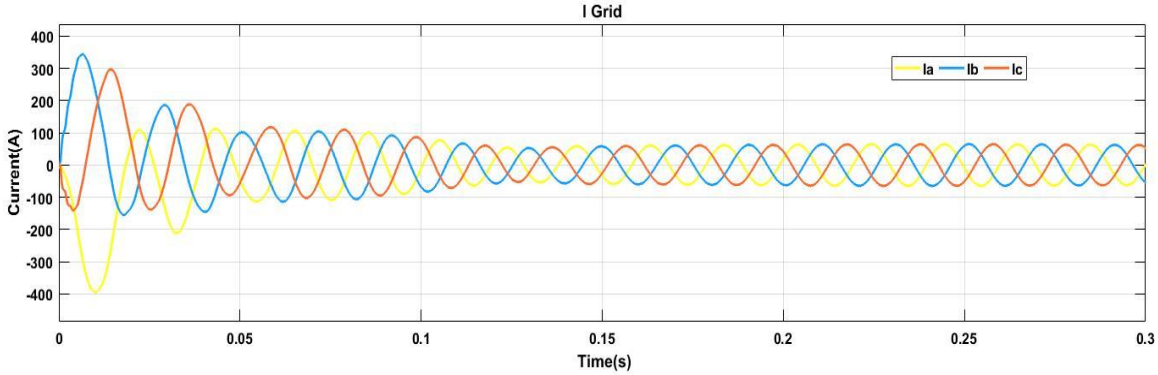

Figure 4-22 Current at Grid side

4.3.2. Simulation result of DFIG during fault condition

During fault conditions the systems is disturbed at time ranges of 0 to 0.1463 s and the systems are normal operations after 0.1463 s when tree phase fault apply to the systems or between substation and wind turbine bus.

.

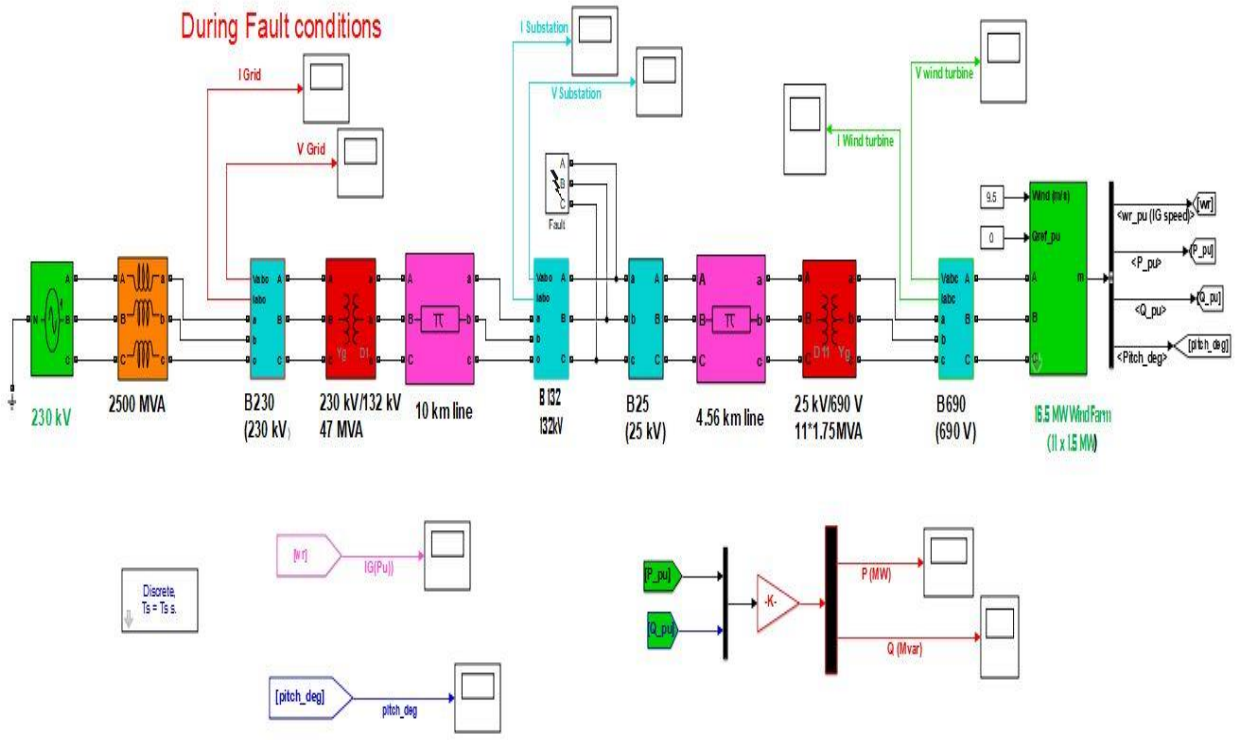

Figure 4-23 Simulation result of DFIG during fault conditions

This three phase fault connected (occurs) to the systems and the systems can be more disturbed due this situations and the result can be as follows:-

During fault conditions the voltage at wind turbine side is decreased during fault time ranges of 0 to 0.1463s. This means the voltage is near to $1 \times 10^3 V$ during fault condition and after fault is removed the voltage level is increased to near $6.75 \times 10^3 V$ after 0.1463s.

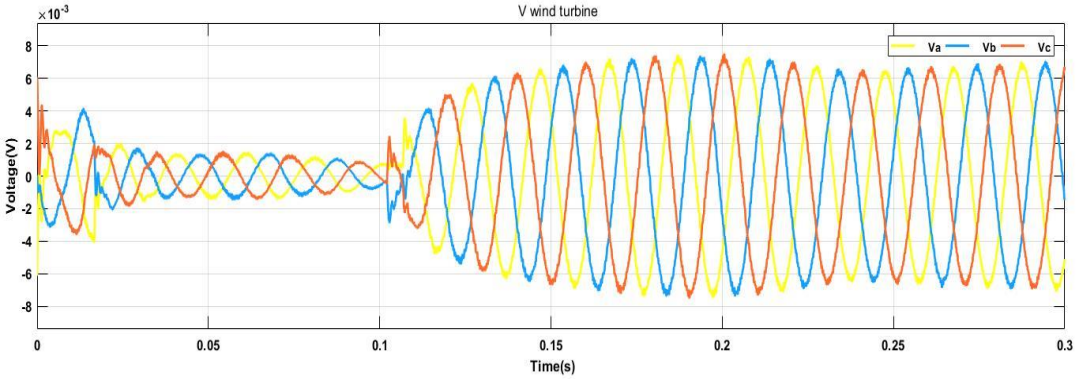

Figure 4-24 Voltages at wind turbine side

During fault conditions the current is increased during fault time. This means during fault time the current is up to $10 \times 10^4 A$ and after fault removed current decrease to near 1×10^4A.

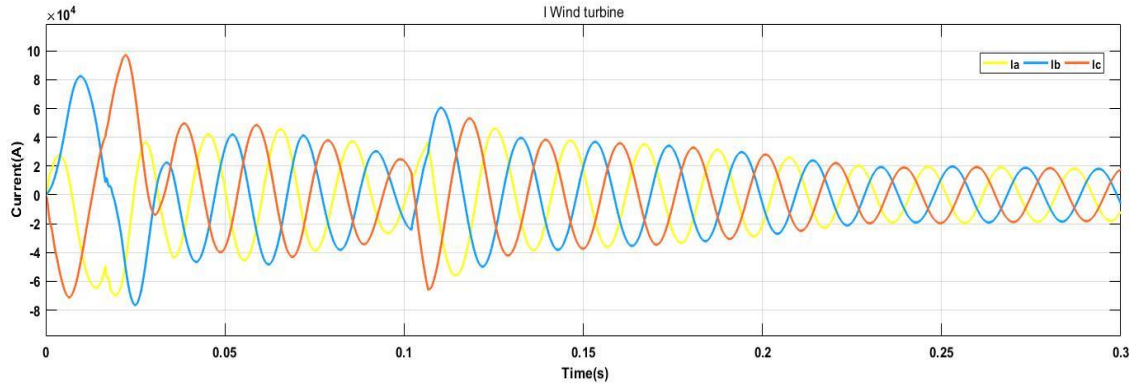

Figure 4-25 Current at wind turbine side

During fault conditions there is over load or loss of power is occurs in real power. In this case during fault time (0-0.1463s) real power is around 0MW and after fault removed real is back to normal condition around 12.5MW.

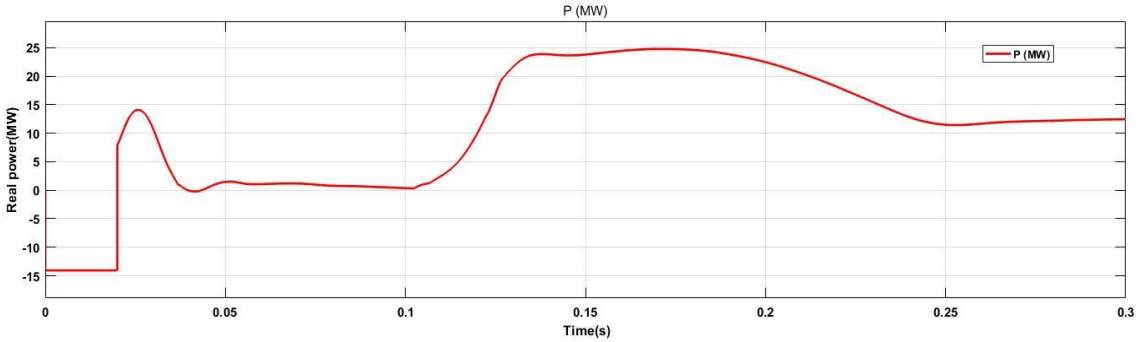

Figure 4-26 Real powers at Wind turbine side

During fault time the reactive power generated is more as we see from the figure below. During fault time reactive power generated by TCSC is 8Mvar during fault time and after fault remove reactive power decline to 0Mvar.

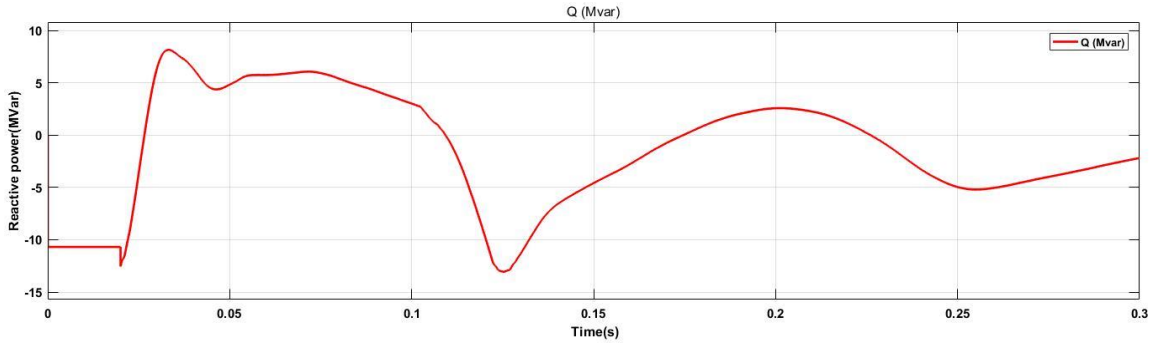

Figure 4-27 Reactive powers at Wind turbine side

The input angle or Pitch angle is increase until the fault is removed from the systems model start from 0 degrees to 1.6degres after the fault removed the angle decrease to zero degrees.

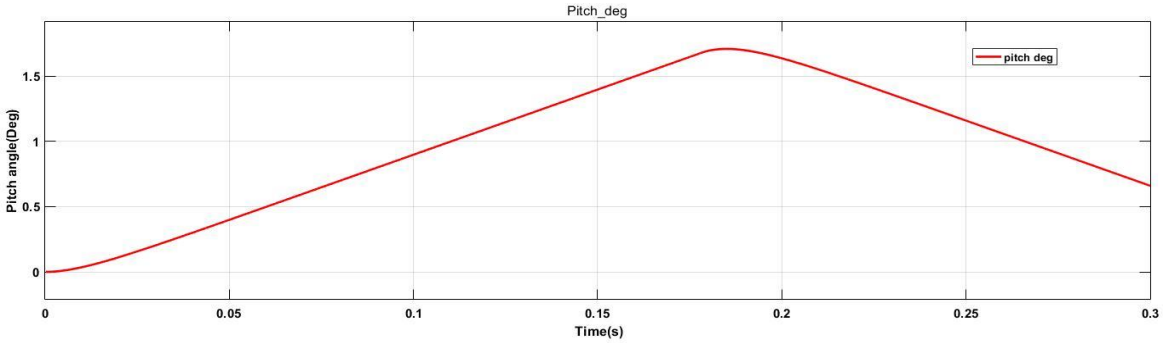

Figure 4-28 Pitch angle at Wind turbine

The input speed of induction generator is around 9.5m/s. during fault time the speed of induction generator is grow up to from 1.2pu to1.23pu after disturbance induction generator speed is near to 1.17pu.

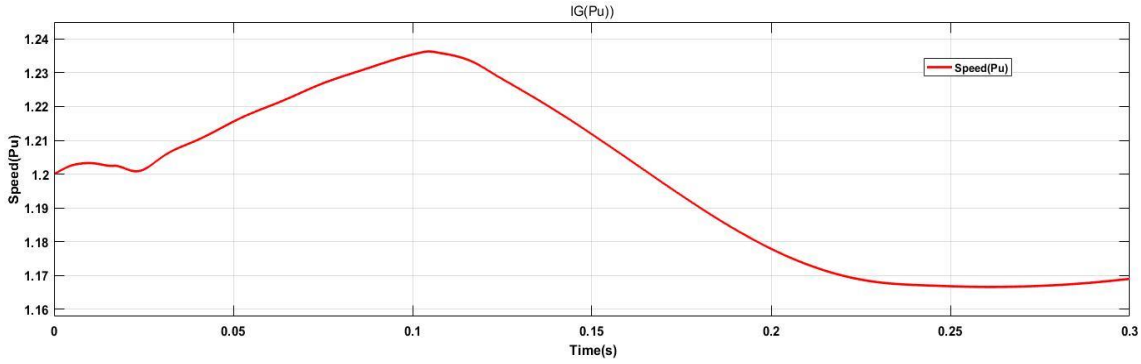

Figure 4-29 Induction generator speed at Wind turbine

Voltage at Adama substation during fault time, the voltage is reduced near zero and after fault removed voltage level is back to normal operation which is 1.32Pu and Voltage more disturbed during fault time.

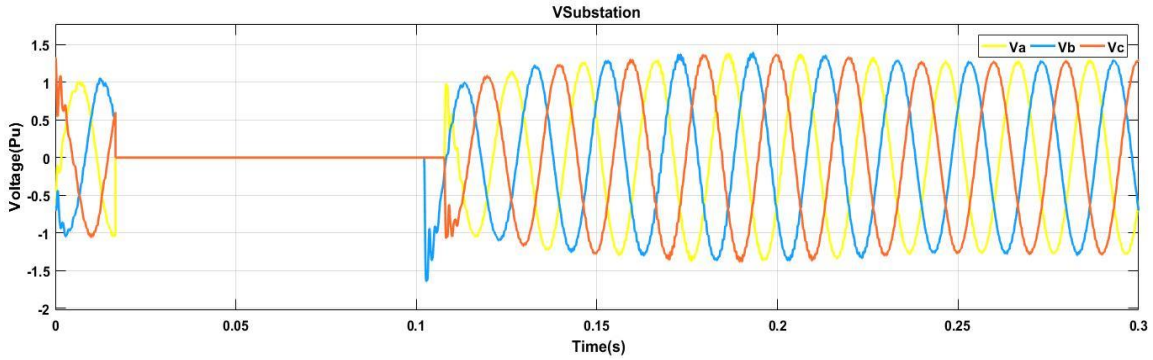

Figure 4-30 Voltage at Adama substations side

The current level at Adama substation is grown up to 5000A and after back from disturbance current is decreased (decline).

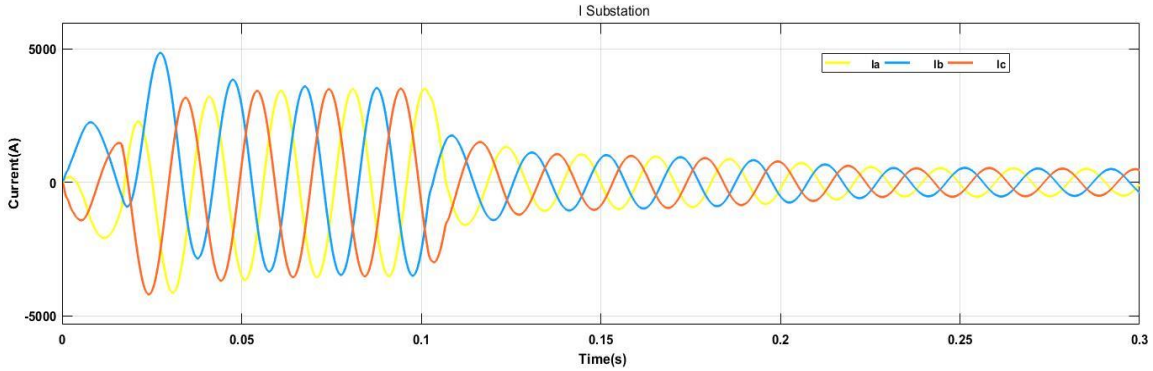

Figure 4-31 Current at Adama substations side

Voltage Level at grid side is affected by three faults, the voltage at grid reduced to 0.9Pu during fault time and after the fault voltage level is increased to 0.976Pu as we see from the figure below.

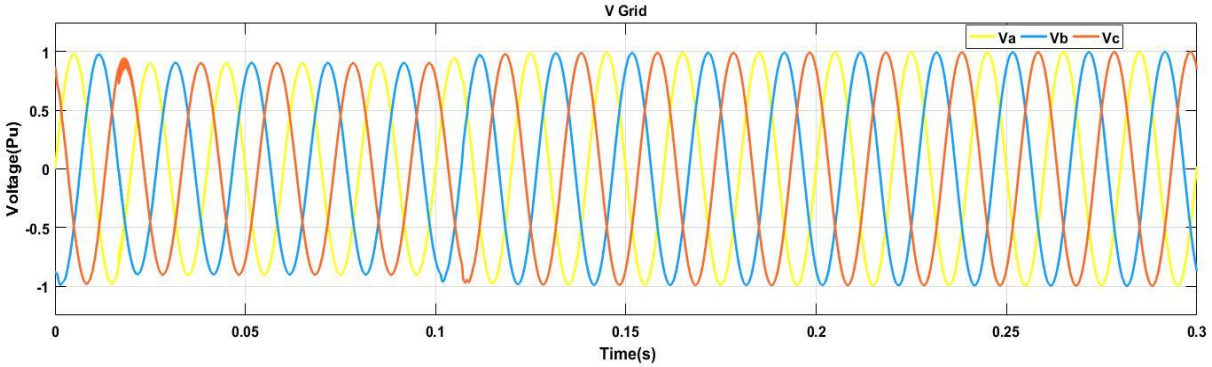

Figure 4-32 Voltage at grid side

Current level is increased during fault time is around 500A and after fault removed the current level is increased to $133A$ as we see from figure below.

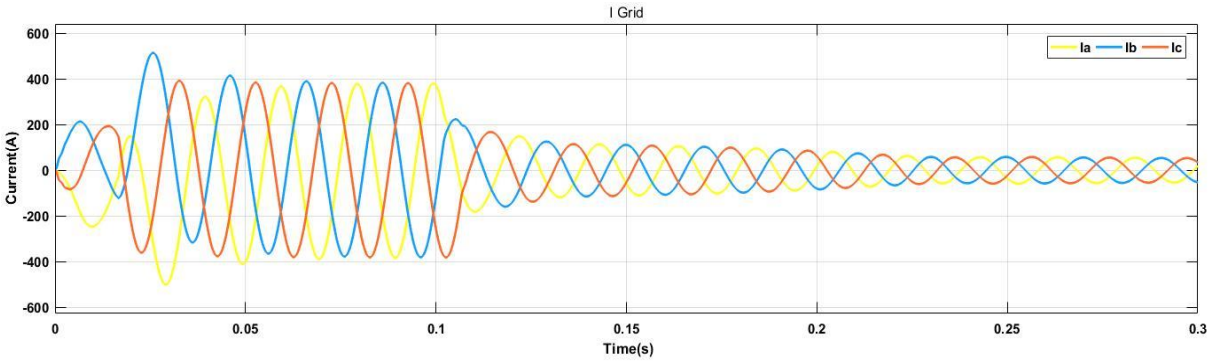

Figure 4-33 Current at grid side

4.3.3. Simulation result of DFIG after fault condition

During fault conditions the systems is almost disturbed at time ranges of 0 to0.1463s and during post fault conditions the systems is only disturbed at starting point the systems, as shows from figure bellows.

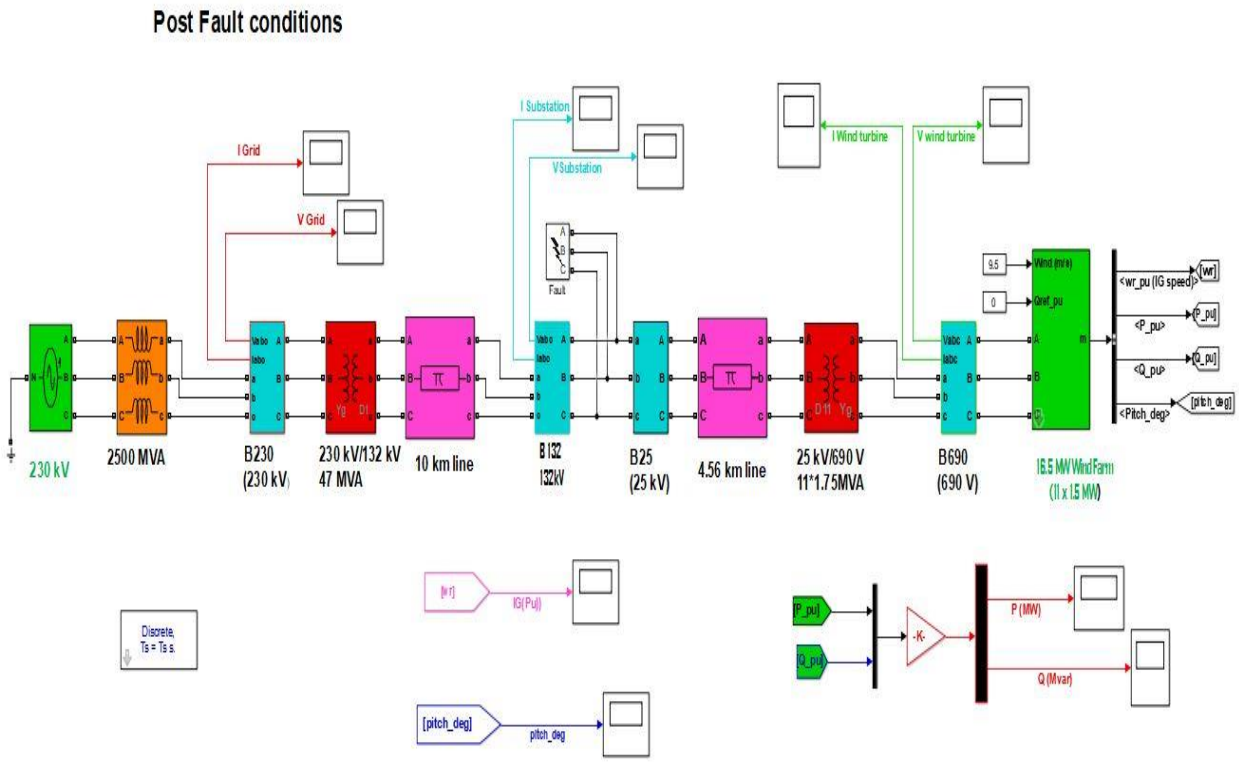

Figure 4-34 Simulation result of DFIG after fault conditions

In this case, the fault is disconnected from the systems, and the DFIG wind turbine system is disconnected from the system because of the grid faults and voltage disturbance on the

voltage source. In this simulation, we understood current, voltage, active power and reactive power, the rotor speed, and the pitch angle of the DFIG wind turbine, and the result can be as follows:-

During post, fault time ranges the starting point the voltage is decreased. This means the voltage is $4 \times 10^3 V$ and after starting points, the voltage level is increased to$6.75 \times 10^3 V$.

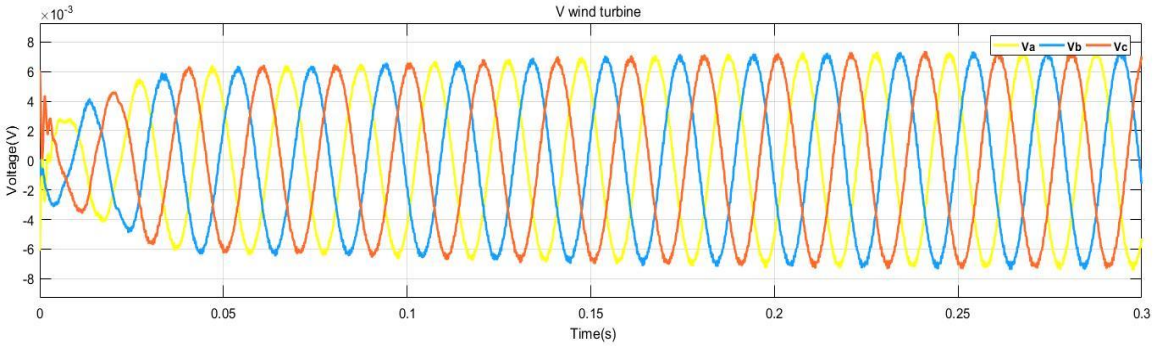

Figure 4-35 Voltages at wind turbine side

During post fault time ranges the current is increased. This means starting point time ranges the current is increased to 8×10^4A and after starting point of current down to 2×10^4A.

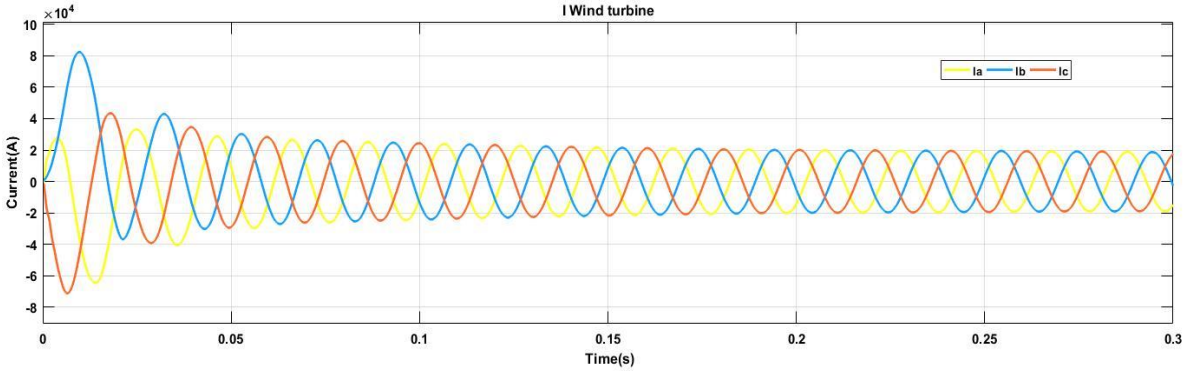

Figure 4-36 Current at wind turbine side

During post fault time there is over load or loss of power is due previous fault (starting times of the systems) occurs in real power. In this case post fault time ranges real power is around 0MW and after time ranges of disturbance real is back to normal condition around 14.5MW.

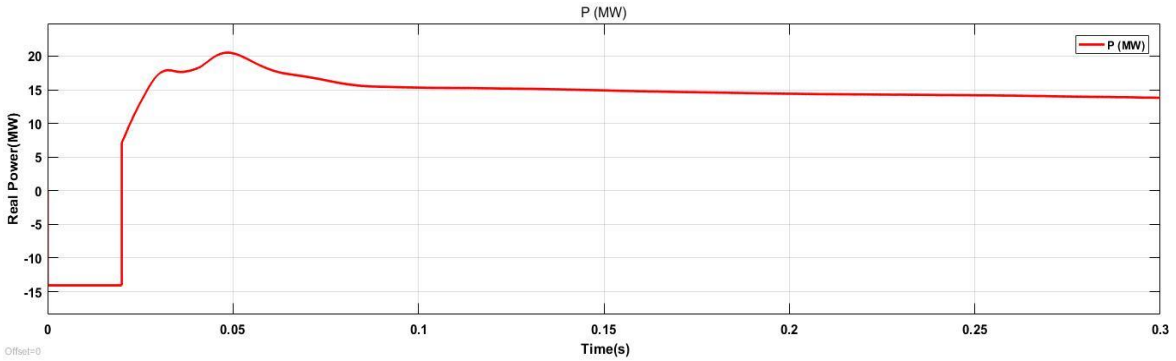

Figure 4-37 Real powers at Wind turbine side

During fault time ranges the reactive power generated is not more as during fault conditions we see from the figure below. During fault time reactive power generated by systems is zero MVar.

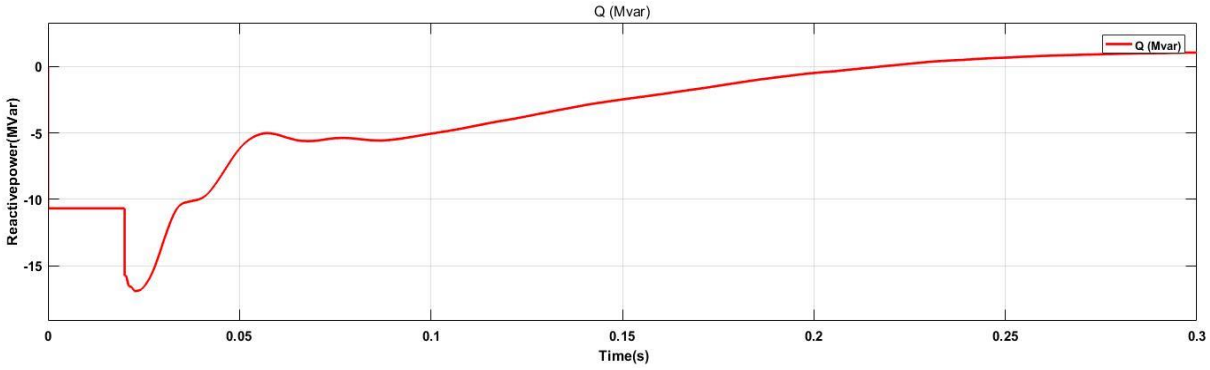

Figure 4-38 Reactive powers at Wind turbine side

The input angle or Pitch angle is increase until the fault time range from 0s-0.056s the DFIG model start from 0 degrees to 0.497 degrees after the time ranges of fault is greater than 0.056s the angle decreases to zero degrees.

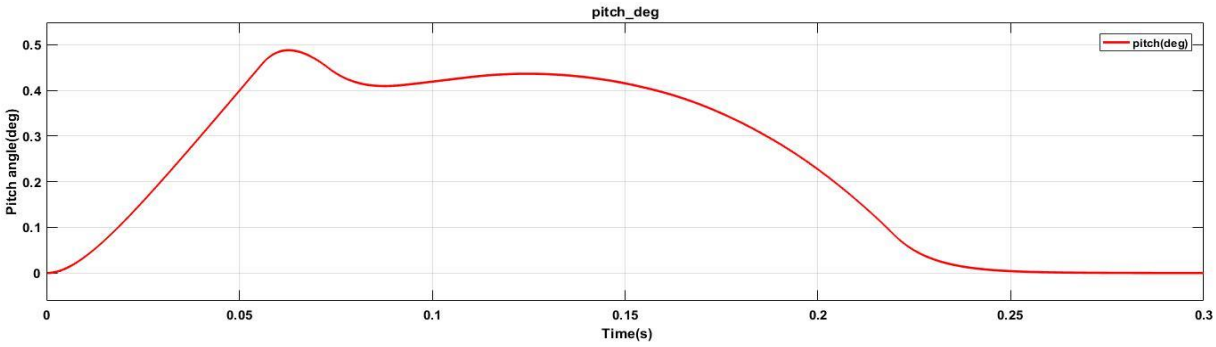

Figure 4-39 Pitch angle at Wind turbine

The input speed of induction generator is around 9.5m/s. during post fault time ranges the speed of induction generator is grownup from 1.2pu to1.204pu after time ranges of disturbance induction generator speed is near to 1.192pu.

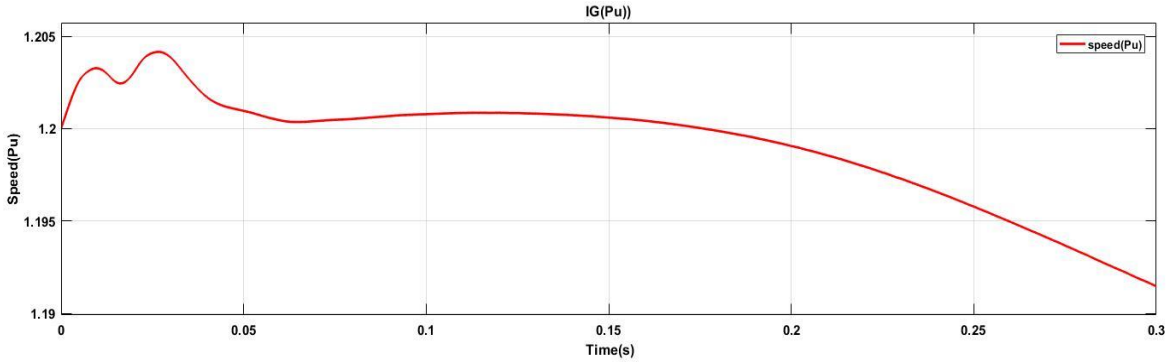

Figure 4-40 Induction generator speed at Wind turbine

Voltage level at Adama substation at post fault time ranges is voltage is reduced $1.18Pu$ and after fault time ranges voltage level is back to normal operation which is $1.32Pu$

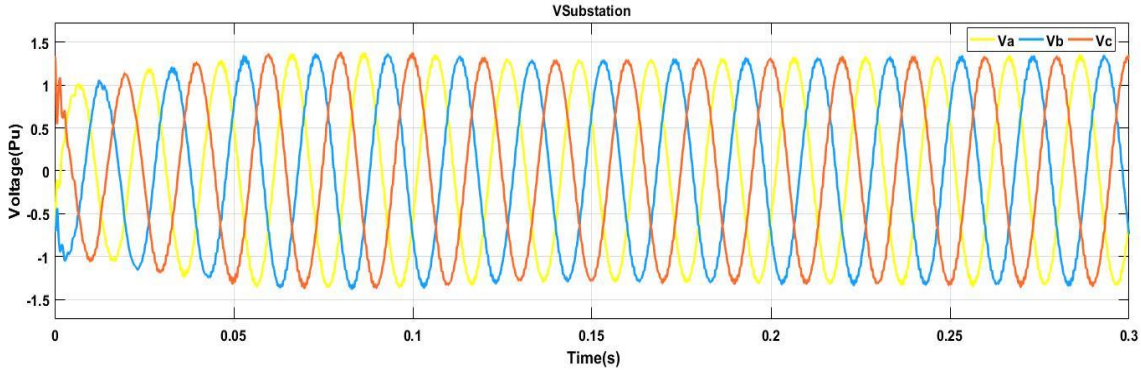

Figure 4-41 Voltage at Adama substations side

The current level at Adama substation is rise at starting point of the systems and after starting time is the current is decreased (decline) to normal operations.

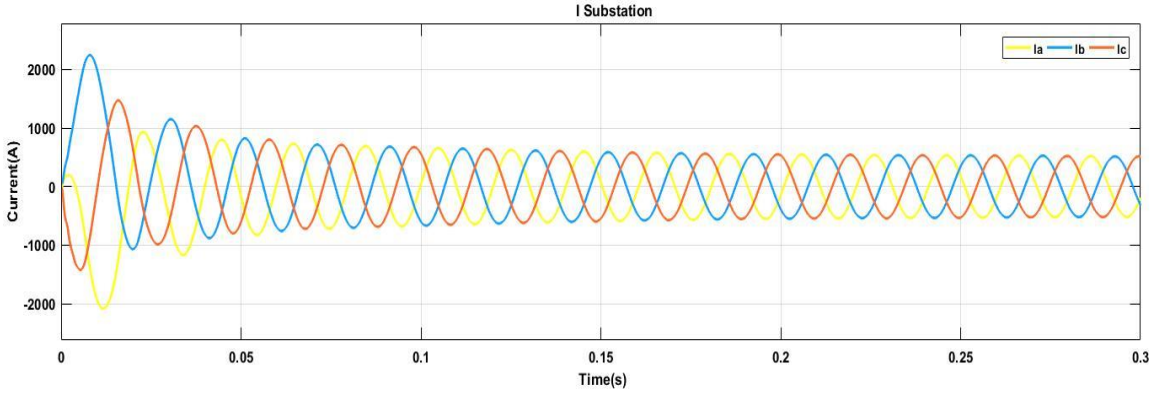

Figure 4-42 Current at Adama substations side

At post fault time voltage Level is doesn't affected by disturbance voltage level is increased to $0.993Pu$ as we see from figure below.

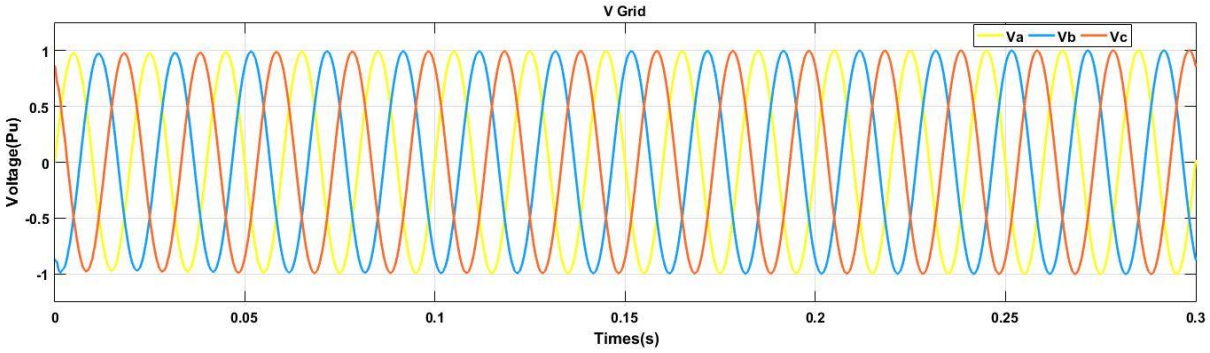

Figure 4-43 Voltage at Grid side

Current level is rise during starting point or initial time range is around $200A$ and after disturbance time, the current level is down to $55A$ as we see from figure below.

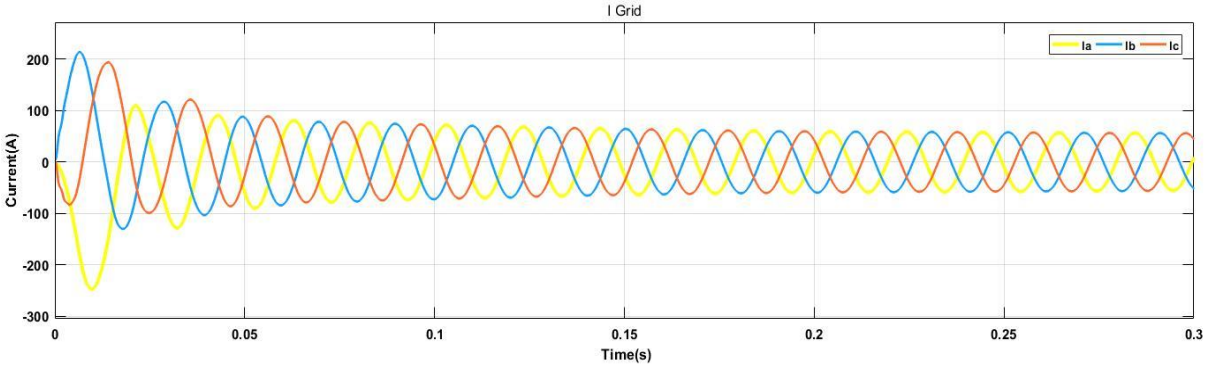

Figure 4-44 Current at Grid side

4.3.4. Simulation result of DFIG improvement using TCSC

For the systems improvement by using TCSC, the TCSC is produce reactive power during fault condition by inject the large amount reactive power in MVar to remove the fault from systems.

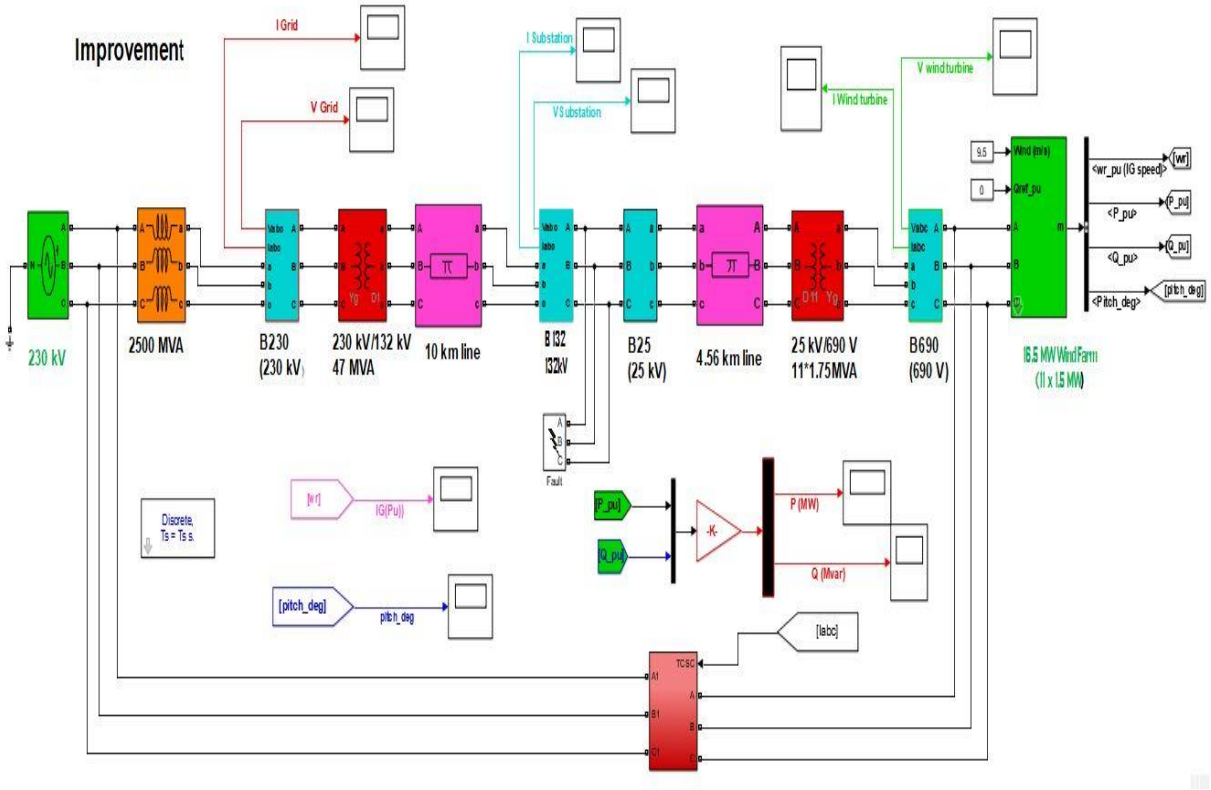

Figure 4-45 Simulation result of DFIG improvement using TCSC

Voltage level is increased during the improvement of the systems (the model). That means the voltage is increased expect at time ranges of 0.1 to 0.15s, at this time ranges the TCSC is does not much control voltage but is more suitable of transient stability improvement.

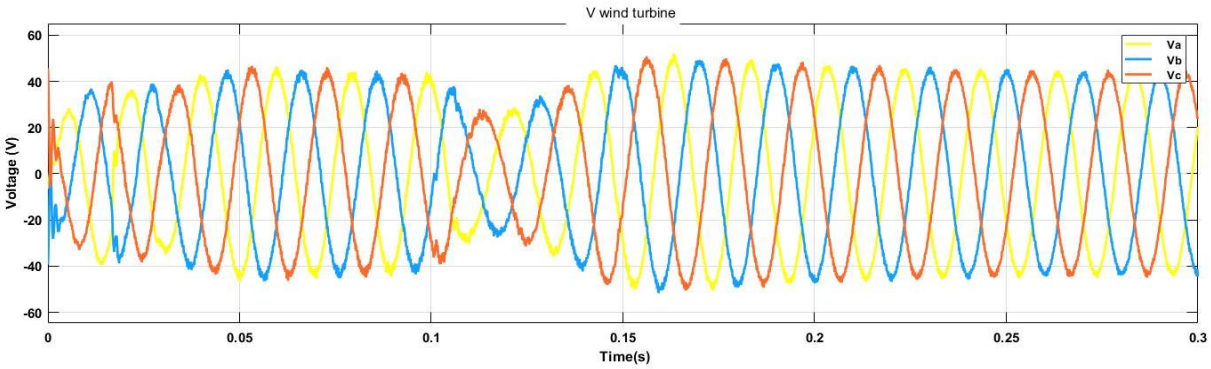

Figure 4-46 Voltage at wind turbine side

The current level is higher at starting point of the systems after steady state the current level decreased (stable) except at initial time.

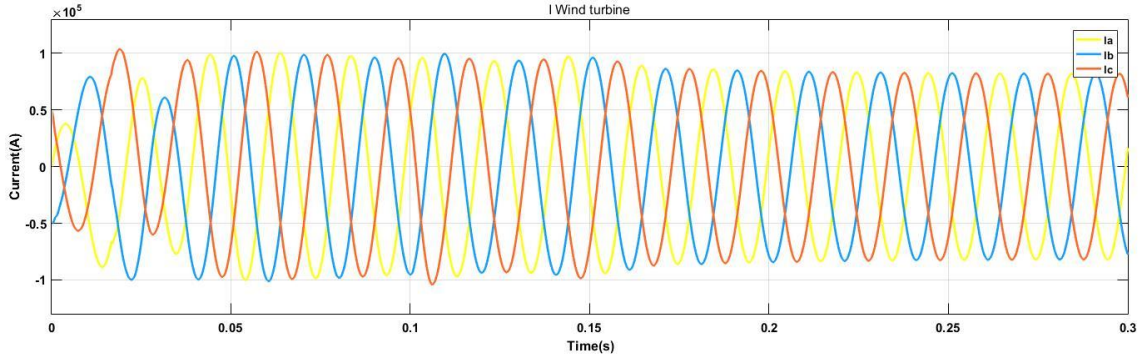

Figure 4-47 Current at wind turbine side

Real power is rise from0 to15.5MW to zero during fault times0to0.1463s and after disturbance real power reach maximum and back to 14.59MW.

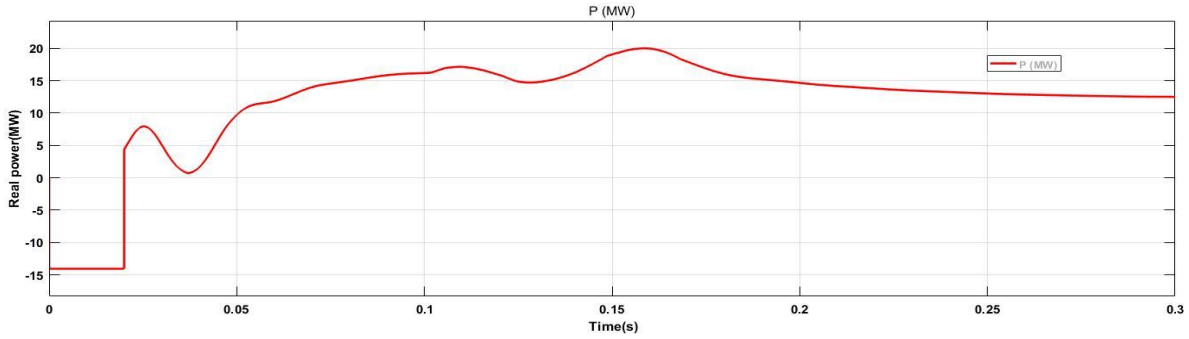

Figure 4-48 Real power of wind turbine

Reactive power is more produced by TCSC during fault time up to 17MVar and after fault is removed from the systems reactive power produced is 0Mvar.

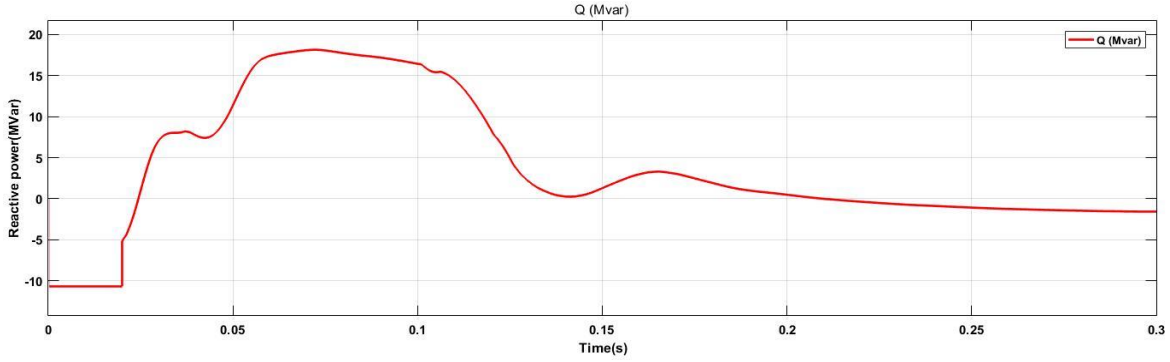

Figure 4-49 Reactive power of wind turbine

Pitch angle is increased up to 1.05degres until the fault removed from the systems and after fault is out from the systems back to Zero degrees.

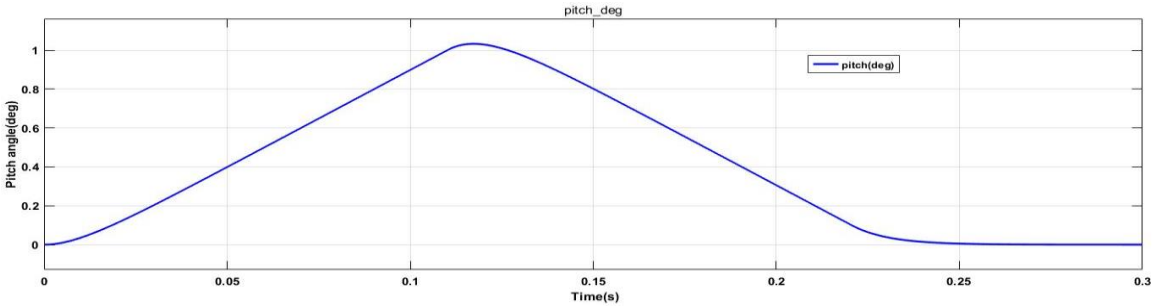

Figure 4-50 Pitch angle of wind turbine

The induction generator speed is increase from 1.2pu to 1.217pu during fault and after fault removed from the systems speed is back to 1.19pu.

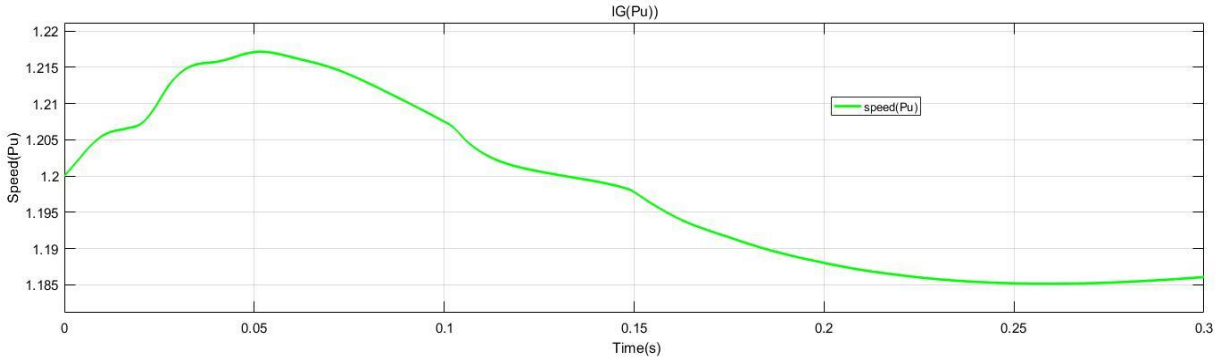

Figure 4-51 Speed of wind turbine

The voltage at substation side during improvement conditions, the voltage is reduced at the initial state 0.86Pu and after initial state the voltage level is back to normal operation near to 1Pu.

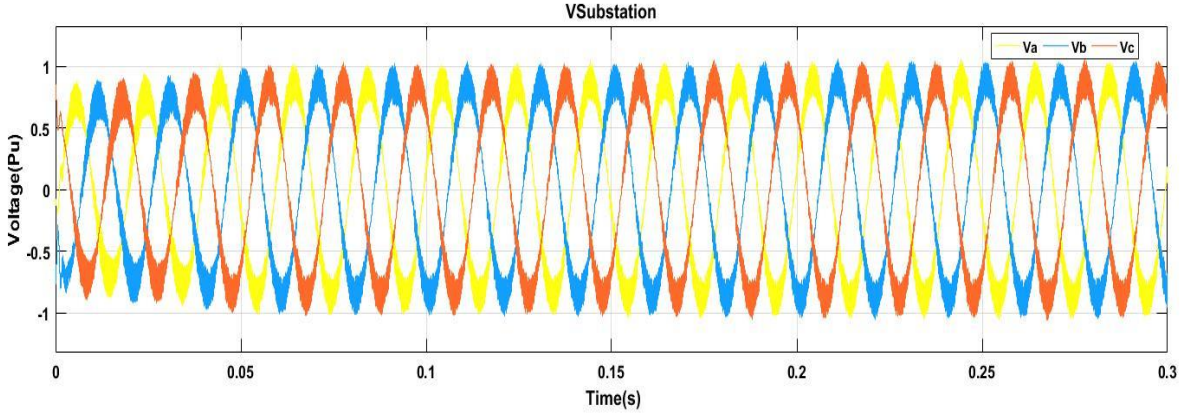

Figure 4-52 Voltage at Adama substation side

At substations the improvement of current disturbed at initial and decreased after initial time ranges or systems current is stable after initial starting point.

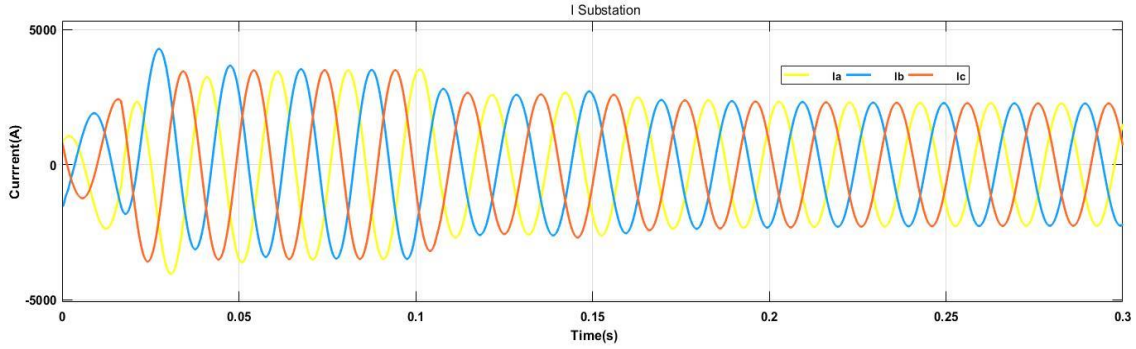

Figure 4-53 Current at Adama substation side

Voltage level at grid side is back normal operation of voltage level is 0.96Pu-0.987Pu and the systems are normal operated at this time.

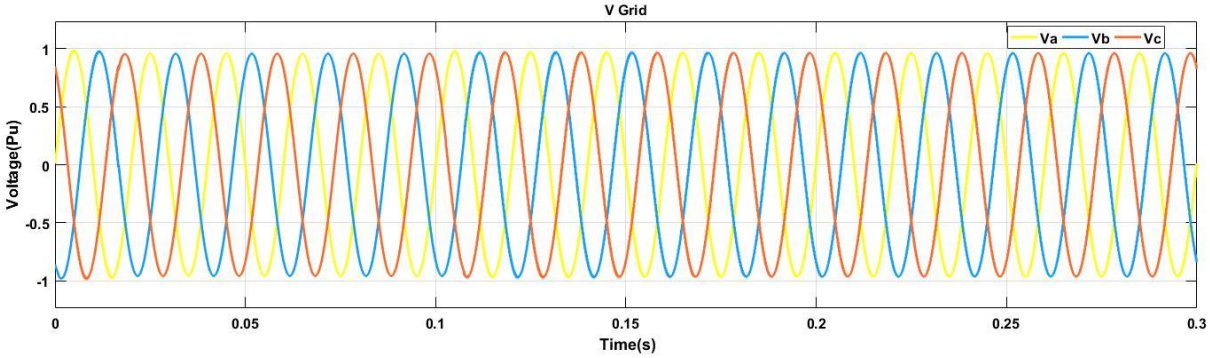

Figure 4-54 Voltage at grid side

During improvement side of the systems current at grid side reduced to 270A and the all systems is more stable.

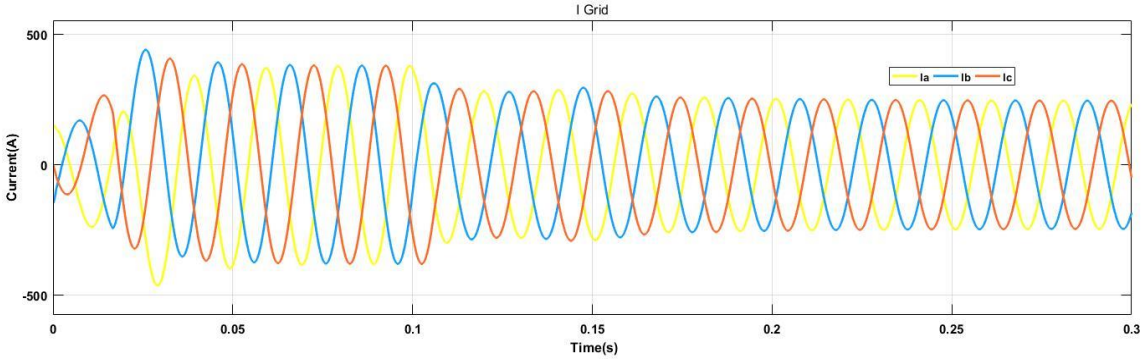

Figure 4-55 Current at grid side

4.4. Comparative results within and without TCSC

The simulation result on figure below is within and figure below is without TCSC, in this simulation result is contains around eight output what I considered in my thesis, real and reactive power, pitch angle and speed of induction generators, voltage and current at wind

turbines, at substation and at grid sides of the systems within and without TCSC and three phase fault is applies in both systems.

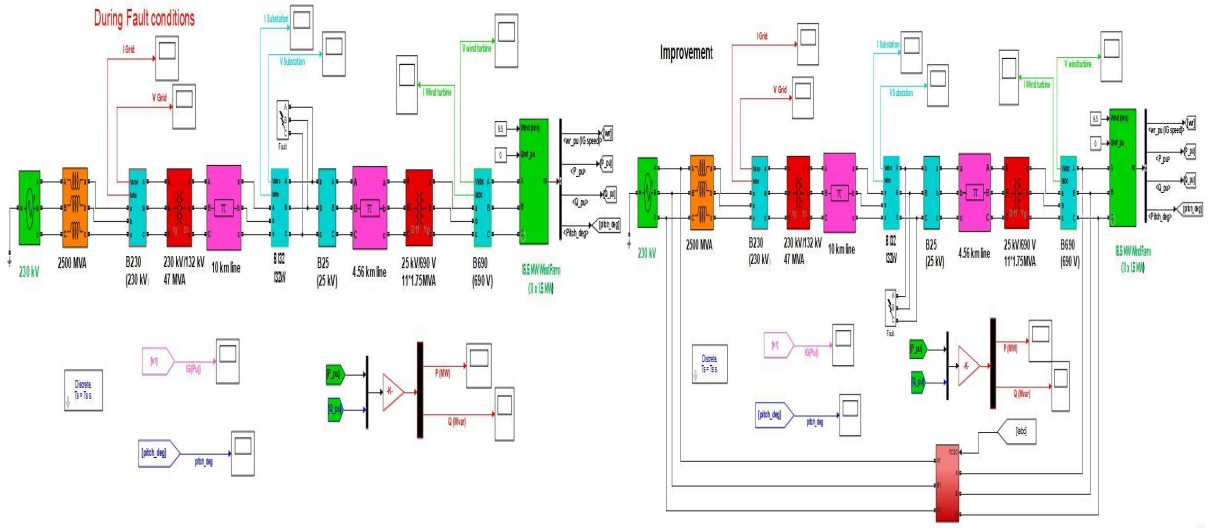

Figure 4-56 simulation result without and within TCSC

During fault conditions means simulation without TCSC the voltage at wind turbine side is decreased during fault time ranges of 0 to 0.1463s. This means the voltage is near to $2 \times 10^3 V$ during fault condition and after fault is removed the voltage level is increased to near $6.75 \times 10^3 V$ after 0.1463s as shown in the figure below but Voltage level is increased during the improvement of the systems. That means the voltage is increased expect at time ranges of 0.1 to 0.15s, at this time ranges because the TCSC is does not much control voltage level but is more suitable of transient stability improvement as seen from figure below.

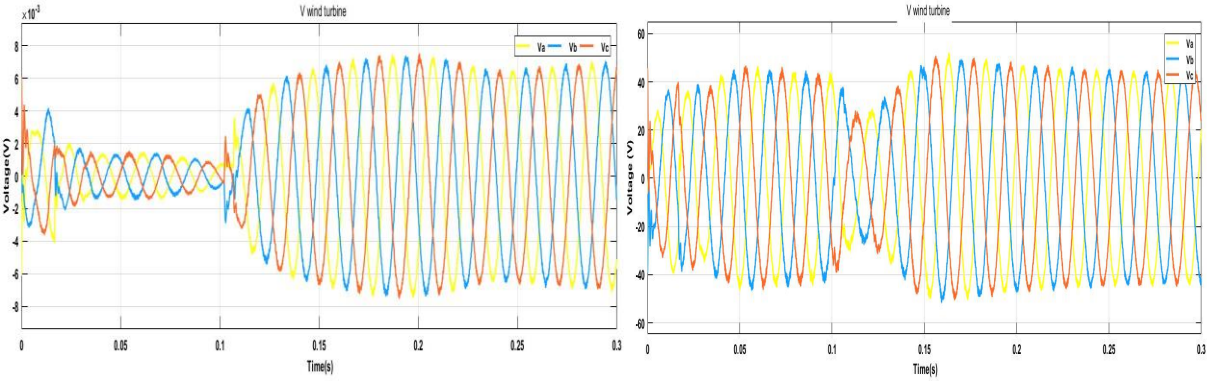

Figure 4-57 Voltage at wind turbine side without and within TCSC

During fault conditions or without TCSC the current is increased during fault time. This means during fault time the current is up (near) to $10 \times 10^4 A$ and after fault removed current

decrease to near 3×10^4A as indicates from figure below, current level is not constant, but the current level is medium except at initial time as shown from figure below its means its constant sinusoidal wave from, general the disturbance is removed from the due to the TCSC.

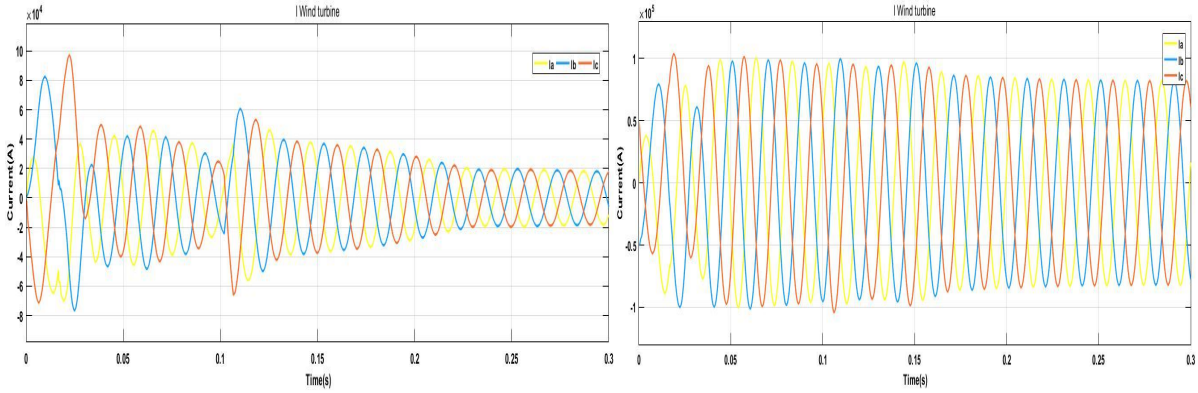

Figure 4-58 Current at wind turbine side without and within TCSC

During fault conditions or without TCSC there is over load or loss of power is occurs in real power. In this case during fault time (0-0.1463s) real power is around 0MW and after fault removed real is back to normal condition around 12.5MW figure below but in within TCSC Real power is rise from0 to15.5MW to zero during fault times 0to0.1463s and after disturbance real power reach maximum and back to 14.59MW in the figure below separately.

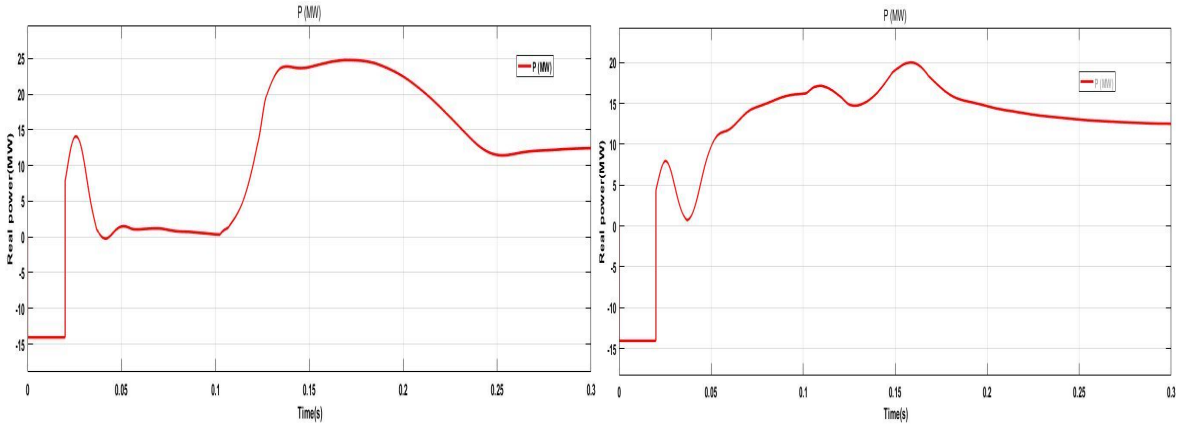

Figure 4-59 Real power without and within TCSC

During fault conditions or without TCSC the reactive power generated is less as we see from the figure below. During fault time reactive power generated by reactive loads is 8Mvar during fault time and after fault remove reactive power decline to 0Mvar. But in within TCSC Reactive power is more produced by TCSC during fault time up to 17MVar and after fault is removed from the systems reactive power produced is 0Mvar shown in the figure below respectively.

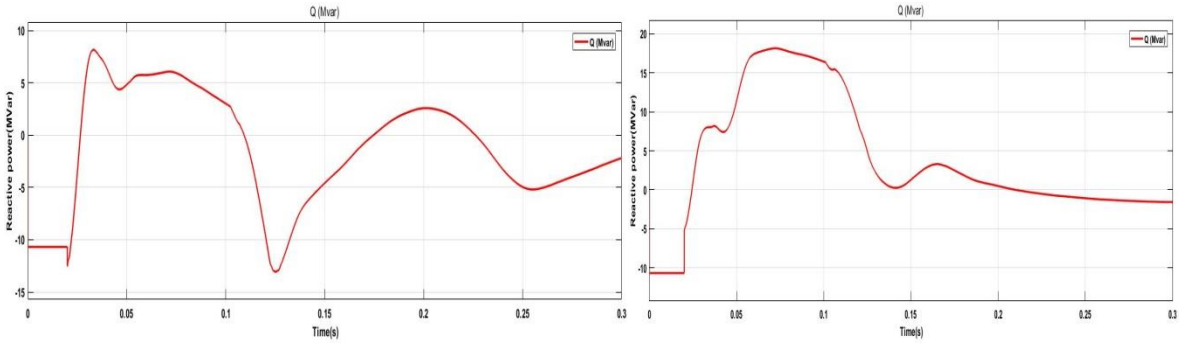

Figure 4-60 Reactive power without and within TCSC

The input angle or Pitch angle is increase until the fault is removed from the systems model start from 0 degrees to 1.6degres after the fault removed the angle decrease to zero degrees as seen from figure below but within TCSC Pitch angle is increased up to 1.05degres until the fault removed from the systems and after fault is out from the systems back to Zero degrees in the figure below separately.

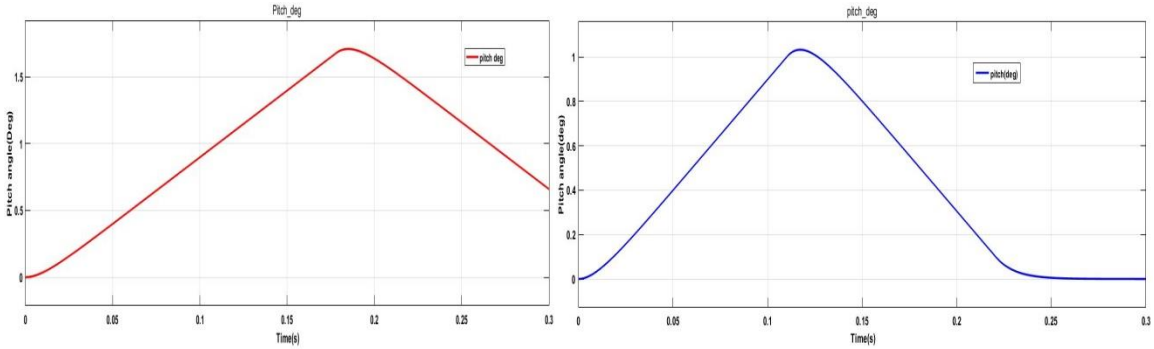

Figure 4-61 Pitch angle without and within TCSC

The input speed of induction generator is around 9.5m/s. during fault time the speed of induction generator is grow up to from 1.2pu to1.23pu after disturbance induction generator speed is near to 1.17pu (figure below) but within TCSC, DFIG speed is increase from 1.2pu to 1.27pu and after fault removed from the systems speed is back to 1.19pu as seen from figure below respectively.

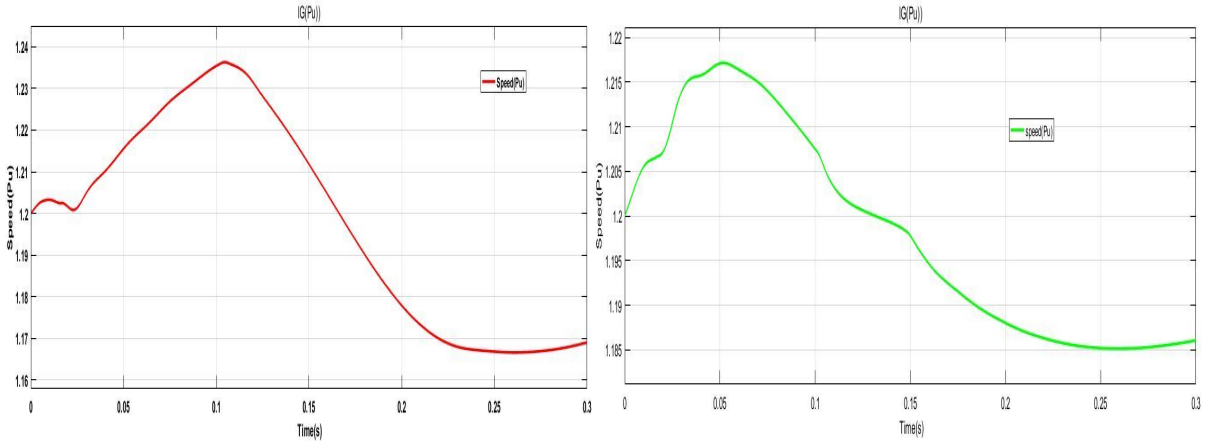

Figure 4-62 Induction generator speed without and within TCSC

Voltage at Adama substation during fault time, the voltage is reduced 1Pu and after fault removed voltage level is back to normal operation which is $1.32Pu$ and Voltage more disturbed during fault time from figure below but within TCSC during fault time, The voltage at substation side during improvement conditions, the voltage is reduced at the initial state 0.86Pu and after initial state, the voltage level is back to normal operation near to 1Pu as we seen from the figure 4-63 correspondingly.

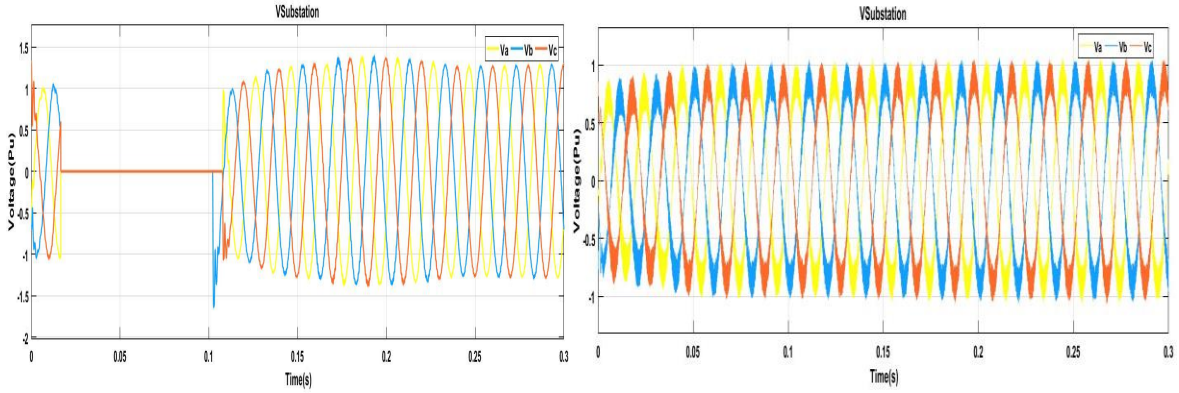

Figure 4-63 Voltage at substation side without and within TCSC

The current level at Adama substation is grown up to 5000A and after back from disturbance current is decreased or decline in the figure below but within TCSC, the improvement of current at substation decreased initial as well as after initial time ranges to constant wave as shown in figure below respectively.

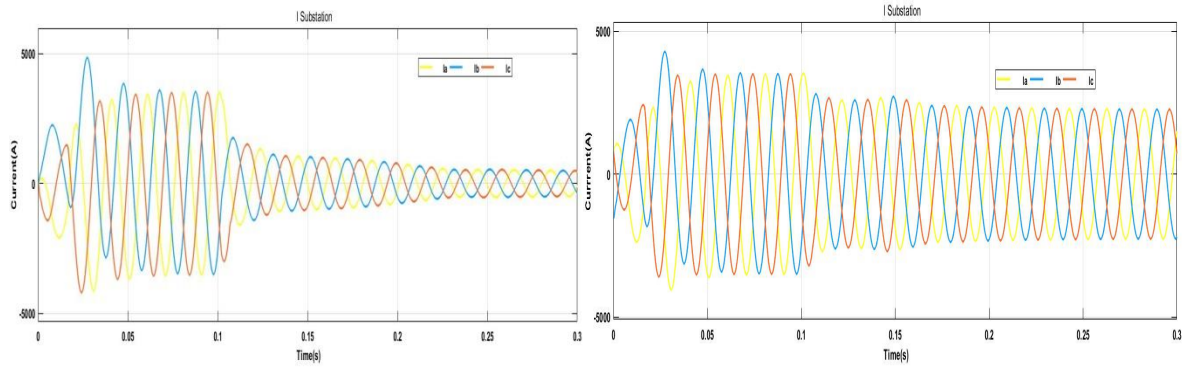

Figure 4-64 Current at substation side without and within TCSC

Voltage Level at grid side small affect by three faults, the is voltage about 0.9Pu and the voltage level is increased to $0.976Pu$ after disorder as we see from figure below but within TCSC Voltage level at grid side is improved because the fault is little bit far from fault location and the grid voltage is ranges from 0.96-0.987Pu in the figure below correspondingly.

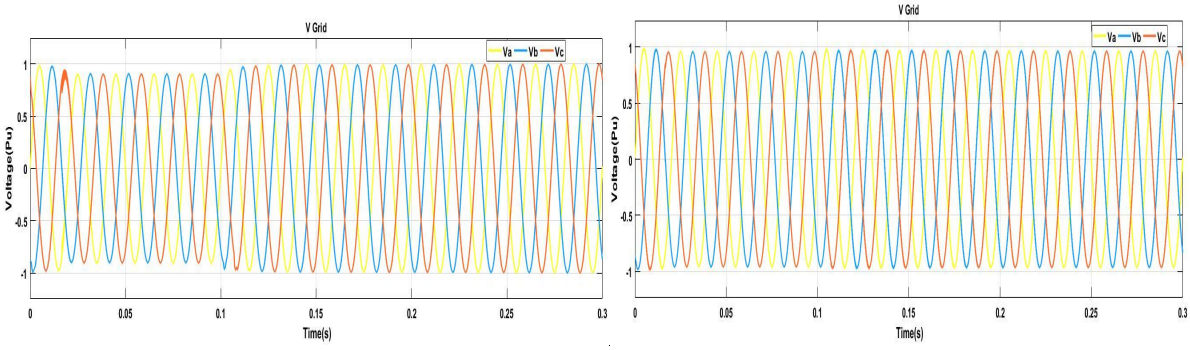

Figure 4-65 Voltage at grid side without and within TCSC

Current level is increased during fault time is around 500A and after fault removed the current level is increased to $133A$ as we see from figure below but within TCSC, the improvement the current at grid side reduced to 100A and the all systems is more stable in the figure below separately .

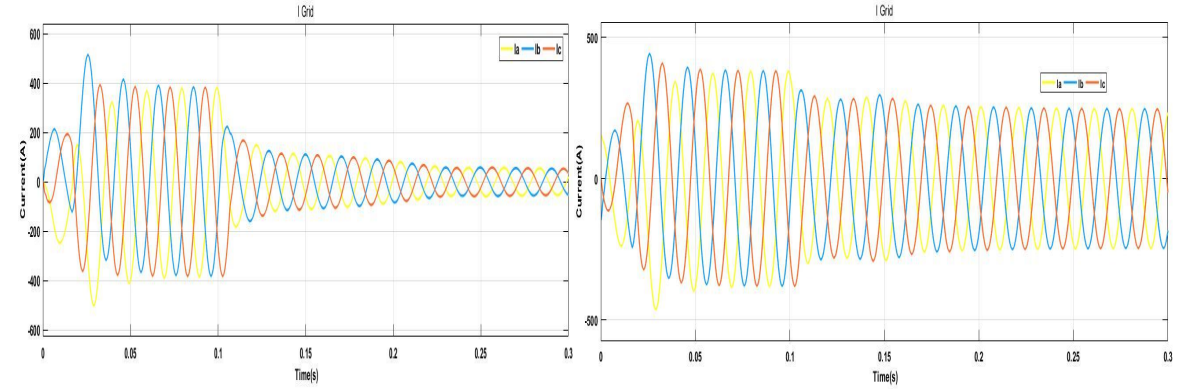

Figure 4-66 Current at grid side without and within TCSC

4.5.Angle clearing fault

Angle clearing fault of DFIG of Adama wind farm from the calculation in chapter three under designing of transient stability analysis of electrical power during pre-fault, post fault, and during fault as well as from mat lab coding on appendix D. This means when a fault occurs on the systems or Adama wind farm of Cluster A is the fault remove at an angle of 53.6 degrees and shown in the figure below.

Transient stability output is as follows:-

Pm1 = 2.0425

Pi = 1

del0 = 29.3143

Pm2 = Inf

Pm3 = 1.3298

delm = 131.2361

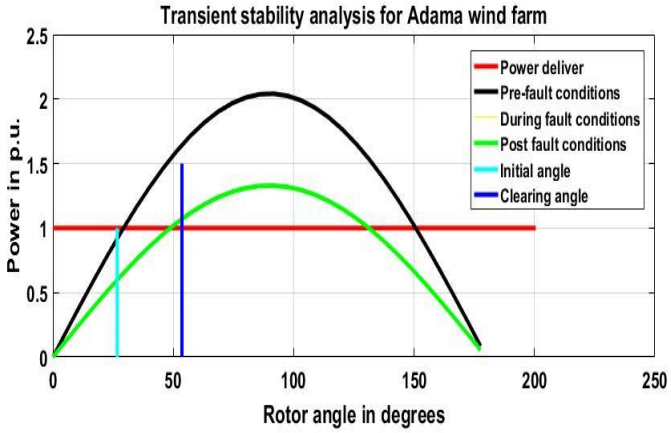

Figure 4-67 Angle clearing fault of Adama wind farm for cluster A

Chapter Five

5. Conclusion and Recommendations

5.1.Conclusion

The Adama II wind farms are located 95Km from Addis Abeba and 7Km Adama. According to Ethiopian statistics has a large(great) wind energy capacity ranges from 2005MW-18645MW with wind speed ranges from 7.5-8-8.8m/s and more than 8.8m/s correspondingly at 50m height of the towers.

Power system stability is the capacity of the power system back to normal working principle after disorder. The wind prediction is depended on weather or climate of the air atmosphere and it's classified into three, one is physical approach, second is a statistical approach, and third is learning approaches. Transient stability assessment is the basis for the study of DFIG transient stability analysis, it's categorized into two, a qualitative assessment is deals with observing post fault state, and a quantitative is about critical clearing angle and critical clearing time of faults. The operation of DFIG is either gird connected or isolated from the grid.

This thesis presents studying of the variable speed DFIG wind turbine and the grid system is subjected to instabilities; like a loss of power, and three-phase faults. The transient behavior of DFIG contains pre-fault, Post fault and during fault system disturbance was simulated using MATLAB/SIMULINK platform using rotor speed control in dictate to control the slip of the machine. The controllers doing of DFIG is suitable in the regular grid conditions and it is originated that, both active and reactive power keeps a study design in spite of changing wind speed and remaining electrical power delivered to grid is kept constant. During grid disruption; voltage, current, pitch angle, induction generator speed, active and reactive power of DFIG has been observed. The dynamic performance of the existing wind farm and hence the stability of the entire power system can be significantly improved through the installation capacity of TCSC when severe network disturbances occur in the system.

5.2.Recommendation

Based on the studies and results found in this thesis, it is recommended to connect TCSC with in the studied Adama II wind farm as it can enhance steady state and transient stability performances of the wind farm as well as the entire system when severe network disturbances

abnormalities occur in the system. We strongly recommend that Ethiopia electric power (EEP) must consider the option of using TCSC such that for grid protection, can save cost, increase transmission line efficiency and reduce the socio-economic problem.

5.3.Future Work

- In this thesis, the Assessment and enhancement of the transient stability of DFIG based wind farm. That can be extended by considering other dynamic compensation technique such as UPFC and comparing the effectiveness in improving dynamic performance of the wind farm
- In order to increase the stability of the system, we can use other FACTS devices like SVC, STATCOM and etc.
- Thesis work may be carried out to study the effects of wind farm integration on system security, power quality, and power system stability.

Reference

[1] Robert Zavadil, Nicholas Miller, Abraham Ellis, and Eduard Muljadi, "Making Connections, IEEE Power & Energy", Vol. 3, No. 6, November/December 2005.

[2] Y. Chen, "A Comparative Analysis: The Sustainable Development Impact of Two Wind Farms in Ethiopia," SAIS China-africa Res. Inst., no. November, p. 28, 2016.

[3] G. Bekele and A. Abdela, "Investigation of wind farm interaction with Ethiopian electric power corporation's grid," Energy Procedia, vol. 14, no. 0, pp. 1766–1773, 2012, doi: 10.1016/j.egypro.2011.12.1165.

[4] Prabha Kundur "Power System Stability and Control.Pdf." p. 1176, 1994.

[5] P. Kundur et al., "Definition and classification of power system stability," IEEE Trans. Power Syst., 2004, doi: 10.1109/TPWRS.2004.825981.

[6] S. Soued, H. S. Ramadan, and M. Becherif, "Effect of doubly fed induction generator on transient stability analysis under fault conditions," Energy Procedia, vol. 162, pp. 315–324, 2019, doi: 10.1016/j.egypro.2019.04.033.

[7] P. Siva, E. Shanmuga Priya, and P. Ajay-D-Vimalraj, "Maximum Power Tracking of Doubly-Fed Induction Generator using Adaptive Neuro-Fuzzy Inference System," Int. J. Eng. Adv. Technol., no. 3, pp. 2249–8958, 2015.

[8] V. Kumar, A. S. Pandey, and S. K. Sinha, "Stability improvement of DFIG-based wind farm integrated power system using ANFIS controlled STATCOM," Energies, vol. 13, no. 18, pp. 1–18, 2020, doi: 10.3390/en13184707.

[9] B. Babypriya and R. Anita, "Modelling, simulation and analysis of doubly fed induction generator for wind Turbines," J. Electr. Eng., vol. 60, no. 2, pp. 79–85, 2009.

[10] K. Pushpak, B. Kumar, and A. Ravi, "Improving Transient Stability of Wind Farm Using Facts Devices Focused on Statcom," Int. J. Eng. Appl. Sci. Technol., vol. 1, no. 7, pp. 2455–2143, 2016, [Online]. Available: http://www.ijeast.com.

[11] N. E. Akpeke, C. M. Muriithi, and C. Mwaniki, "Contribution of FACTS Devices to the Transient Stability Improvement of a Power System Integrated with a PMSG-based Wind Turbine," Eng. Technol. Appl. Sci. Res., vol. 9, no. 6, pp. 4893–4900, 2019, doi: 10.48084/etasr.3090.

[12] S. S. A. Alhalim and L. A. Alnabi, "Enhancement transient stability of wind power system of doubly-fed induction generator using STATCOM and PI controller," Int. J. Power

Electron. Drive Syst., vol. 10, no. 4, pp. 1977–1985, 2019, doi: 10.11591/ijpeds.v10.i4.1977-1985.

[13] M. N. Eskander, M. A. Saleh, M. N. F. Nashed, and S. Amer, "Superiority of LVRT of Grid Connected Wind Energy Conversion System Using Unified Power Quality Controller," vol. 6, no. 6, pp. 1925–1930, 2015.

[14] R. Syahputra and I. Soesanti, "DFIG control scheme of wind power using ANFIS method in electrical power grid system," Int. J. Appl. Eng. Res., vol. 11, no. 7, pp. 5256–5262, 2016.

[15] M. Rama Sekhar Reddy and M. Vijaya Kumar, "Performance analysis of facts devices for reduction of power quality issues in DFIG based WECS integrated to grid," Int. J. Eng. Technol., vol. 7, no. 3, pp. 49–56, 2018, doi: 10.14419/ijet.v7i3.29.18460.

[16] T. K. Renuka, P. Reji, and S. Sreedharan, "Enhancement of small signal stability of a DFIG-based wind power system using fuzzy logic control," Int. J. Eng. Sci. Technol., vol. 8, no. 3, p. 48, 2016, doi: 10.4314/ijest.v8i3.5.

[17] A. Rashad, S. Kamel, and F. Jurado, "Stability improvement of power systems connected with developed wind farms using SSSC controller," Ain Shams Eng. J., vol. 9, no. 4, pp. 2767–2779, 2018, doi: 10.1016/j.asej.2017.03.015.

[18] I. E. T. Renewable and P. Generation, "Enhancement of transient stability of distribution system with SCIG and DFIG based wind farms using STATCOM," no. 1, pp. 1–16, 2016.

[19] A. Sode-yome, N. Mithulananthan, and K. Y. Lee, "Comprehensive Comparison of FACTS Devices for Exclusive Loadability Enhancement," pp. 7–18, 2013, doi: 10.1002/tee.21785.

[20] M. A. Chowdhury, W. X. Shen, N. Hosseinzadeh, and H. R. Pota, "A review on transient stability of DFIG integrated power system," Int. J. Sustain. Eng., vol. 8, no. 6, pp. 405–416, 2015, doi: 10.1080/19397038.2015.1050480.

[21] D. Azeez, M. A. M. Ali, K. B. Gan, and I. Saiboon, "Comparison of adaptive neuro-fuzzy inference system and artificial neutral networks model to categorize patients in the emergency department," Springerplus, vol.2, no.1, pp. 1–10, 2013, doi: 10.1186/2193-1801-2-416.

[22] N. Rout,) Jagadish, and K. Sethy, "Implementation of Fuzzy Logic Controller for Load Frequency Control in Two Area Power System," 2010.

[23] K. S. Aprameya, “Performance Evaluation Of TCSC Fuzzy Logic Controller In Transient Stability Analysis,” vol. 2, no. 7, pp. 305–309, 2013.

[24] F. Cavallaro, “A Takagi-Sugeno fuzzy inference system for developing a sustainability index of biomass,” Sustain., vol. 7, no. 9, pp. 12359–12371, 2015, doi: 10.3390/su70912359.

[25] A. Narain, “An Overview of Facts Devices used for Reactive Power Compensation Techniques,” vol. 4, no. 12, pp. 81–85, 2015.

[26] L. F. Casey, L. E. Zubieta, J. T. Mossoba, B. S. Borowy, and B. Semenov, “FACTS-Devices and Applications,” pp. 1–30, 2012.

[27] A. Elmitwally, A. Eladl, and J. Morrow, “Long-term economic model for allocation of FACTS devices in restructured power systems integrating wind generation,” IET Gener. Transm. Distrib., vol. 10, no. 1, pp. 19–30, 2016, doi: 10.1049/iet-gtd.2014.1189.

[28] P. Engineering et al., “Study and Analysis of Thyristor Controlled Series Capacitor for Improving of Transmission,” 2017.

[29] Grainger J.J., Stevenson W.D. (1994). “Power System Analysis, New York, NY: McGraw-Hill”.

[30] R. N. Nayak, Y. K. Sehgal, and S. Subir, “Ehv transmission line capacity enhancement Through increase in surge impedance loading level, in Proceedings of the Power India Conference. IEEE”, April 2006, p. 4

[31] B. S. Hsu and D. Ph, “Power Systems - Basic Concepts and Applications Part I,” Power, vol. 105, pp. 1–19, 2012.

[32] A. Y. Abdelaziz, A. M. Ibrahim, and Z. G. Hasan, “Transient stability analysis with equal-area criterion for out of step detection using phasor measurement units,” Int. J. Eng. Sci. Technol., vol. 5, no. 1, p. 1, 2018, doi: 10.4314/ijest.v5i1.1.

[33] S. Paudyal, G. Ramakrishna, and M. S. Sachdev, “Application of equal area criterion conditions in the time domain for out-of-step protection,” IEEE Trans. Power Deliv, vol. 25, no. 2, pp. 600–609, 2010, doi: 10.1109/TPWRD.2009.2032326.,

Appendix

Appendix A: Parameters of all the Clusters of Adama II Wind Farm

Table1: GPS data, distance between each tower and branch impedance of all clusters

Cluster A									
Tower ID No.	Y(m)	X(m)	Branch		Distance (KM)	R(pu/KM)	X(pu/KM)	C($\mu F/KM$	Z(pu/KM)
			From	To					
S 14	944583.1	517705.6	S 14	S 15	0.45	0.011	0.005	0.270	0.012
S 15	944955.2	517959.1	S 15	S 16	0.29	0.007	0.003	0.270	0.008
S 16	945238.8	518020.9	S 16	S 17	0.33	0.008	0.003	0.270	0.009
S 17	945516.4	518207.1	S 17	CCG1	0.10	0.003	0.001	0.270	0.003
S 18	945829.5	516805.6	S 18	CCG1	1.40	0.035	0.014	0.270	0.038
S 19	945564.4	516657.8	S 19	S 18	0.30	0.008	0.003	0.270	0.008
S 20	945353.4	516572.1	S 19	S 20	0.23	0.006	0.002	0.440	0.006
S 21	945211.1	516761.8	S 20	S 21	0.24	0.006	0.002	0.270	0.006
S 22	944405.9	516021.5	S 21	S 22	1.09	0.027	0.011	0.270	0.029
S 23	944187.0	515947.1	S 22	S 23	0.23	0.006	0.002	0.270	0.006
S 24	944001.8	516018.5	S 23	S 24	0.20	0.005	0.002	0.440	0.005
Total					**4.86**	**0.122**	**0.048**	**3.14**	**0.13**
Cluster B									
Tower ID No.	Y(m)	X(m)	Branch		Distance (KM)	R(pu/KM)	X(pu/KM)	C($\mu F/KM$	Z(pu/KM)
			From	To					
S1	942168.1	520288.1	S1	S2	0.24	0.006	0.002	0.270	0.006
S2	942385.6	520384.9	S2	S3	0.29	0.007	0.003	0.270	0.008
S3	942152.1	520563.6	S3	S4	0.30	0.007	0.003	0.270	0.008
S4	942358.7	520774.3	S4	S5	0.18	0.004	0.002	0.270	0.005
S5	942536.0	520774.0	S5	S6	0.20	0.005	0.002	0.270	0.005
S6	942713.6	520687.9	S6	S7	0.20	0.005	0.002	0.270	0.005
S7	942917.4	520687.9	S7	S8	0.18	0.004	0.002	0.270	0.005
S8	943086.2	520639.4	S8	S9	0.21	0.005	0.002	0.270	0.006
S9	943279.6	520727.9	S9	S10	0.20	0.005	0.002	0.270	0.005
S10	943441.0	520614.8	S10	S11	0.39	0.010	0.004	0.270	0.011
S11	943638.4	520273.9	S11	S12	0.45	0.011	0.004	0.270	0.012
S12	944008.3	520522.9	S12	S13	0.17	0.004	0.002	0.270	0.005
S13	944164.8	520458.7	S13	CC	3.57	0.053	0.038	0.440	0.065
Total					**6.18**	**0.126**	**0.068**	**3.14**	**0.146**
Cluster C									
Tower ID No.	Y(m)	X(m)	Branch		Distance (KM)	R(pu/KM)	X(pu/KM)	C($\mu F/KM$	Z(pu/KM)
			From	To					
N59	953525.3	526422.1	N59	N60	0.47	0.012	0.005	0.270	0.013
N60	953063.8	526352.7	N60	N61	0.38	0.010	0.004	0.270	0.010
N61	952684.0	526390.6	N61	N62	0.25	0.006	0.003	0.270	0.007
N62	952452.6	526283.9	N62	N69	2.14	0.053	0.021	0.270	0.057

N69	950671.6	525106.4	N69	N70	0.65	0.016	0.006	0.270	0.017
N70	950364.8	524534.2	N70	N71	0.50	0.013	0.005	0.270	0.013
N71	950165.1	524074.3	N71	N72	2.46	0.062	0.025	0.440	0.066
N74	947705.8	523943.9	N74	N72	0.41	0.010	0.004	0.270	0.011
N72	948012.1	523667.6	N72	N73	0.56	0.014	0.006	0.440	0.015
N73	947627.2	523267.0	N73	N77	0.50	0.013	0.005	0.270	0.014
N76	947185.9	523511.1	N76	N77	0.43	0.011	0.004	0.270	0.012
N77	947169.4	523083.2	N77	N78	0.37	0.009	0.004	0.440	0.010
N78	946794.7	523087.2	N78	CC	0.15	0.002	0.002	0.440	0.003
Total					**9.27**	**0.231**	**0.093**	**4.19**	**0.248**
Cluster D									
Tower ID No.	Y(m)	X(m)	Branch		Distance (KM)	R(pu/KM)	X(pu/KM)	C($\mu F/KM$	Z(pu/KM)
			From	To					
N57	954520.9	527455.0	N57	N58	0.33	0.008	0.003	0.270	0.009
N58	954196.9	527490.3	N58	N29	1.00	0.025	0.010	0.270	0.027
N28	953134.7	527633.2	N28	N29	0.20	0.005	0.002	0.270	0.005
N29	953195.3	527445.9	N29	N30	0.31	0.008	0.003	0.270	0.008
N30	952904.5	527326.0	N30	CCG2	0.85	0.013	0.009	0.270	0.015
N27	952843.8	527678.3	N27	N31	0.25	0.006	0.003	0.270	0.007
N31	952620.8	527564.5	N31	N30	0.37	0.009	0.004	0.440	0.010
N63	952258.8	526775.1	N63	N64	0.23	0.006	0.002	0.270	0.006
N64	952073.0	526645.5	N64	N65	0.23	0.006	0.002	0.270	0.006
N65	951862.4	526556.8	N65	CCG3	0.46	0.007	0.005	0.270	0.008
N68	950968.2	526196.4	N68	N66	0.51	0.013	0.005	0.270	0.014
N66	951475.5	526213.4	N66	N67	0.47	0.012	0.005	0.270	0.013
N67	951424.2	526684.7	N67	CCG4	5.00	0.074	0.053	0.440	0.091
Total					**10.21**	**0.192**	**0.106**	**3.85**	**0.219**
Cluster E									
Tower ID No.	Y(m)	X(m)	Branch		Distance (KM)	R(pu/KM)	X(pu/KM)	C($\mu F/KM$	Z(pu/KM)
			From	To					
N16	954609.9	528324.1	N16	N21	0.61	0.015	0.006	0.270	0.016
N25	953467.7	528093.3	N25	N21	0.74	0.019	0.007	0.270	0.020
N21	954050.2	528555.0	N21	CCG1	0.25	0.004	0.003	0.270	0.004
N22	954023.4	528800.7	N22	N21	0.25	0.006	0.002	0.440	0.007
N19	954265.0	529004.5	N19	N20	0.25	0.006	0.002	0.270	0.007
N20	954030.9	529079.0	N20	CCG2	0.28	0.004	0.003	0.270	0.005
N23	953586.0	528809.9	N23	N24	0.37	0.009	0.004	0.270	0.010
N24	953257.0	528647.6	N24	N26	1.01	0.025	0.010	0.270	0.027
N26	952623.9	527858.4	N26	CCG3	1.06	0.027	0.011	0.270	0.029
N32	951994.7	527314.2	N32	N33	0.16	0.004	0.002	0.270	0.004
N33	951851.8	527381.4	N33	CCG4	0.18	0.003	0.002	0.270	0.003
N34	951667.6	527394.3	N34	N35	0.90	0.023	0.009	0.270	0.024
N35	950908.8	526903.7	N35	CCG5	5.61	0.083	0.059	0.440	0.102
Total					**10.61**	**0.228**	**0.11**	**3.85**	**0.258**

Cluster F									
Tower ID No.	Y(m)	X(m)	Branch		Distance (KM)	R(pu/KM)	X(pu/KM)	C($\mu F/KM$	Z(pu/KM)
			From	To					
N52	956614.1	528029.8	N52	N51	0.25	0.006	0.003	0.270	0.007
N51	956591.6	528281.3	N51	N53	0.44	0.011	0.004	0.270	0.012
N50	957327.4	528524.1	N50	N51	0.77	0.019	0.008	0.270	0.021
N53	956156.5	528265.3	N53	N54	0.64	0.016	0.006	0.270	0.017
N54	955745.8	527779.4	N54	N55	0.46	0.011	0.005	0.270	0.012
N56	955066.4	527772.9	N56	N55	0.23	0.006	0.002	0.270	0.006
N55	955289.3	527813.8	N55	CCG1	0.79	0.012	0.008	0.440	0.014
N49	957195.6	528984.1	N49	N48	0.42	0.010	0.004	0.270	0.011
N48	956782.0	528948.1	N48	N47	0.27	0.007	0.003	0.270	0.007
N47	956520.6	528890.9	N47	N13	1.17	0.029	0.012	0.270	0.032
N13	955368.5	528684.4	N13	N15	0.42	0.011	0.004	0.270	0.011
N15	954972.7	528536.9	N15	CCG2	5.00	0.074	0.053	0.440	0.091
N78	947143.9	523995.6	N78	CCG3	0.09	0.001	0.001	0.440	0.002
Total					**10.95**	**0.213**	**0.113**	**4.02**	**0.243**
Cluster G									
Tower ID No.	Y(m)	X(m)	Branch		Distance (KM)	R(pu/KM)	X(pu/KM)	C($\mu F/KM$	Z(pu/KM)
			From	To					
N1	959170.0	530089.7	N1	N2	0.21	0.005	0.002	0.270	0.006
N2	958996.4	529977.2	N2	N3	0.18	0.004	0.002	0.270	0.005
N3	958835.3	530046.6	N3	N5	0.67	0.017	0.007	0.270	0.018
N5	958172.4	529930.3	N5	N6	0.38	0.009	0.004	0.270	0.010
N6	957824.7	529785.3	N6	N7	0.35	0.009	0.004	0.270	0.009
N7	957496.3	529658.7	N7	N9	0.24	0.006	0.002	0.270	0.007
N9	957253.7	529659.7	N9	N10	0.71	0.018	0.007	0.270	0.019
N10	956550.4	529577.4	N10	N11	0.27	0.007	0.003	0.270	0.007
N11	956307.8	529458.6	N11	CCG1	1.08	0.027	0.011	0.440	0.029
N14	955314.1	529034.9	N14	N12	0.36	0.009	0.004	0.270	0.010
N12	955660.7	528927.7	N12	CCG2	0.55	0.014	0.006	0.440	0.015
N17	954770.4	529087.1	N17	N18	0.27	0.007	0.003	0.270	0.007
N18	954498.1	529062.6	N18	CCG3	5.45	0.136	0.058	0.440	0.148
Total					**10.72**	**0.268**	**0.113**	**3.85**	**0.29**
Cluster H									
Tower ID No.	Y(m)	X(m)	Branch		Distance (KM)	R(pu/KM)	X(pu/KM)	C($\mu F/KM$	Z(pu/KM)
			From	To					
N4	958099.1	530324.5	N4	N8	0.86	0.021	0.009	0.270	0.023
N8	957300.6	530010.1	N8	N36	1.48	0.037	0.015	0.270	0.040
N36	955818.3	529938.3	N36	N37	0.24	0.006	0.002	0.270	0.007
N37	955575.6	529910.8	N37	N39	0.24	0.006	0.002	0.270	0.007
N38	955551.4	530443.4	N38	N37	0.53	0.013	0.005	0.270	0.014
N39	955342.2	529975.3	N39	N40	0.30	0.007	0.003	0.270	0.008
N40	955044.3	529984.8	N40	CCG1	0.48	0.007	0.005	0.270	0.009

N46	954723.3	530485.3	N46	N45	0.28	0.007	0.003	0.270	0.008
N45	954514.9	530299.2	N45	N41	0.29	0.007	0.003	0.270	0.008
N41	954565.6	530018.5	N41	CCG2	0.32	0.005	0.003	0.440	0.006
N42	954296.8	529853.2	N42	N43	0.24	0.006	0.002	0.270	0.006
N44	954077.8	530136.1	N44	N43	0.30	0.008	0.003	0.270	0.008
N43	954061.7	529834.1	N43	CCG3	5.00	0.074	0.053	0.440	0.09
Total					**10.56**	**0.204**	**0.108**	**3.85**	**0.234**

Appendix B: Adama- II wind farm DFIG parameters

Doubly fed induction generator parameters		
Rated Power	1.5MW	1.0pu
Rated stator line-to-line voltage	690V(rms)	
Rated Stator Phase Voltage/Base voltage	398.4V(rms)	1.0pu
Rated Rotor Phase Voltage	79V(rms)	79/398.4=0.1983
Rated Stator current	1110A(rms)	$1110/I_B$=0.8844
Efficiency at rated power	>=97%	
Base current, I_B=1.5MW/sqrt3*690V	1255.11A(rms)	1.0pu
Rated Rotor current	1209.852A(rms)	0.964
Rated stator Frequency	50Hz	1.0pu
Rated Power factor	from cosφ =0.95 inductive to cosφ =0.95capacitive	
Rated stator speed, ωs	1500rpm	1.0pu
Rated Rotor speed	1800rpm	1.0pu
Nominal Rotor speed Range	1000-2000rpm	0.56-1.11pu
Wind Turbine rotor speed range	10.6-21.1rpm	
Rated speed of wind turbine rotor	19rpm	
Rated slip, rated	ws-wr/ws=15001800/1500=0.2	
Number of pole pairs	2	
Transformation Ratio, u	0.42	
Rotor/Stator connection	Delta/Star	
Rated mechanical torque	8.5922KN-m	1.0
Stator winding resistance, R_s	0.006243 Ω	0.006243/0.3174=0.0197
Rotor winding resistance, R_r	0.011074 Ω	0.0349
Stator leakage inductance, Lls	0.198822mH	$Lls*\omega_s/Z_B$=0.000198822*2*л*50/0.3174=0.197
Rotor leakage inductance, Llr	0.198822mH	0.197
Magnetizing Inductance, Lm	3.976mH	3.9354
Base flux linkage, $\psi_B=V_B/\omega s$	1.2681Wb(rms)	1.0pu

Base Impedance, $Z_B=V_B/I_B$=398.4/1255.1	0.3174Ω	1.0pu
Base inductance, LB=ψ_B/I_B	1.0103	1.0pu
Turbine inertia, Jt	85.8	
Generator inertia, Jg(Kg-m2)	67	
Gear box ratio	94.7	
Base capacitance, CB=1/2лfZ_B	10028.7μF	=1.0pu
Air density, p	1.225Kg/m3	
Converter	**Rotor side (two modules are connected in parallel)**	
	IGBT voltage level	1700V
	Max. continuous operating voltage	1100V
	Rated continuous DC voltage	975V
	Grid side(single module)	
	IGBT voltage level	1700V
	Max. continuous operating DC voltage	1100V
	Rated continuous DC voltage	975V
Cpmax	0.4865	
Lambda opt	9	
Stator wiring	Δ	
Rotor wiring	Y	
Δ-winding (stator side)	220V(L-L)	
Y-winding (stator converter)	220V(L-L)	
Induction Generator Used in the Wind Turbine		
Nominal values	values	
Voltage	690V	
Frequency (electrical)	50Hz	
Power	1.8MW	
Machine Parameter		
Stator resistance		0.043pu
Rotor leakage Inductance		0.0613pu
Stator Leakage Inductance		0.0613pu

Mutual inductance		1.0pu
Angular moment of inertia(J)		1.0se
Control model parameter		
Cut in speed	1000r/min	
Speed limit	1800r/min	
Shutdown speed	2000r/min	
Turbine Data		
Shaft stiffness	2.5pu/rad	
Turbine rotor speed range	9.5-2.1rpm	
Rated wind speed	12m/s	
Rotor diameter	75m	
Gear ratio	1:86.5	
Generator Data		
Rated power	2MW	
Rated voltage	690V	
Rated frequency	50Hz	
Stator resistance		0.048pu
Stator reactance		0.075pu
Mutual reactance		3.8pu
Rotor resistance		0.018pu
Rotor reactance		0.12pu
Generator rotor inertia	0.5s	
Number of pole pairs	2	
DC-bus	C=38μF,V_{dc}=1200V	
RI, filter	R_f=0.075Ω,L_f=0.75mH	

Appendix C Coding of input/output characteristics of systems using ANFIS

```
% >>Coding for ANFIS
X=(0:0.1:10)';
y=sin(2*X)./exp(X/5);
trnData=[X y];
numMFs=5;
mfType='gbellmf';
in_fis=genfis1(trnData,numMFs,mfType);
epoch_n=20;
Out_fis=anfis(trnData,in_fis,20);
plot(X,y,X,evalfis(X,Out_fis));
```

```
legend ('TrainingData','ANFISOutput');
```

Appendix D: Angle clear fault using Mat lab coding

```
>> %: Given the Adama wind farm and apply a three phase fault is to wind turbine generator of cluster A
% is carrying 1.0 p.u. Megawatt at the direct preceding the fault.
% Pre fault condition
X1 = 0.612;
E = 1.25;
V = 1.0;
Pm1 = E*V/X1
% Electric power output before fault
%Pe1 = Pm1*sin(del0)
% Pe1 = Pi; Pi = input mechanical power
Pi = 1.0
del0 = asin(Pi/Pm1)*180/pi
% during fault condition, power transfer = Pe2
X2 =0;
E = 1.25;
V = 1.0;
Pm2 = E*V/X2
%Pe2 = Pm2*sin(del0)
% Post fault condition
X3 = 0.94;
E = 1.25;
V = 1.0;
Pm3 = E*V/X3
% Power transfer after fault = Pe3
% delm = maximum del angle
delm = 180-asin(Pi/Pm3)*180/pi
% delc = clearing angle
```

```
delc = acos((Pi*(delm-del0)*pi/180)-Pm2*cos(del0)+Pm3*cos(delm))/(Pm3-Pm2) % delc in radians
delc = delc*180/pi % delc in degrees
del = [0,0.5,1.0,1.5,2.0,2.5,3.0,3.5];
Pi=[1.0,1.0,1.0,1.0,1.0,1.0,1.0,1.0];
plot(del*180/pi,Pi,'r-'),hold
del = 0:0.1:pi;
Pe1 = Pm1*sin(del);
Pe2= Pm2*sin(del);
Pe3 = Pm3*sin(del);
x = [26.72  26.72];
y= [0.0 1.0];
xx= [53.6  53.6  ];
yy = [0.0 1.5];
plot(del*180/pi,Pe1,'k-',del*180/pi,Pe2,'y-',del*180/pi,Pe3,'g-',x,y,'b-',xx,yy,'b-'),hold off
%legend('Pre- fault Power Transfer', 'During fault Power Transfer', 'Post fault power transfer','del0 Vs Power','delc Vs Power')
Grid title ('Transient stability analysis for Adama wind farm')
xlabel('Rotor angle in degrees')
ylabel('Power in p.u.')
```